

# Influence of supplementary cementitious materials on durability of calcium aluminate cement under different curing regimes

---

**Bašić, Alma-Dina**

**Doctoral thesis / Disertacija**

**2024**

*Degree Grantor / Ustanova koja je dodijelila akademski / stručni stupanj:* **University of Zagreb, Faculty of Civil Engineering / Sveučilište u Zagrebu, Građevinski fakultet**

*Permanent link / Trajna poveznica:* <https://um.nsk.hr/um:nbn:hr:237:302283>

*Rights / Prava:* [In copyright](#) / [Zaštićeno autorskim pravom.](#)

*Download date / Datum preuzimanja:* **2025-03-29**

*Repository / Repozitorij:*

[Repository of the Faculty of Civil Engineering,  
University of Zagreb](#)





University of Zagreb

Faculty of Civil Engineering

Alma-Dina Bašić

**INFLUENCE OF SUPPLEMENTARY  
CEMENTITIOUS MATERIALS ON DURABILITY  
OF CALCIUM ALUMINATE CEMENT UNDER  
DIFFERENT CURING REGIMES**

DOCTORAL THESIS

Zagreb, 2024.



University of Zagreb

Faculty of Civil Engineering

Alma-Dina Bašić

**INFLUENCE OF SUPPLEMENTARY  
CEMENTITIOUS MATERIALS ON DURABILITY  
OF CALCIUM ALUMINATE CEMENT UNDER  
DIFFERENT CURING REGIMES**

DOCTORAL THESIS

Supervisor: Assoc. Prof Marijana Serdar, Ph.D

Zagreb, 2024.



Sveučilište u Zagrebu

GRAĐEVINSKI FAKULTET

Alma-Dina Bašić

**UTJECAJ MINERLNIH DODATAKA NA TRAJNOST  
KALCIJ ALUMINATNOGA CEMENTA PRI  
RAZLIČITIM TEMPERATURAMA NJEGOVANJA**

DOKTORSKI RAD

Mentor: izv. prof. dr. sc. Marijana Serdar

Zagreb, 2024.

## Acknowledgement

First, I would like to thank my mentor Assoc. Prof. Marijana Serdar. Thank you for believing in me since my master's studies and thank you for giving me the opportunity to be a part of your LATOM group almost four years ago. Your guidance and support helped me a lot to complete my PhD. The last few months of writing my PhD were very challenging. And when I did not believe I could do it, you were there to encourage me that I could. Thank you for believing in me and helping me to believe in myself.

I am very thankful to all my girls from Sveti Duh. There were so many beautiful days and unforgettable moments along this journey. Matea, Ivana, Vanja, Branka and Josipa, thank you girls for all your help, advice and discussions. I would also like to thank Kiran for his support during my PhD. Katarina, Petra and Olivera, I am incredibly grateful to have you in my life. Thank you for all your support and help throughout my PhD journey. I would like to thank everyone from the Department of Materials for their selfless help, professional advice and support during these years. Furthermore, I would like to thank the Calucem company employees who participated in the ECO2Flex project.

Finally, I would like to express my deepest gratitude to my boyfriend Krešo, my parents, my brother, my sister-in-law Ivona and all my friends who have stood by me during my PhD. Your support has meant everything to me over these years. I could not have done this without you, through both the good times and the challenging ones. Thank you!

Alma-Dina

## Extended Summary

The cement industry is facing a global problem of environmental pollution during cement production. To reduce the negative impact on the environment, the possibility of using supplementary cementitious materials – SCMs, e.g. industrial by-products or natural materials, as a replacement for part of the cement in concrete has been already investigated for many years. Calcium aluminate cement (CAC) has been used for more than 100 years and is mostly used for special purposes where resistance to aggressive environments is required. However, the application of CAC is limited by the occurrence of the conversion process, which increases the porosity of the cement matrix and reduces its mechanical properties. The use of SCMs as a replacement for part of the CAC could reduce the negative environmental impact of cement production and improve the mechanical properties of concrete, especially when exposed to higher curing temperatures. Previous research has shown that the application of blast furnace slag reduces the impact of the conversion process. However, due to challenges with the availability and cost of slag, there is a need to investigate other possible SCMs. In this dissertation, calcined clay, which is available in the region and has a medium kaolin content, was used. Although the rate of the conversion process is reduced by the use of SCMs, the question of the durability of such binders arises.

In the first phase of this dissertation, the research focused on the influence of slag and calcined clay on the mechanical properties of CAC cement. At the same time, the changes in hydration products and pore structure were analysed under the influence of two different curing regimes (20°C and 38°C). It was found that calcined clay can be used as a replacement for part of the CAC instead of slag to reduce the effects of the conversion process. Furthermore, the results show that the addition of calcined clay to CAC strätlingite is formed, which densifies the structure and inhibits the conversion process.

In the second phase, the research focused on evaluating the durability of concrete based on CAC with and without the addition of slag or calcined clay. The durability assessment included tests on resistance to carbonation, resistance to chloride penetration, resistance to acid attack and sulphate resistance. The tests were carried out on systems before and after the conversion process, whereby the conversion process was accelerated by curing at 38°C. The results show that the addition of slag or calcined clay reduces the resistance of CAC under different environmental conditions. However, while the resistance of systems without SCMs was significantly affected by these influences, the resistance of systems with slag or calcined clay was only slightly affected after the conversion process.

The research conducted in this dissertation shows that slag and calcined clay can be used as a replacement for 30% of CAC. Understanding the effects of slag and clay on microstructural changes, their contribution to mitigating the effects of the conversion process and their effects on durability properties allows for a wider application of CAC-based systems.

Keywords: calcium aluminate cement, conversion process, slag, calcined clay, porosity, chloride diffusion, carbonation, sulphates, acids

## Produženi sažetak

Cementna industrija suočava se s globalnim problemom zagađenja okoliša tijekom proizvodnje cementa. Kako bi se smanjio negativan utjecaj na okoliš, već dugi niz godina istražuje se mogućnost primjene mineralnih dodataka (nusproizvodi industrije ili prirodni materijali) kao zamjena za dio cementa u betonu. Kalcij aluminatni cement koristi se već više od 100 godina, a najčešće se primjenjuje za posebne namjene gdje je potrebna otpornost na agresivni okoliš. Međutim, primjenu CAC cementa ograničava pojava procesa konverzije kojim se povećava poroznost cementne matrice i smanjuju mehanička svojstva. Upotrebom mineralnih dodataka za zamjenu dijela CAC cementa smanjuje se negativni utjecaj proizvodnje cementa na okoliš te se poboljšavaju mehanička svojstva betona pogotovo pri izloženosti povišenim temperaturama prilikom njegovanja. Dosadašnja istraživanja pokazala su da se primjenom zgure visokih peći smanjuje utjecaj procesa konverzije, no zbog izazova s dostupnošću i troškovima zgure, postoji potreba za istraživanjem drugih mogućih mineralnih dodataka. U ovoj disertaciji korištena je kalcinirana glina, koja je dostupna u regiji, sa srednjim sadržajem kaolina. Iako se stopa procesa konverzije smanjuje primjenom mineralnih dodataka, otvara se pitanje trajnosti takvih veziva.

U prvoj fazi ove disertacije istraživanje je usmjereno na utjecaj zgure i kalcinirane gline na mehanička svojstva CAC cementa. Istovremeno su analizirane promjene produkata hidratacije i strukture pora pod utjecajem dva različita režima njegovanja (20°C i 38°C). Utvrđeno je da se kalcinirana glina može koristiti kao zamjena za dio CAC cementa umjesto zgure, za smanjenje utjecaja procesa konverzije. Također, rezultati pokazuju da se dodatkom kalcinirane gline CAC cementu stvara stratlingit koji smanjuje poroznost i inhibira proces konverzije.

U drugoj fazi istraživanje je usmjereno na procjenu trajnosti CAC cementa sa i bez dodatka zgure ili kalcinirane gline. Procjena trajnosti obuhvaća ispitivanja otpornosti na karbonatizaciju,



otpornost na prodor klorida, otpornost na djelovanje kiselina te sulfatnu otpornost. Ispitivanja su provedena za sustave u kojima nije bilo procesa konverzije i za sustave u kojima je proces konverzije ubrzan njegovanjem na 38°C. Rezultati pokazuju da dodatak zgure ili kalcinirane gline smanjuje otpornost CAC cementa na razna djelovanja iz okoliša. Međutim, dok je u sustavu bez mineralnih dodataka otpornost na navedena djelovanja značajno narušena nakon konverzije, otpornost sustava sa zgurom ili kalciniranom glinom nije značajno narušena nakon procesa konverzije.

Istraživanje provedeno u ovoj disertaciji pokazuje da se zgura i kalcinirana glina mogu primjenjivati kao zamjena za 30% CAC cementa. Poznavanje utjecaja zgure i gline na promjene u mikrostrukturi, njihov doprinos na suzbijanje utjecaja procesa konverzije te utjecaj na trajnosna svojstva, omogućuje širu primjenu sustava na bazi CAC cementa.

Ključne riječi: kalcij aluminatni cement, proces konverzije, zgura, kalcinirana glina, poroznost, difuzija klorida, karbonatizacija, sulfati, kiseline

## Glossary

CA	Monocalcium aluminate
CAH <sub>10</sub> , CaO • Al <sub>2</sub> O <sub>3</sub> • 10H <sub>2</sub> O	Dicalcium aluminate decahydrate
C <sub>2</sub> AH <sub>8</sub> , 2CaO • Al <sub>2</sub> O <sub>3</sub> • 8H <sub>2</sub> O	Dicalcium aluminate octahydrate
C <sub>3</sub> AH <sub>6</sub> , 3CaO • Al <sub>2</sub> O <sub>3</sub> • 6H <sub>2</sub> O	Hydrogarnet
AH <sub>3</sub> , 2Al(OH) <sub>3</sub>	Aluminium hydroxide
C <sub>2</sub> ASH <sub>8</sub> , 2CaO • Al <sub>2</sub> O <sub>3</sub> • SiO <sub>2</sub> • 8H <sub>2</sub> O	Strätlingite
NaCl	Sodium chloride
Na <sub>2</sub> SO <sub>4</sub>	Sodium sulphate
H <sub>2</sub> SO <sub>4</sub>	Sulfuric acid
CaCO <sub>3</sub>	Calcium carbonate
CO <sub>2</sub>	Carbon dioxide
XRF	X-ray fluorescence
XRD	X-ray diffraction
TGA	Thermogravimetric analysis
MIP	Mercury intrusion porosimetry
SCM	Supplementary cementitious materials
S	Slag
C	Calcined clay
OPC	Ordinary Portland cement
CAC	Calcium aluminate cement

---

## DECLARATION OF ORIGINALITY

I declare that my doctoral dissertation is the original result of my work and that I did not use any sources other than those listed in it.

Alma-Dina Bašić, mag. ing. aedif

*Bašić A.D.*

---

## Table of contents

<b>Acknowledgement.....</b>	<b>iv</b>
<b>Extended Summary .....</b>	<b>v</b>
<b>Produženi sažetak.....</b>	<b>vii</b>
<b>Glossary .....</b>	<b>ix</b>
<b>Chapter 1 Introduction .....</b>	<b>14</b>
1.1 Hydration and conversion process of calcium aluminate cement .....	15
1.2 Durability of calcium aluminate cement.....	20
1.3 Research scope .....	23
<b>Chapter 2 Materials and methods.....</b>	<b>27</b>
2.1 Materials.....	27
2.2 Methods.....	30
2.2.1 Particle size distribution .....	30
2.2.2 Reactivity.....	30
2.2.3 Setting time.....	31
2.2.4 Workability.....	31
2.2.5 Compressive strength .....	31
2.2.6 Thermogravimetric analysis .....	32
2.2.7 Mercury intrusion porosimetry .....	32
2.2.8 X-ray diffraction .....	32
2.2.9 Carbonation resistance .....	33
2.2.10 Gas permeability .....	33
2.2.11 Chloride migration .....	34
2.2.12 Chloride diffusion .....	34
2.2.13 Water permeability.....	35
2.2.14 Freezing and thawing with de-icing salts.....	35
2.2.15 Sulphate resistivity .....	36
2.2.16 Acid resistance .....	36

---

<b>Chapter 3 Impact of slag and calcined clay on CAC properties.....</b>	<b>37</b>
3.1 Introduction .....	37
3.2 Impact of slag .....	39
3.2.1 Optimisation of laboratory milling .....	39
3.2.2 Impact of slag on calcium aluminate cement-based mortar .....	42
3.2.3 Impact of slag on conversion process of calcium aluminate cement .....	45
3.2.4 Impact of slag on basic durability properties of calcium aluminate cement-based concrete .....	54
3.3 Impact of calcined clay .....	62
3.3.1 Impact of calcined clay on calcium aluminate-based mortar .....	62
3.3.2 Impact of calcined clay on conversion process of calcium aluminate cement .....	65
3.4 Discussion .....	72
3.5 Conclusion.....	76
<b>Chapter 4 Carbonation of CAC with the addition of slag/calcined clay .....</b>	<b>79</b>
4.1 Introduction .....	79
4.2 Results.....	80
4.2.1 Depth of carbonation.....	80
4.2.2 Compressive strength development .....	81
4.2.3 Microstructural changes during carbonation .....	83
4.2.4 Pore structure changes during carbonation.....	90
4.3 Discussion .....	92
4.4 Conclusion.....	98
<b>Chapter 5 Chloride transfer in CAC with the addition of slag/calcined clay.....</b>	<b>100</b>
5.1 Introduction .....	100
5.2 Results.....	101
5.2.1 Compressive strength .....	101
5.2.2 Thermogravimetric analysis .....	102
5.2.3 Mercury intrusion porosimetry .....	103
5.2.4 Chloride diffusion results .....	105

---

5.2.5 X-ray diffraction .....	108
5.3 Discussion .....	112
5.4 . Conclusion.....	115
<b>Chapter 6 Sulphate and acid resistance of CAC with the addition of slag/calced clay ....</b>	<b>116</b>
6.1 Introduction .....	116
6.2 Results.....	118
6.2.1 Analysis of samples after exposure to sodium sulphate.....	118
6.2.2 Analysis of samples after exposure to sulphuric acid .....	124
6.3 Discussion .....	133
6.3.1 Exposure to sodium sulphate solution.....	134
6.3.2 Exposure to sulfuric acid solution.....	137
6.4 Conclusion.....	140
<b>Chapter 7 Conclusions.....</b>	<b>142</b>
7.1 Conclusions .....	142
7.2 Scientific contribution.....	143
7.3 Future recommendations.....	146
<b>References .....</b>	<b>147</b>
<b>List of figures .....</b>	<b>159</b>
<b>List of tables.....</b>	<b>164</b>
<b>Biography.....</b>	<b>165</b>
List of published papers .....	165
<b>Papers in journal.....</b>	<b>165</b>
<b>Papers, posters, and presentations in conferences.....</b>	<b>165</b>

## Chapter 1 Introduction

The production of cement emits a large amount of CO<sub>2</sub>, currently accounting for 5-8% of the total CO<sub>2</sub> emissions worldwide. Looking at the development of the cement industry, it is estimated that this proportion will be 25% or more by 2050 [1]. Following the commitments of the cement industry to achieve net-zero emissions by 2050, the focus is on reducing the clinker-to-cement ratio and developing innovative cement manufacturing technologies [2]. In order to reduce the clinker-to-cement ratio, supplementary cementitious materials are often used in practise. Additionally, the production of alternative cementitious materials, such as calcium aluminate cement (CAC), contributes to the reduction of CO<sub>2</sub> emissions [3]. Calcium aluminate cement has been used in the construction industry for over 100 years and was patented by Jules Bied in 1908. It was originally used to increase resistance to aggressive sulphates and chlorides, due to the poor durability of ordinary Portland cement in such environments [4]. In addition, it offers further advantages compared to Portland cement, such as a rapid increase in early strength, high wear resistance and resistance to various chemical attacks. Due to its unique properties, it is used for various purposes: emergency and rapid repairs, dam overflows, sewers, industrial floors, as a refractory material, for concreting in cold conditions and as an injection mix for tunnel linings [5]. Although it is used for various applications, its use is limited by the occurrence of conversion and the limited availability of the primary raw material (high-quality bauxite) [6]. The production of calcium aluminate cement amounts to 2 million tons per year [7], and it is more than four times more expensive than ordinary Portland cement [5].

## 1.1 Hydration and conversion process of calcium aluminate cement

Monocalcium aluminate (CA) is the main phase of calcium aluminate cement [8]. In contact with water, calcium ( $\text{Ca}^{2+}$ ) and aluminate ( $\text{Al}(\text{OH})_4^-$ ) ions dissolve and form four main phases during cement hydration. The phases that occur first,  $\text{CAH}_{10}$  and  $\text{C}_2\text{AH}_8$ , are called metastable hydrates. Over time, the metastable hydrates form the stable hydrate  $\text{C}_3\text{AH}_6$  [5][7]. The transformation of metastable hydrates into stable hydrates is called conversion. Along with the appearance of  $\text{C}_3\text{AH}_6$ ,  $\text{AH}_3$  gel is formed, and subsequent water release occurs. The conversion process is highly dependent on the temperature and relative humidity of the environment. Furthermore, conversion is an unavoidable process. During the aging of calcium aluminate cement [7], a transformation of the hydrates occurs. At temperatures up to  $15^\circ\text{C}$ , the metastable  $\text{CAH}_{10}$  forms as the first phase. At temperatures above  $30^\circ\text{C}$ , the metastable  $\text{C}_2\text{AH}_8$  forms as the first phase, while at temperatures between  $15^\circ\text{C}$  and  $30^\circ\text{C}$  both forms of metastable hydrates and  $\text{AH}_3$  hydrate are formed. However, the formation of metastable phases becomes more difficult when temperatures are close to  $30^\circ\text{C}$ . At temperatures above  $30^\circ\text{C}$ , the reaction kinetics accelerate, leading to the rapid formation of  $\text{C}_3\text{AH}_6$  (stable hydrate) and  $\text{AH}_3$  [5][9]. Figure 1.1 schematically illustrates the formation of the main phases of calcium aluminate cement (CAC) as a function of temperature. The temperature to which the material is exposed determines the relative amounts of hydrates that form during the hydration of calcium aluminate cement. Stable hydrates form after a certain time if the material is exposed to sufficient relative humidity and if the temperature of the material is above  $20^\circ\text{C}$  for at least part of its lifetime [5]. The hydration process of monocalcium aluminate is shown in the equations 1.1, 1.2, 1.3, 1.4, 1.5 [4][8][10][11].



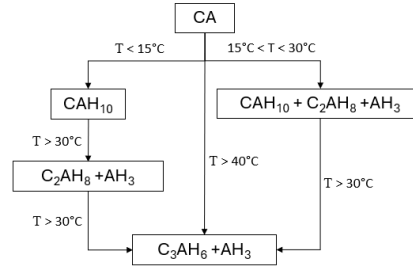
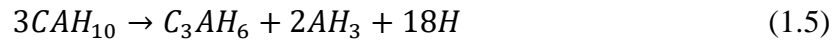
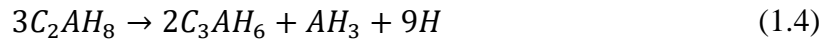
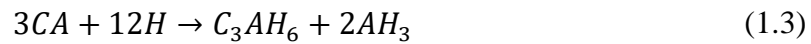
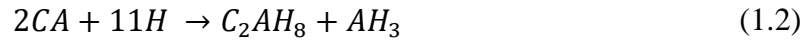


Figure 1.1 Formation of the main phases under the influence of temperature



Metastable hydrates usually decompose at temperatures from 100°C to 200°C, while stable hydrates decompose at temperatures from 250°C to 350°C [4]. The low-density hexagonal phases of the metastable hydrates ( $CAH_{10}$  and  $C_2AH_8$ ) fill the space at the beginning of CA cement hydration and thus ensure high early strengths. The conversion process, reduces this space and fills it with the cubic phases of the stable hydrates ( $C_3AH_6$  and  $AH_3$ ), leading to a decrease in strength [10]. The densities of the hydrates formed through the conversion process are shown in Table 1.1. As the density increases, the porosity of the cement matrix also increases, which leads to a reduction in strength. The bonds between  $C_3AH_6$  and  $AH_3$  are weaker than the bonds between  $CAH_{10}$  and  $C_2AH_8$ , even with the same porosity [12]. When the minimum strength is reached, the water released during the conversion process can continue to participate in the hydration of the remaining (non-hydrated) cement particles, thus increasing the strength over time [4].

Table 1.1 Densities of the calcium aluminate cement hydrates

Hydrates	Density (g/cm <sup>3</sup> )
$CAH_{10}$	1.72
$C_2AH_8$	1.75
$C_3AH_6$	2.52
$AH_3$	2.40

The development of the compressive strength in CAC depends on the water-to-cement ratio, the relative humidity of the environment and the curing temperature to which it is exposed. Figure 1.2 shows the influence of curing temperature on the development of compressive strength. A higher curing temperature leads to a lower initial compressive strength, as conversion process takes place in very short period. However, when curing at lower temperatures initial compressive strength is higher, but after a longer curing time, the compressive strength decreases. Only when curing at 20°C the compressive strength is constant over a longer period of time. During conversion of metastable hydrates into stable hydrates phases with a higher density are formed, which leads to a reduction in the volume of hydrates. This results in increased porosity of the cement matrix and lower compressive strength. The conversion process can take up to ten years if the concrete is exposed to low temperatures (10°C-20°C). Once the conversion process is complete, it can be said that the strength is stable, i.e. there is no further significant decrease or increase in strength.

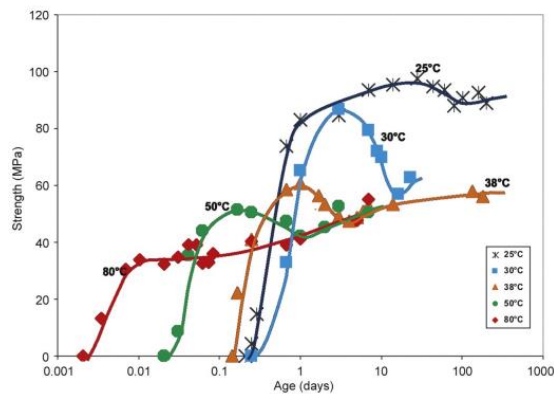
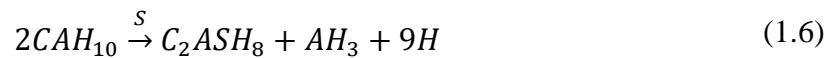


Figure 1.2 Development of compressive strength in relation to curing temperature [5]

During the hydration of calcium aluminate cement metastable hydrates are formed, which convert into stable hydrates under the influence of temperature and relative humidity. The conversion process results in a decrease in compressive strength. The effects of the conversion process on compressive strength can be reduced by the use of chemical and/or mineral additives. Most research has been carried out with the addition of pozzolanic materials such as slag, fly ash, and silica fume

[13][14][15][16]. The most commonly used supplementary cementitious material is ground granulated blast furnace slag (GGBFS). The high glass content enables latent hydraulic reactivity, which allows slag to be used to produce composite cements concrete. To achieve compatibility with cement and higher reactivity, the slag needs to be ground to smaller particle sizes [17]. Slag contains 32-42% silicon dioxide ( $\text{SiO}_2$ ) in its chemical composition. The high  $\text{SiO}_2$  content in slag forms hydrates that inhibit the conversion process during the transformation of hydrates [18]. Silicon dioxide reacts with the hydrates of calcium aluminate cement and forms the hydrate  $\text{C}_2\text{ASH}_8$  (strätlingite hydrate) [19]. The amount of  $\text{C}_2\text{ASH}_8$  formed depends on the slag ability to release silicon dioxide upon activation. Activation is favoured by the presence of alkali metal hydroxides in the CA cement [20]. The process of  $\text{C}_2\text{ASH}_8$  hydrate formation is shown in the following equations [5][10].



The reaction of silica with the hydrates of CAC reduces the formation of  $\text{C}_2\text{AH}_8$ , and at the same time  $\text{C}_2\text{ASH}_8$  is formed, depending on the amount of slag used to replace the cement. This reaction is beneficial as since it reduces the effects of the conversion process, i.e. there is no significant decrease in compressive strength [21]. Moreover, the strength will continuously increase until the hydration process is complete. Slag has a positive effect on the mechanical properties up to a certain replacement percentage. If the replacement percentage is too high, the hydraulic phases in the composition decrease, resulting in a large amount of unreacted slag particles. This hinders the hydration of the non-hydrated CAC particles, which leads to a reduction in compressive strength. Figure 1.3 shows the development of calcium aluminate-based mortar with partial replacement (40%, 60%, 80%) by slag. It can be seen that the initial strength of mortars with partial cement

replacement is lower but increase continuously over time. Mortars without slag addition show the greatest increase in strength during the first few days, but later the strength decreases due to the conversion process.

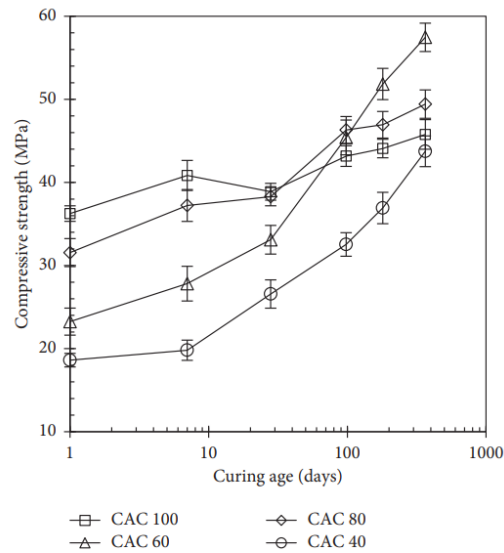


Figure 1.3 Compressive strength development of mortar in relation to curing time [10]

The positive influence of slag on the development of compressive strength was confirmed by Majumdar et.al [20]. They investigated the development of the compressive strength in cement paste and concrete with the addition of slag, as a function of the water-to-cement ratio and the curing temperature. The cement paste was cured at 20°C and 40°C, the mortar samples at 20°C and 38°C. By replacing a significant proportion of the cement with slag (50%), the reduction in strength caused by the conversion process is prevented. The measurement of the compressive strength of cement paste and mortar with the addition of slag showed a stable compressive strength compared to mixtures without slag. Kirca [21] came to similar results in his research. A 20% replacement of cement with slag had no significant effect on the hydration products formed during the hydration of CAC. The conversion from metastable to stable hydrates was not hindered, suggesting that a 20% addition of slag is not sufficient to prevent a decrease in strength during the conversion

process. However, if the percentage of replacement is increased to 40%, 60%, and 80%, the reduction in strength is avoided by the formation of sufficient quantities of strätlingite. At elevated curing temperatures, strätlingite forms more slowly than  $C_3AH_6$  and cannot completely replace it. The main disadvantage of replacing cement with slag is that increasing the replacement percentage reduces the early strength of the concrete.

## 1.2 Durability of calcium aluminate cement

The durability of calcium aluminate cement is often cited as the greatest advantage of this material [4][5][22]. In contrast to Portland cement, which is mainly used in construction, CAC has its niche applications [23]. The main purpose of CAC cement was to improve the resistance of OPC to sulphates and chlorides [5]. The primary oxides in ordinary Portland cement (OPC) are silicon dioxide ( $SiO_2$ ) and limestone ( $CaO$ ) [24]. In contrast to OPC, the primary oxides in calcium aluminate cement (CAC) are limestone ( $CaO$ ) and aluminum oxide ( $Al_2O_3$ ), which together form monocalcium aluminate (CA,  $CaO \cdot Al_2O_3$ ), dicalcium aluminate ( $CA_2$ ,  $2CaO \cdot Al_2O_3$ ), aluminum oxide ( $Al_2O_3$ ), gehlenite ( $Ca_2Al_2SiO_7$ ), and mayenite ( $C_{12}A_7$ ,  $12CaO \cdot 7Al_2O_3$ ) in smaller quantities [25]. The hydration of CAC cement depends on the temperature and relative humidity of the environment. The high early strength is a result of the formation of metastable hydrates ( $CAH_{10}$  and  $C_2AH_8$ ) of hexagonal phases, which have low density. However, over time or with an increase in temperature, these metastable hydrates transform into stable cubic hydrates ( $C_3AH_6$  and  $AH_3$ ), which have a high density [26]. The conversion process affects mechanical properties and durability. During the conversion process, the porosity of the cement matrix increases and the compressive strength decreases [27]. The increased porosity of the cement matrix impairs the durability of the cement during exposure to aggressive substances from the environment.

CAC is considered to have superior durability compared to OPC. However, most studies have been conducted with unconverted CAC or as an addition of CAC to OPC to improve desired properties [22][28]. Research has mainly focused on sulphate, chloride and carbonation resistance. The resistance to aggressive substances from the environment is highly dependent on the hydration products and the porosity of the cement matrix [29]. The penetration of aggressive sulphates into the concrete structure is one of the factors that cause the formation of ettringite, monosulphate and gypsum [30]. To reduce the effects of aggressive sulphates, sulphate resistant cement (sulphate resistant cement-SR) has been produced. The proportion of C3A in sulphate-resistant cement is less than 5%, which contributes to improved durability and reduced formation of secondary ettringite [31]. It has been shown that CAC exhibits a smaller decrease in compressive strength compared to sulphate resistant cement when exposed to sulphate solution (Figure 1.4). CAC is more resistant to sulphates due to the absence of calcium hydroxide, the presence of  $AH_3$  gel and the low reactivity of the metastable hydrate  $CAH_{10}$  with sulphate ions [32].

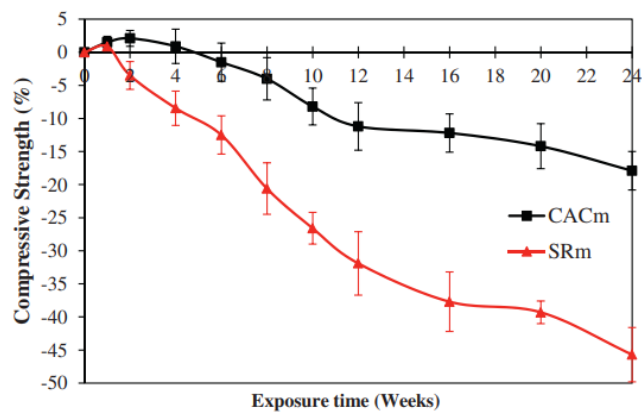


Figure 1.4 Change in compressive strength in relation to exposure time [22]

One of the durability properties raising additional attention in concrete research is resistance to carbonation, as concrete-based materials play a role as carbon sinks in the carbon neutrality strategy [33][34]. According to the literature, reaction with  $CO_2$  in CAC leads to the formation of  $CaCO_3$

and  $AH_3$  gel, regardless of the hydrates present [35][36]. Alapati and Kurtis [37] showed that CAC concrete has a faster carbonation rate compared to OPC concrete. They also showed that the decomposition of the primary hydration products as a result of carbonation can lead to a significant decrease in compressive strength and capillary porosity. On the contrary, some of the researches attempted to inhibit conversion process by carbonation curing [38][39]. Exposure of CAC to a large amount of  $CO_2$  during early age can suppress the conversion process. Metastable hydrates, which would convert into stable hydrates, can carbonate during curing with high level of  $CO_2$ . The product of metastable hydrates after carbonation is  $AH_3$  gel (Figure 1.5).

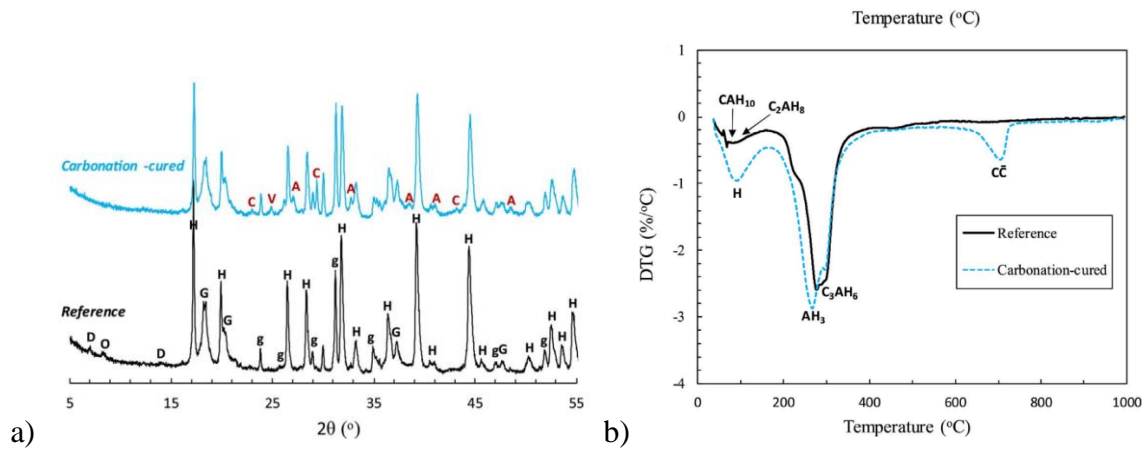


Figure 1.5 a) XRD of non-carbonated and carbonated CAC, b) dTG of non-carbonated and carbonated CAC [39]

Chloride ions in the concrete structure can be free in the pore solution, adsorbed on surfaces, or react with hydration products to form new compounds [40]. Only the free ions in the pore solution are considered in the mechanism of chloride movement in concrete, as they are the only ones that influence the corrosion processes [41]. A higher chloride binding capacity slows down the process of chloride transport through the concrete and leads to a lower degree of chloride-induced corrosion [42]. The high content of aluminum oxide ( $Al_2O_3$ ) in the chemical composition of calcium aluminate cement (more than 30%) enables greater chloride binding in the pores of the concrete, reducing the degree of concrete corrosion. Chlorides react with the hydration products of CAC and

forms a new product in the form of Friedel salt ( $3\text{CaO}\cdot\text{Al}_2\text{O}_3\cdot\text{CaCl}_2\cdot 10\text{H}_2\text{O}$ ) [43][44][45]. In addition, replacing part of the cement with mineral additives can increase the resistance of the cement matrix to chloride penetration. The addition of materials such as slag and fly ash make the structure of the cement matrix more compact. Li et.al [46] investigated the influence of supplementary cementitious materials on chloride penetration. By determining the content of free and total chlorides, they found that a mixture of CAC without SCMs and a mixture of OPC, CAC, gypsum, and slag had the lowest content of free and total chlorides after exposure to seawater.

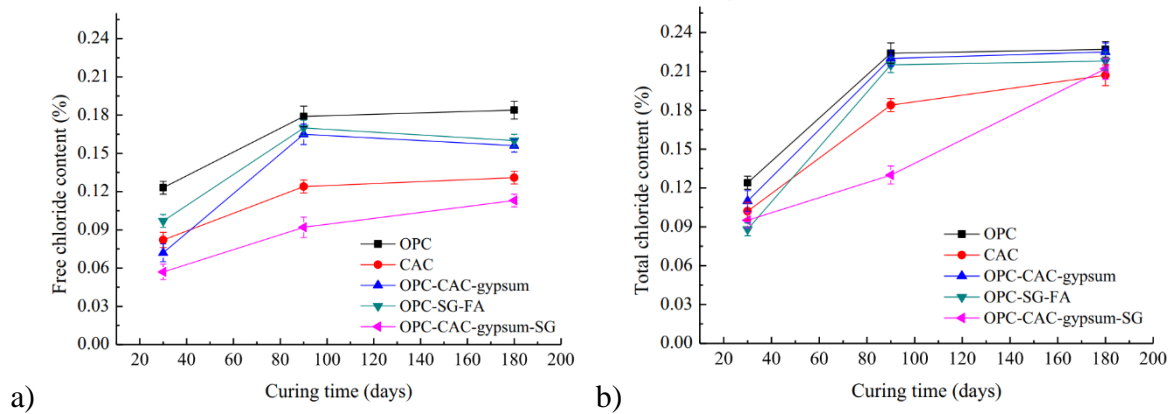


Figure 1.6 a) Free chloride content, b) Total chloride content

### 1.3 Research scope

The main objective of the doctoral dissertation was to evaluate the durability of concrete based on calcium aluminate cement with and without SCMs under different curing regimes. Research was focused on the assessment of durability before and after the conversion process with and without the addition of slag and calcined clay in CAC. The research was carried out in cooperation with the Calucem company (whose cement was used during the preparation of the entire dissertation), and in addition to scientific research, cooperation between industry and research institutions was developed. In total, six slags and two clay were used in the initial phase of this research, leading to one slag and one clay that were chosen for further investigation on durability properties.



Specific objectives of the research were:

- characterisation of the available SCMs and determination of their effects on the basic mechanical and durability of concrete based on calcium aluminate cement (Chapter 3),
- effects of the conversion process on the changes in the microstructure of the cement matrix with and without the addition of SCMs (Chapters 3, 4, 5 and 6),
- changes in the durability properties of CAC with and without mineral additives at different curing temperatures (Chapters 4, 5 and 6).

The outline of this dissertation is as follows:

### *Chapter 1*

This chapter is an introduction to doctoral dissertation covering the most important literature review related to calcium aluminate cement such as the hydration, conversion process, and durability. After condensed state of the art, research gaps were identified, and research scope and hypothesis of the research were set.

### *Chapter 2*

The first part of this chapter includes the characterisation of the materials used during the research. The second part of the chapter contains a detailed description of all the methods used in the research.

### *Chapter 3*

This chapter represents the first phase of the experimental research. An initial assessment of the influence of slag and calcined clay on the compressive strength of CAC based mortar was investigated. Also, the possibility of inhibiting the conversion process by replacing 30% of CAC with slag or calcined clay was tested. Furthermore, influence of slag on basic durability properties

of CAC based concrete was established. Based on this chapter the durability properties for further investigation were defined.

#### *Chapter 4*

This chapter examines carbonation resistance of CAC based mortar without and with partial replacement by slag or calcined clay. The carbonation was evaluated through mechanical properties by testing compressive strength, and microstructural changes induced by carbonation through TGA and MIP analysis. In addition, depth of carbonation was determined by phenolphthalein indicator.

#### *Chapter 5*

This chapter investigates potential of using slag or calcined clay as partial replacement of CAC in chloride environment. The chloride environment was stimulated by exposure of samples to NaCl solution. Chloride concentration was determined using titration method. In addition, chloride concentration was correlated to porosity and phase assemblage obtained by MIP and TGA analysis.

#### *Chapter 6*

The aim of this chapter was to evaluate sulphate and acid resistance of CAC based mortar without and with the addition of slag or calcined clay. The influence of aggressive sulphates and acid solutions was determined through mass change, compressive strength, and microstructural analysis obtained by TGA, MIP and XRD.

#### *Chapter 7*

In this chapter, all the conclusions obtained from the research are presented and original scientific contributions highlighted. Additionally, recommendations are given for future research on this topic.

## **Hypothesis of the research**

1. The addition of SCMs induces changes in the microstructure of alumina cement that affect durability in aggressive environments.
2. The changes in durability properties are highly dependent on the temperature that occurs during the early age of CAC hydration.

## Chapter 2 Materials and methods

### 2.1 Materials

This research is focused on understanding the influence of supplementary cementitious materials on micro and macrostructural changes in CAC. For this purpose, six different slags and two clays were analysed in the first phase of the research. As a result of the first phase, one slag and one clay were selected for further investigation. A calcium aluminate cement supplied by manufacturer was used for all investigations.

The calcium aluminate cement used in this research was provided by Calucem company from Pula, Croatia. The percentage of  $\text{Al}_2\text{O}_3$  in the chemical composition of the used CAC was 57.67 %. The complete chemical composition of the CAC cement is not available due to the non-disclosure agreement with the manufacturer of CAC cement, Calucem d.o.o. The cement was delivered three times in batches of 25 kg each. After shipment, the cement was stored in sealed plastic bags and in a plastic box until use.

In the first phase of the research, six different types of slag samples were analysed as possible additions to CAC. All slags are of different origin and are labelled as S1, S2, S3, S4, S5, and S6. The particle size distribution of the slags (as received) is shown in Figure 2.1. The slags S1, S2, S3, S4, S5 were received as grains. Slag S6 was received as finish product and in the form of powder. Two clays labelled as C1 and C2, supplied from South-East Europe, were also used for this research. The chemical composition of all SCMs is listed in Table 2.1. The raw materials chemical oxides composition was measured using X-ray fluorescence.

In the second research phase, slag S1 and calcined clay C1 were used to investigate a possible addition to calcium aluminate cement and its influence on the mechanical and durability

properties. Figure 2.2 shows the results obtained by thermogravimetric analysis of the raw clays C1 and C2. The first peak ( $< 100^{\circ}\text{C}$ ) is related to the moisture content, and the significant mass loss (%) from  $350 - 600^{\circ}\text{C}$  is related to the dihydroxylation of the clay minerals kaolinite and/or illite. According to the mass loss (%) from  $350 - 600^{\circ}\text{C}$ , the calcined clay contained 40% kaolinite. The kaolinite content determined from the mass loss curve is 40% for C1, 25.3% for C2. The heat of hydration obtained by the R3 test using calorimetry according to the test developed for the RILEM TC-267 committee (ASTM C1897-20) is shown in Figure 2.3. Slag showed a higher reactivity compared to calcined clay with a higher amount of heat released during the 7 days, but also a slightly higher initial reaction in the first 20 hours.

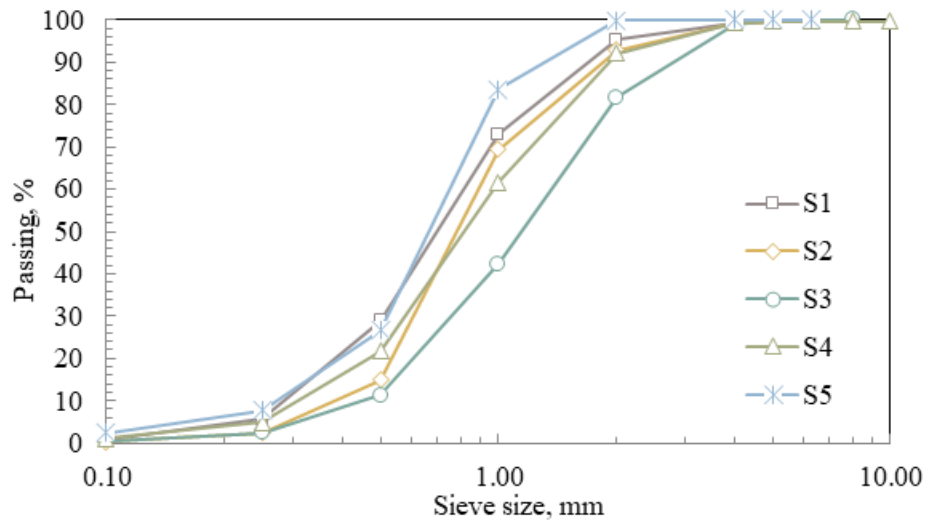


Figure 2.1 Particle size distribution of slags (as received)

Table 2.1 Chemical composition of used materials

Components	S1	S2	S3	S4	S5	S6	C1	C2
Al <sub>2</sub> O <sub>3</sub>	11.7	12.1	13.5	10.8	12	8.4	28.72	26.81
SiO <sub>2</sub>	35.4	38.2	35.6	36.6	39.8	40.6	61.77	62.22
TiO <sub>2</sub>	0.6	0.6	1.2	0.5	1.4	0.3	0.87	0.81
MnO	0.2	1.8	0.3	0.4	1.6	3.6	< 0.01	< 0.01
Fe <sub>2</sub> O <sub>3</sub>	0.5	0.5	0.5	0.3	0.8	2.3	3.03	2.08
CaO	42.5	34.7	38.8	41.9	34.6	36.1	2.39	2.06
MgO	6.4	10.3	8.7	7.3	7.3	6.3	0.68	1.39
K <sub>2</sub> O	0.3	1.3	0.7	0.4	1	1.2	2.3	3.97
Na <sub>2</sub> O	0.3	0.4	0.4	0.2	0.2	0.2	0.01	0.67
SO <sub>3</sub>	1.2	0.3	0.6	1.4	0.4	0.7	0.22	0.1
P <sub>2</sub> O <sub>5</sub>	0	0	0	0	0	0	0.01	0.01

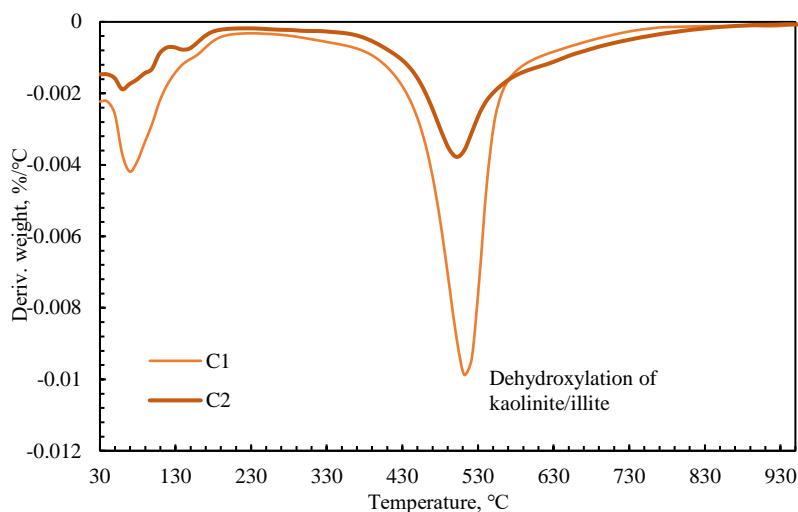


Figure 2.2 dTG of raw clay

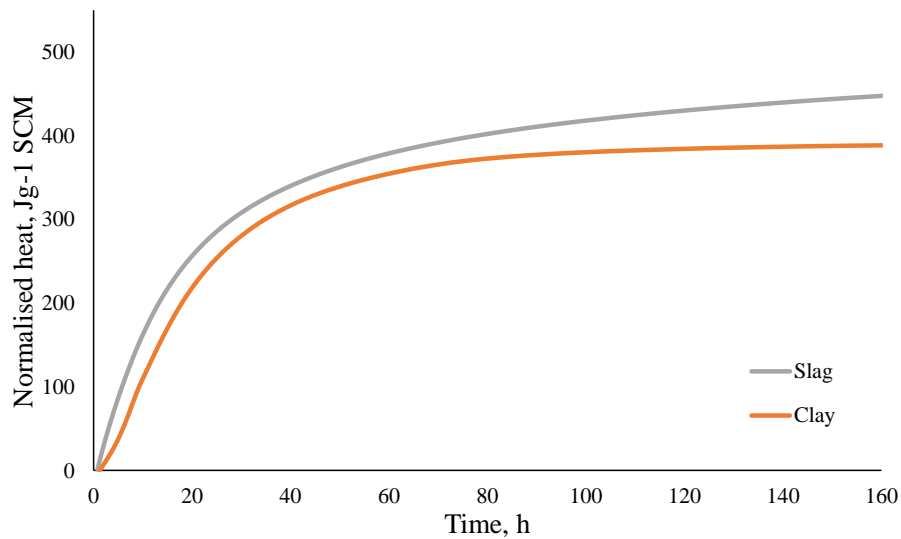


Figure 2.3 Heat of hydration obtained by R3 test using calorimetry for 7 days

## 2.2 Methods

### 2.2.1 Particle size distribution

Air jet sieving of slags was carried out in accordance with the standard HRN EN 933-10 [47] using the MATEST air jet sieve machine. A minimum quantity of 50 g of material was required for effective screening. The particle size distribution by laser diffraction was carried out by the Calucem company, Pula, Croatia.

### 2.2.2 Reactivity

The reactivity of the materials was investigated using a calorimetry test and bound water measurement developed by the RILEM TC-267 committee, called the R3 test (ASTM C1897-20) [48]. Samples of the pastes containing SCMs, sulphate and alkali additive were placed in an isothermal calorimeter at a temperature of 40 °C for 3 and 7 days to determine the total heat release. A ratio of  $\text{Ca}(\text{OH})_2/\text{SCM}$  and  $\text{CaCO}_3/\text{SCM}$  of 3 and 1/2, respectively, was used for each mixture, while the alkali solution was prepared with 3M of K in the form of KOH and  $\text{K}_2\text{SO}_4$ . All materials and reagents were weighed, mixed and stored at 40 °C for 24 h prior to the experiment. A high shear mixer was used at  $1600 \pm 50$  rpm for 2 minutes to

ensure a homogeneous paste, which was immediately poured into a glass vial and placed in an isothermal calorimeter.

### 2.2.3 Setting time

The setting time of mortars was determined according to HRN 480-2:2007 [49]. The mortars were cast in conical moulds immediately after mixing. The initial and final setting times are determined based on the extent of needle penetration into the sample. The initial setting time of the mortar is defined as the time from the completion of mixing until the needle is 4 mm above the bottom of the mould. To determine the final setting time, the mould should be rotated to the bottom of the mould. The setting time, which is measured from the end of the mixing process to the point at which the needle no longer penetrates 2.5 mm into the mortar, is defined as the final setting time of the mortar.

### 2.2.4 Workability

The workability of the mortar was determined according to EN 1015-3:2000/A1:2005/A2:2008 [50]. The workability of the fresh mortar was tested immediately after mixing. The mortar is cast into the mould in two layers, each layer being compacted by at least 10 short strokes with the tamper to ensure uniform filling of the mould. After 15 seconds, the mould is slowly removed vertically, and the mortar is spread by turning the flow table 15 times, approximately once per second. The average value of two measured diameters of mortar indicates the workability of the fresh mortar.

### 2.2.5 Compressive strength

The compressive strength of concrete was measured according to EN 196-1:2016 [51]. The compressive strength was determined after 24h, 7d, 28d and 56d of curing. Immediately after mixing the concrete was cast in 15x15x15 cm cube samples. The concrete samples were



demoulded after 24h and tested for 24-hour compressive strength. The rest of the samples were stored in tap water until testing.

The compressive strength of mortar samples was tested according to EN 14647 [11]. The compressive strength was measured after 6h, 24h, 5d, 7d, 14d, 21d, 28d, 42d, 56d and 91d depending on the specific part of the research being conducted. The samples were cast in 4x4x16 cm prisms moulds. The samples were demoulded after 6 or 24 hours and cured in tap water until testing.

#### 2.2.6 Thermogravimetric analysis

The TG was conducted using TA Instrument Discovery TGA 55. After a certain time of curing, a part of the sample was cut, and hydration was stopped by the solvent exchange method by immersion in isopropanol for 7 days. The samples were then stored in a vacuum until testing. The samples were heated from 30 to 950 °C at a heating rate of 10°/min in an N<sub>2</sub> environment with a flow rate of 60 Cc/min.

#### 2.2.7 Mercury intrusion porosimetry

The porosity changes were analysed using AutoPore IV 9500 in a pressure range from 0.0033 MPa to 206.69 MPa and contact angle of 130°. Similar to TGA, the sample was cut, and hydration was stopped by the solvent exchange method using immersion in isopropanol for 7 days. The samples were then stored in a vacuum until testing.

#### 2.2.8 X-ray diffraction

Qualitative XRD analysis was used for the mineralogical identification of the crystalline phases in the CAC mortar before and after curing in water, and before and after exposure to aggressive solutions. For each sample, the mortar powder was packed into a sample holder. XRD was performed with a Bruker D8 Discover diffractometer using a Cu tube with a

wavelength of 1.54 Å. The 2 $\theta$ -degree angle was scanned from 5 to 70° with a step size of 0.017°.

### 2.2.9 Carbonation resistance

The carbonation resistance of concrete and mortar was determined according to EN 12390-12 [52]. The samples were covered and stored in 15x15x15 cm cube moulds for 24h in humidity chamber at 20 °C with relative humidity of 95 %. After 24h, the samples were demoulded and stored in water at 20 °C in humidity chamber for 28 days. After 28 days of curing in water, the cubes were removed from the water and placed in an air-drying environment in the laboratory (18 °C to 25 °C and 50 % to 65 % relative humidity) for 14 days. After 42 days of curing, the samples were placed in carbonation chamber with a carbon dioxide concentration of  $3.0 \pm 0.5$  %, a temperature of  $20 \pm 2$  °C and a relative humidity of  $57 \pm 3$  % for 7 and 28 days. After each exposure time, the samples were split in half and sprayed with phenolphthalein to measure the depth of carbonation.

### 2.2.10 Gas permeability

The gas permeability measurement was carried out according to EN 993-4:2008 [53]. The gas permeability of the mortar was tested on cylinder samples,  $\phi 100/50$  mm. The test is carried out by placing the sample in the test cell and placing the plates below and above. Nitrogen is released into the system at a pressure of 5 bar. The pressure regulator on the device applies pressure to the sample cell and is tested at three different pressures of 2, 2.5 and 3 bar. For each individual pressure, the travel time of the soap bubble is measured for an arbitrary measuring volume with a minimum travel time of 20 s and a maximum travel time of 60 s. Three measurements are taken for each pressure and each volume and the mean value of these measurements is taken.

### 2.2.11 Chloride migration

The chloride migration coefficient measurement was carried out according to NT BUILD 492 [54]. Samples 28 days and 56 days old were used. An external electrical potential is applied axially across the sample and forces chloride ions to migrate into the sample from the outside. After a certain test duration, the sample is split axially, and a silver nitrate solution is sprayed onto one of the freshly split sections. The chloride penetration depth is measured by the visible white silver chloride precipitation, after which the chloride migration coefficient is calculated from penetration depth. Table 2.2 shows the resistance of concrete according to the migration coefficient values.

*Table 2.2 The resistance of concrete according to chloride migration coefficient values*

<b>Chloride migration coefficient (<math>m^2/s</math>)</b>	<b>Concrete resistance</b>
$< 2 \times 10^{-12}$	Very good
$2 \times 10^{-12} - 8 \times 10^{-12}$	Good
$8 \times 10^{-12} - 16 \times 10^{-12}$	Satisfactory
$> 16 \times 10^{-12}$	Unsatisfactory

### 2.2.12 Chloride diffusion

Chloride diffusion was tested according to NT BUILD 443 [55]. Cylindrical samples ( $\phi 10/h 20$  cm) were prepared for measurements of chloride resistance of the CAC. After 28 days of curing, the samples were divided into three 5 cm long samples. Before exposure to the NaCl solution, the samples were preconditioned in a  $Ca(OH)_2$  solution for minimum of 18 hours. After preconditioning samples were coated with epoxy on all sides except the side to be exposed to chlorides. When the coating has hardened (after 24 hours), the samples were immersed in 16.5 % NaCl solution for 35 days. After the defined exposure, a profile grinding was performed according to the standard. The samples were ground at 2, 4, 6.5, 10, 14, 18,

and 22 mm depth. The obtained powder was then tested for chemical analysis. The chloride content was determined by using titration method according to standard EN 14629-2007.

### 2.2.13 Water permeability

The water permeability measurement was carried out on cube samples according to HRN EN 12390-8 [56]. Three samples were tested for each mixture after 28 days of curing. The water is injected from below, and the tightness is ensured by a rubber seal. After  $72 \pm 2$  hours, the sample should be split in half. After dividing the sample, the penetration of water through the sample is marked with a marker and the depth is measured in millimetres. The maximum water penetration is noted. Table 2.3 lists the limiting values for different quality classes of concrete based on water permeability. These limiting values are proposed in the Croatian national standard HRN 1128 [57], which is a national annex to the standard EN 206-1.

*Table 2.3 Limiting water permeability values for different quality classes of concrete*

<b>Water permeability classes</b>	<b>Maximum water penetration allowed (mm)</b>
VDP1	50
VDP2	30
VDP3	15

### 2.2.14 Freezing and thawing with de-icing salts

The freezing and thawing measurements were carried out according to HRN CEN/TS 12390-9 [58]. Freezing and thawing was tested after  $7 \pm 1$  cycles,  $14 \pm 1$  cycles,  $28 \pm 1$  cycles,  $42 \pm 1$  cycles, and  $56 \pm 1$  cycles. After each cycle, the material is scaled off the sample surface and its mass is measured. The mean value and the individual values for each sample after 56 cycles are used for the evaluation of the scaling resistance. According to the Croatian national standard HRN 1128 for exposure class XF4, the restriction is that after 56 cycles the average mass loss  $\Delta m_{\text{mean}} < 0.5 \text{ kg/m}^2$  and the individual mass loss  $\Delta m < 1 \text{ kg/m}^2$ .

### 2.2.15 Sulphate resistivity

The sulphate resistivity was tested according to ASTM 1012 [59]. The prism (4x4x16 cm) samples were exposed to a 5% Na<sub>2</sub>SO<sub>4</sub> solution for 13 weeks. After each exposure time, the mass change and compressive strength of the samples was tested. The solution in which the samples were immersed was changed every 4 weeks. The samples were tested after 1, 2, 3, 4, 8, and 13 weeks.

### 2.2.16 Acid resistance

The acid resistance was tested according to ASTM 1012[59], and according to Khan et. al., “Durability of calcium aluminate and sulphate resistant Portland cement-based mortars in aggressive sewer environment and sulphuric acid” [22]. The prism (4x4x16 cm) samples were immersed in 1.5% H<sub>2</sub>SO<sub>4</sub>. After each exposure time, the mass change and compressive strength of the samples were tested. The solution in which the samples were immersed was changed every 4 weeks. The samples were tested after 1, 2, 3, 4, 8, and 13 weeks.

## Chapter 3 Impact of slag and calcined clay on CAC properties

### 3.1 Introduction

The cement industry faces the global challenge of reducing emission of CO<sub>2</sub> during production, while maintaining equal technical requirements and price of the final products [60]. To reduce emissions, the greatest emphasis is on reducing the ratio of clinker within cement and cement within concrete and on developing innovative cement production technologies [61]. Supplementary cementitious materials (SCMs) are increasingly used in the OPC industry as a substitute for part of the cement [62]. However, their use in other specialty cements, such as CAC, is not yet fully developed [63]. CAC is used for special applications where improved resistance to aggressive environments is required, such as rapid repairs, sewers, industrial floors, etc. [6] which means that the niche market and annual production is significantly smaller compared to OPC. Nevertheless, the production of CAC still contributes to environmental pollution and opportunities are needed to reduce the environmental impact [7].

Specificity of CAC cement is that depending on the temperature and humidity of the environment, it undergoes a conversion process that consequently leads to a decrease in strength [4]. At the beginning of hydration the main phase of CAC cement, monocalcium aluminate (CA), reacts with water and forms metastable CAH<sub>10</sub> and C<sub>2</sub>AH<sub>8</sub> hydrates [8]. The hexagonal phases of the metastable hydrates provide high early compressive strength. At temperatures up to 15°C, the first phase to form is metastable CAH<sub>10</sub>. At temperatures above 30°C, the first phase to form is metastable C<sub>2</sub>AH<sub>8</sub>, while at temperatures between 15°C and 30°C, both forms of metastable hydrates and AH<sub>3</sub> hydrate form [7]. The metastable hydration

products will over time transform to stable  $C_3AH_6$  and  $AH_3$  hydrates, in a process known as conversion. The conversion process is accelerated when the temperature exceed  $30^\circ C$  and the rapid formation of stable  $C_3AH_6$  and  $AH_3$  occurs [10]. The precipitation of metastable to stable hydrates with cubic phases changes the porosity of the cement matrix and causes a decrease in compressive strength [12]. Several previous studies [5][21] have confirmed that the conversion process can be mitigated by the use of Ground granulated blast furnace slag (GGBFS). The reaction of silica in the slag with CAC hydrates leads to the formation of the stable phase strätlingite ( $C_2ASH_8$ ). By the formation of strätlingite, the conversion process rate can be decreased, since the formation of metastable  $C_2AH_8$  hydrate is reduced. The formation of strätlingite stabilizes the compressive strength regardless of the curing temperature. Despite all the advantages obtained by using slag as a partial replacement of CAC, certain challenges of slag utilisation in cement industry exist. More than 90% of the available slag is already used in the production of cement or as addition to cement-based mixtures [61]. Furthermore, the availability of slag does not follow the trend of global cement production. Moreover, the largest growth of the cement industry is expected in developing countries, and slag is mainly available in industrialized countries [64]. Therefore, it is necessary to find other alternative materials that are available in sufficient quantities and at the same time suitable for use in CAC. In the case of OPC, calcined clay (CC) in combination with limestone (LC3) emerged as a possible solution for reducing environmental footprint of cement without jeopardizing mechanical properties and durability of OPC [65][66][67][68]. As calcined clay is rich in  $SiO_2$ , the question remains whether calcined clay could be a promising material for use in combination with CAC.

The main objective of this study is to understand the influence of slag and calcined clay on the mechanical properties and durability of calcium aluminate cement. In the first phase, the influence of slag was investigated. Six slags of different origins were compared based on fresh and mechanical properties of calcium aluminate cement-based mortar. Based on the results, one slag was selected for further investigation of the conversion process of CAC mortar and the durability of CAC concrete. In the second phase, the possibility of replacing part of CAC with calcined clay was investigated. Two clays of different origins were compared and one clay was selected for further testing of the conversion process.

## **3.2 Impact of slag**

### 3.2.1 Optimisation of laboratory milling

Five of the slags were obtained in grains ( $d_{50}=0,66$  to  $1,2$  mm) of different sizes (Figure 2.1) and one slag was industrially milled (slag S6). The reactivity of slags is strongly dependent on the particle size. Therefore, prior to the experimental investigation, it was important to define a protocol for the laboratory milling of slags in grains to ensure a fair comparison between different slags. In order to investigate the optimum milling time to obtain a similar particle size for all the slags studied, the slags S3 and S4 were selected for comparison. Slags were milled in laboratory disk mill. Prior to milling, the slags were dried in an oven at a temperature of  $105$  °C until a constant weight was reached. The slags were milled for 30 s, 90 s, 3 min and 5 min. The results of the air jet sieving are shown in Figure 3.1. The results show that the same time of milling leads to the same fineness of the slag, regardless of the initial particle (grain) size. Furthermore,  $d_{50}$  decreases with increasing milling time. The results show the finest particle size distribution of the dry slag samples when the milling time is increased to 5 minutes. Also, compared with industrially milled slag S6, the slags milled



for 5 minutes show the most similar particle size distribution. From this, it was concluded that the optimum grinding time is 5 minutes.

The air jet sieving particle size distribution for all slags in grains milled for 5 minutes in a disc mill is shown in Figure 3.2. The results show a similar particle size distribution for the studied slags,  $d_{50}$  is in the range of 32 to 39  $\mu\text{m}$ , confirming that 5 minutes of milling is an optimal time, regardless of the initial particle (grain) size of the slags. Additionally, the particle size distribution of the slags was analysed by laser diffraction at Calucem company. The results are shown in Figure 3.3. Both methods show a similar particle size distribution with the exception of quartz which was milled for 10 minutes.

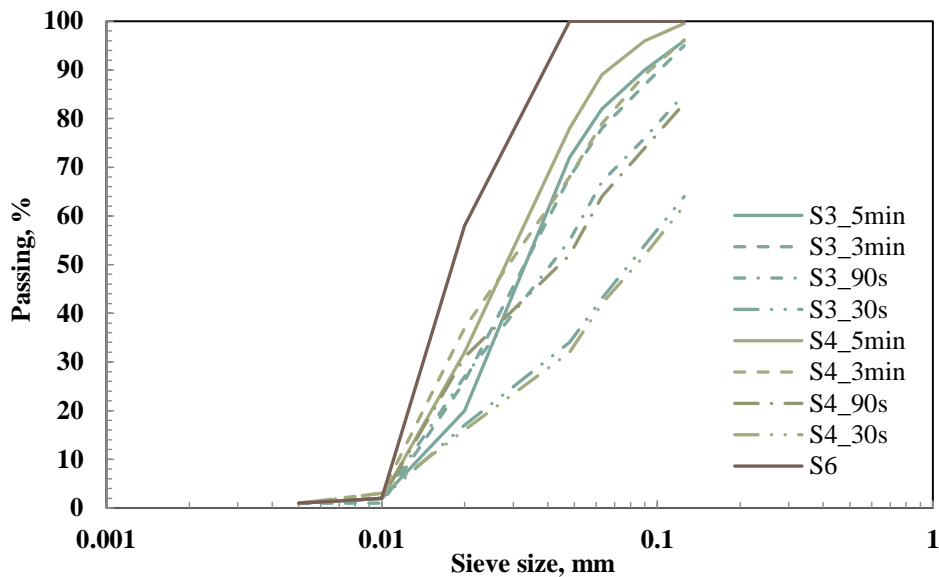


Figure 3.1 Particle size distribution-air jet sieving for different time of milling

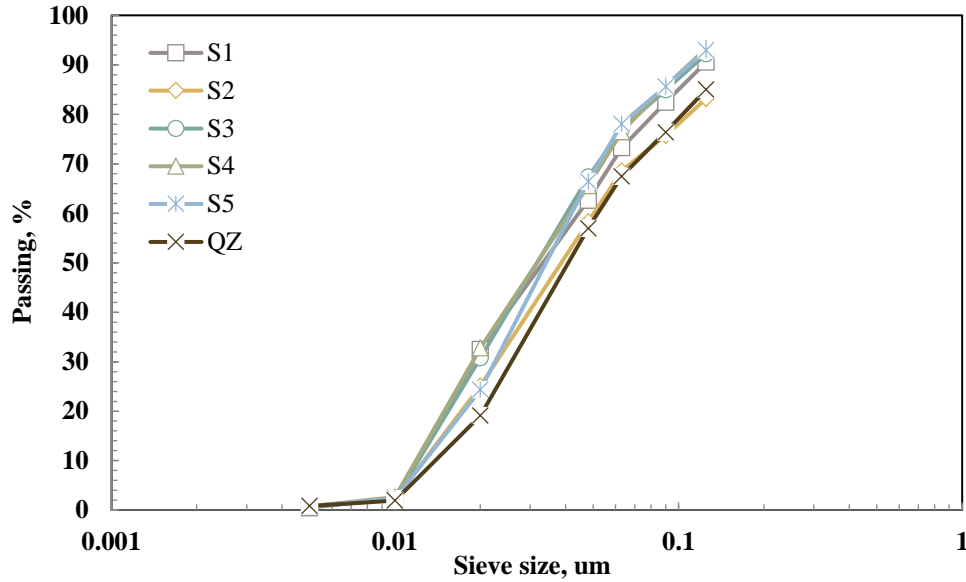


Figure 3.2 Particle size distribution - air jet sieving

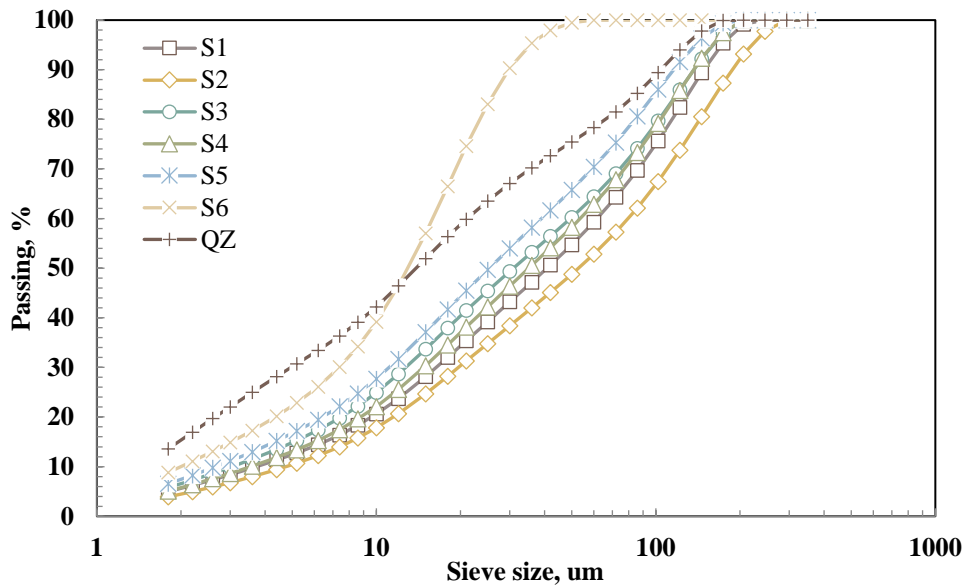


Figure 3.3 Particle size distribution - laser diffraction

The Blaine size values of  $d_{10}$ ,  $d_{50}$  and  $d_{90}$  for slag and quartz are listed in Table 3.1. The Blaine sizes are compared with the Blaine sizes of CAC used in this research. It can be observed that the industrially milled slag (S6) has the finest particle size distribution compared to then other slags, but also compared to cement and quartz. Furthermore, then slag S4 has the coarsest particles, and the lowest Blaine size.

Table 3.1 Comparison of Blaine,  $d_{10}$ ,  $d_{50}$  and  $d_{90}$ 

	<b>Blaine (cm<sup>2</sup>/g)</b>	<b>d<sub>10</sub> (µm)</b>	<b>d<sub>50</sub> (µm)</b>	<b>d<sub>90</sub> (µm)</b>
<b>CAC</b>	4000	1,9	14	49
<b>S1</b>	2076	3,6	41	160
<b>S2</b>	2178	3,6	36	145
<b>S3</b>	2407	3	31	145
<b>S4</b>	1768	4,9	52	190
<b>S5</b>	2668	2,6	26	125
<b>S6</b>	3715	2,1	12	29
<b>QZ</b>	2800	0	15	110

### 3.2.2 Impact of slag on calcium aluminate cement-based mortar

For the investigation of the influence of slag on the properties of CAC mortar, 8 mixtures were prepared, one reference mixture with 100% CAC, 6 mixtures with a CAC replacement of 30 % slag and one mixture with a CAC replacement of 30 % with inert material – quartz. The mixtures were prepared according to EN 14647 standard. The mortar mixtures were prepared using 500 g binder (CAC and/or slag), 200 g water and 1350 g silicious CEN standard sand. The water to binder ratio was kept constant for all mixtures – 0.4.

#### *Fresh properties*

To evaluate the effects of the different slags on the fresh properties, the workability, temperature and the initial and final setting times were determined. The results of the workability and temperature of the fresh mortar are shown in Figure 3.4. The results of the workability and temperature of the fresh mortar show that the 30 % replacement of CAC with slag improves the workability of the fresh mortar and has no effect on the temperature.

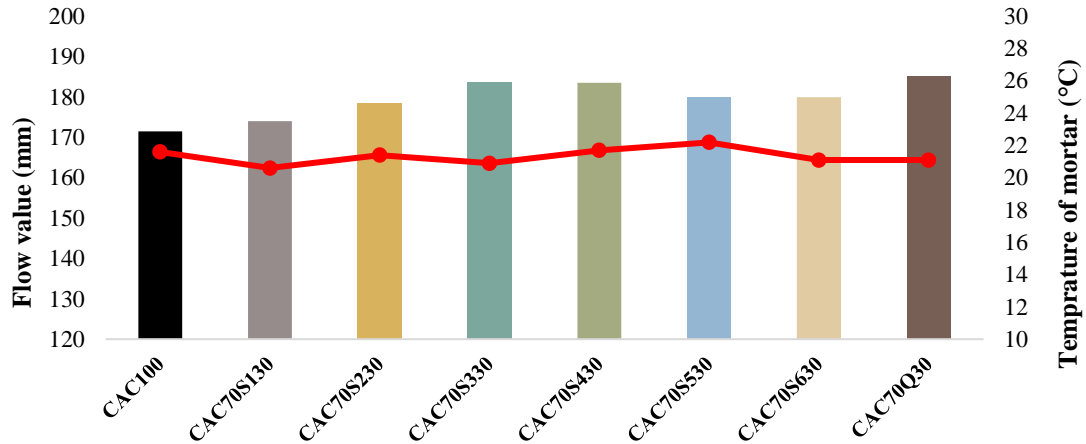


Figure 3.4 Flow value and temperature of fresh mortar

According to EN 14647, the setting time should not be less than 90 minutes. The results of the initial and final setting time, shown in Figure 3.5, indicate that all mixtures meet the requirements of the standard. Moreover, all mixtures with 30% slag replacement have prolonged setting time, with the exception of the mixture with S1 slag.

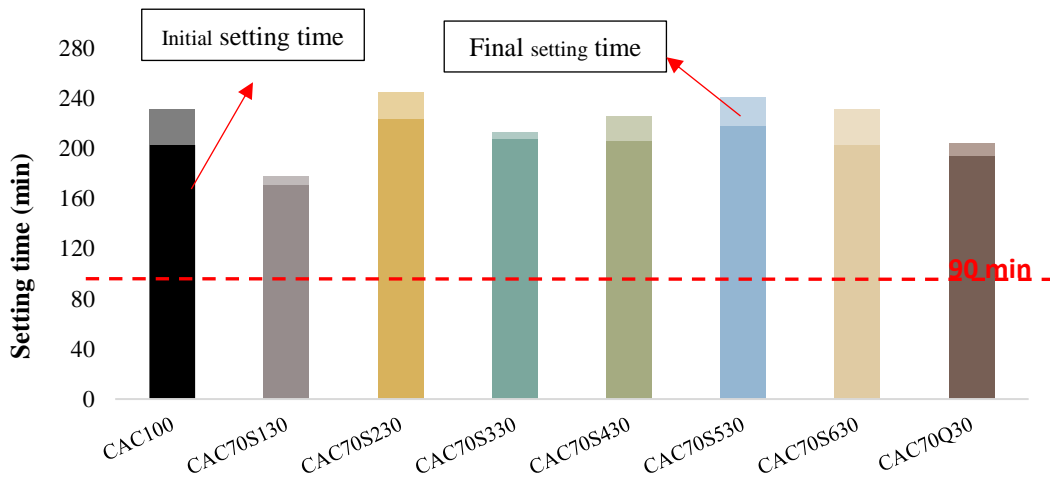


Figure 3.5 Initial and final setting time of fresh mortar

### Compressive strength

The effect of cement replacement by slag on the development of compressive strength was also investigated. The compressive strength measurements were carried out on the mortar samples after 6 hours, 24 hours, 7 days and 28 days. The results of the compressive strength

test are shown in Figure 3.6 and the results of the compressive strength relative to the pure CAC mix are shown in Figure 3.7. The results show that the tested mixtures developed between 31.3% (for CAC70S330) and 61.7% (for CAC100) of their 28-day compressive strength at 6 hours, while after 24 hours the compressive strength development was between 65.5% (for CAC70S130) and 81.6 % (for CAC70QZ30). Furthermore, the development of compressive strength after 7 days ranged from 79.0 % (for CAC70S130) to 94.35 % (for CAC70QZ30) of its 28-day compressive strength. Compared to the reference mix CAC100, the replacement of CAC with slag reduced the compressive strength by 30-50% after 6 hours. After 24 hours, the slag started to contribute to the development of compressive strength and a negligible difference in compressive strength (less than 8 %) was observed compared to the reference mix CAC. In addition, mixtures with 30 % alumina replaced by slag showed a slightly higher compressive strength after 7 days than mixtures with 100 % CAC. After 28 days, the compressive strength values of the tested mixtures were between 92.66 MPa (for CAC70S530) and 106.89 MPa (for CAC100). For these mixtures, it can be observed that the replacement of CAC with 30% slag had no influence on the compressive strength after 28 days. Mixtures with S1, S3, S4 and S6 slag have an even higher compressive strength compared to the reference mixture. Mixtures with a 30% replacement of CAC by quartz show the same compressive strength as the reference mixture after 28 days of curing. The results show that a 30% replacement of CAC with slag can provide higher compressive strength for later ages ( $\geq 24$ h), while the compressive strength decreases at early ages ( $< 24$ h).

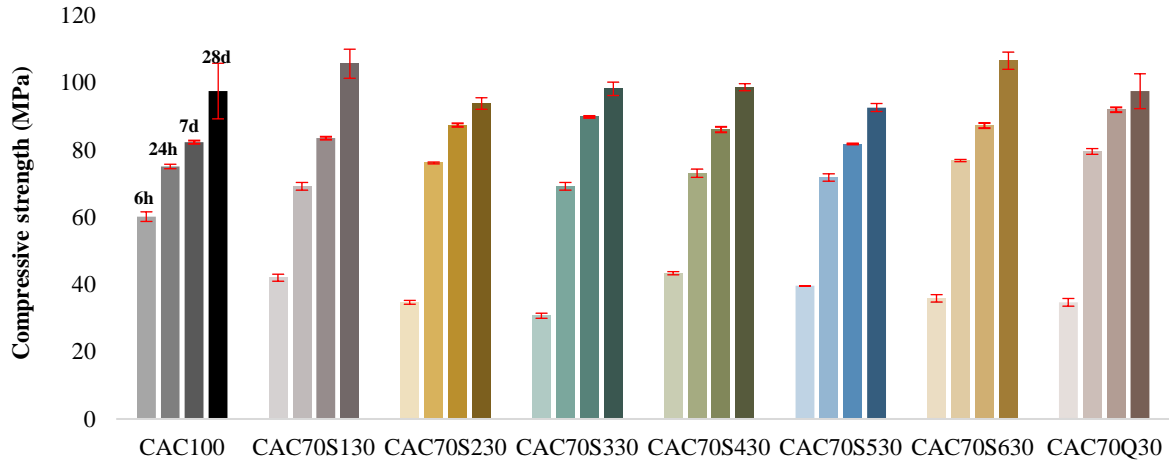


Figure 3.6 Compressive strength of mortars of the following ages: 6 hours, 24 hours, 7 days and 28 days

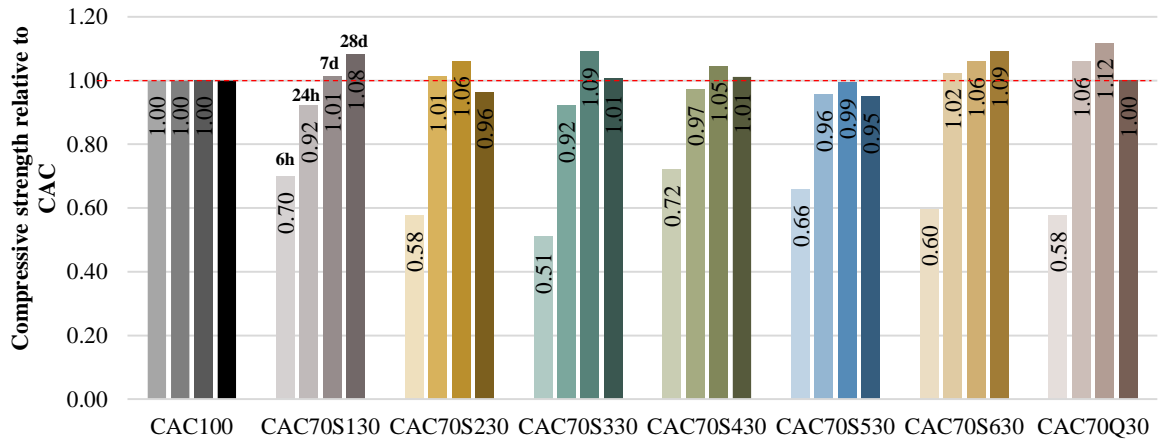


Figure 3.7 Relative compressive strength of mortars of the following ages: 6 hours, 24 hours, 7 days and 28 days

### 3.2.3 Impact of slag on conversion process of calcium aluminate cement

Based on the initial tests of six different slags and their influence on the compressive strength of CAC mortar, one slag was selected for further investigation of the conversion process. Slag S1 was selected for further testing of the conversion process and microstructural changes due to most optimal development of compressive strength and regional availability.

A special calcium aluminate cement with 52.67%  $\text{Al}_2\text{O}_3$  produced by the Calucem company in Pula, Croatia, was used. The slag S1 used in this study was obtained industrially milled with a Blaine size of  $4580 \text{ cm}^2/\text{g}$ , while the Blaine size of CAC was  $4570 \text{ cm}^2/\text{g}$ . The particle

size distribution of CAC cement and S1 slag obtained by laser diffraction is shown in Figure 3.8.

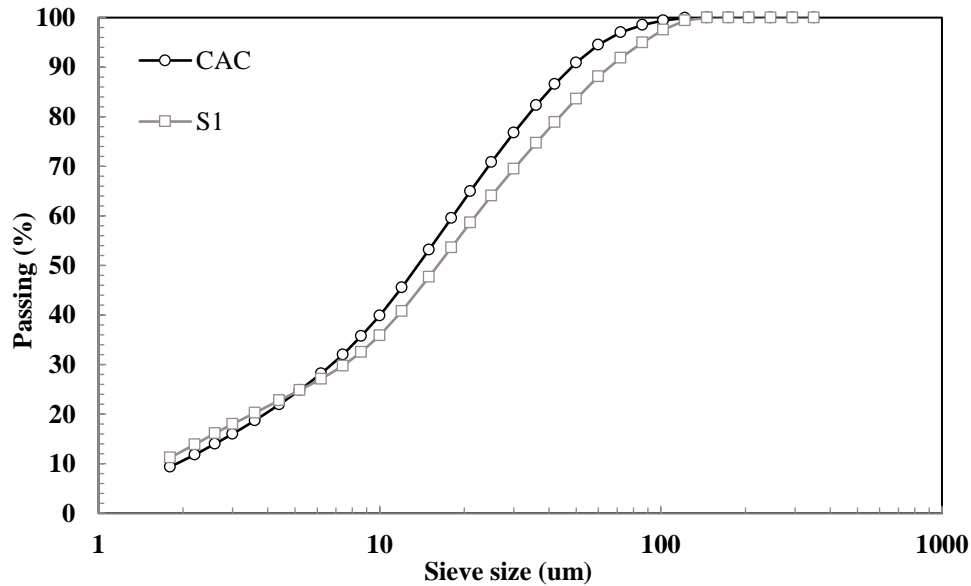


Figure 3.8 Particle size distribution of CAC cement and slag S1

To access conversion process of CAC , two different mixtures were prepared. A one reference mixture (labelled CAC100) and a mixture with 30 % replacement of CAC by slag (labelled CAC70S130). The replacement level of 30% was used to ensure that any changes induced by the addition of SCM are visible in mechanical properties and microstructure. The mixtures were prepared according to EN 14647. The mortar mixtures were prepared from 500 g binder (CAC and/or slag), 200 g water and 1350 g silicious CEN standard sand. The water to cement ratio was kept constant for all mixtures – 0.4. The conversion process is highly dependent on the temperature and relative humidity of the environment. Therefore, the laboratory and all components were conditioned to 20 °C before casting to prevent temperature from influencing the early hydration of CAC. For the first 24 hours, the samples were covered and stored in a humidity chamber at 20 °C and 95% relative humidity. After 24 hours, the samples were demoulded. To access conversion process one group of samples

was cured in a water bath at 20 °C and one group in a water bath at 38 °C. Compressive strength, thermogravimetric analysis (TGA), and mercury intrusion porosimetry (MIP) were tested to evaluate effect of slag on the inhibition of the conversion process.

### *Compressive strength*

The development of compressive strength over 56 days for samples cured at 20°C and 38°C is shown in Figure 3.9 a) and b), respectively. When cured at 20°C, the mixture with slag exhibits a comparable compressive strength to the reference mixture despite the reduction of CAC by 30%. Furthermore, both mixtures showed an increase in compressive strength during 56 days of curing at 20°C. After curing at 38°C, the compressive strength of the reference CAC mix started to decrease after five days, indicating the occurrence of the conversion process. By prolonged curing, the conversion process rate i.e. the precipitation of metastable hydrates into stable hydrates started to increase, and compressive strength started to decrease. After 28 days of curing, the lowest compressive strength was reached, implying that the conversion process is completed and there are no more metastable hydrates that could transform into stable hydrates. In contrast, once cured at 38°C, mix with slag exhibited an increase in compressive strength during 7-day curing. After the 7<sup>th</sup> day of curing at 38°C, this mixture showed a slight decrease in compressive strength, but by the end of the test (56 days), the compressive strength value increased again and is equal to the compressive strength after 7 days of curing. This slight decrease in compressive strength indicates that a conversion process also occurred in system with slag, but in smaller rate than for reference mix.



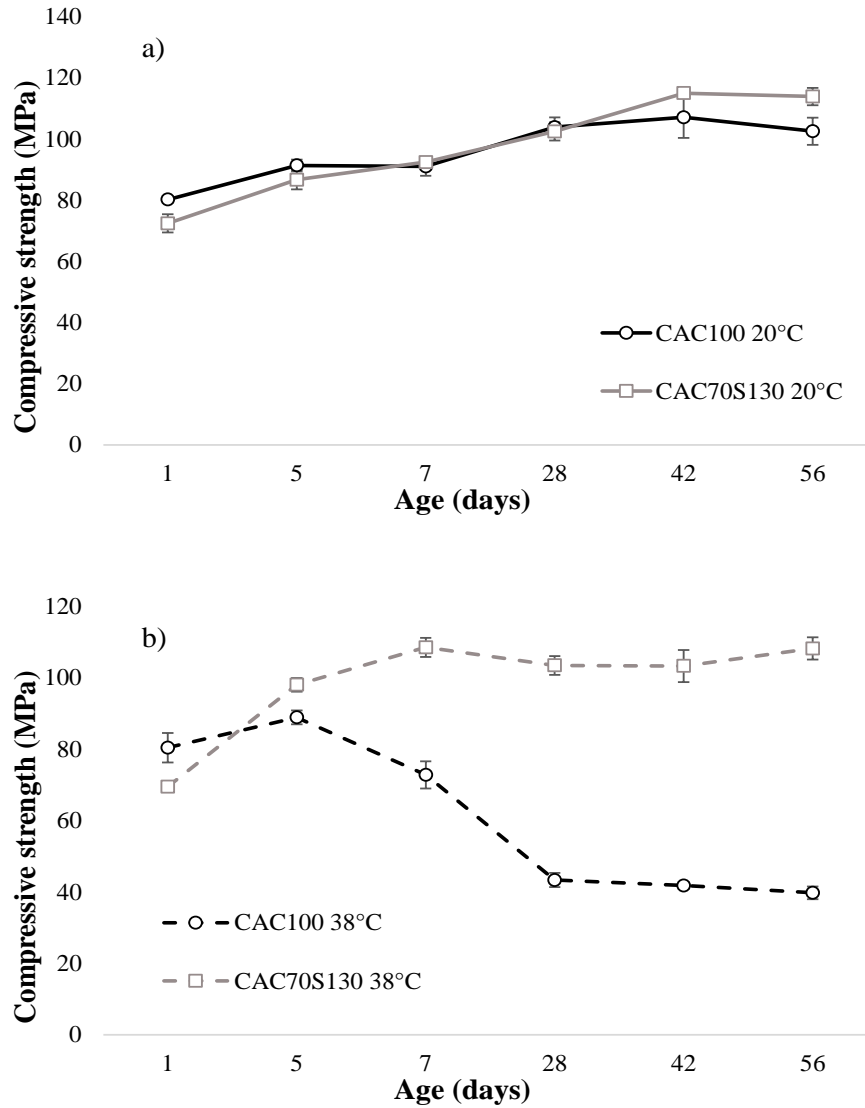


Figure 3.9 Development of compressive strength over 56 days for samples cured at: a) 20°C, b) 38°C

### Thermogravimetric analysis

Thermogravimetric analysis was performed on samples cured at 20°C and 38°C for 28 days. The derivatives of the mass loss curve obtained are shown in Figure 3.10. The DTG curves show that hydrate formation occurs in a similar temperature range for all samples. The decomposition of the metastable hydrate  $\text{CAH}_{10}$  was observed in the temperature range of 40-80 °C, the decomposition of  $\text{C}_2\text{HA}_8$  at 70-130 °C. The formation of the stable hydrate  $\text{C}_3\text{AH}_6$  was observed between 230°C and 300°C, the formation of the  $\text{AH}_3$  hydrate in the

temperature range of 170-230 °C. The decomposition of strätlingite in samples with slag and calcined clay was visible from 140°C to 190°C.

After 28 days of curing CAC100 mix at 20°C (Figure 3.10a) metastable hydrates ( $\text{CAH}_{10}$  and  $\text{C}_2\text{AH}_8$ ) and stable hydrate hydrogarnet ( $\text{C}_3\text{AH}_6$ ) as well as  $\text{AH}_3$  hydrate were detected. For the same mixture cured at 38°C significantly lower peaks of metastable hydrates and significantly higher peak for stable hydrate hydrogarnet were detected. Moreover, it was not possible to distinguish between hydrogarnet and  $\text{AH}_3$  hydrates, as only a one broad peak was observed at around 230°C. The formation of stable hydrate with higher intensity during curing at 38°C confirmed that a conversion process occurred, which was observed as compressive strength decrease, Figure 3.9b. For the sample with 30% replacement of CAC by slag (Figure 3.10b) metastable and stable hydrates were also observed after 28 days of curing at 20°C and 38°C. In both curing regimes, the formation of a new peak, referred to as strätlingite hydrate ( $\text{C}_2\text{ASH}_8$ ), was observed [69]. The intensity of the peaks for metastable hydrates and strätlingite hydrate was very similar regardless of the curing temperature, but hydrogarnet and  $\text{AH}_3$  hydrate had a higher peak intensity when cured at 38°C.

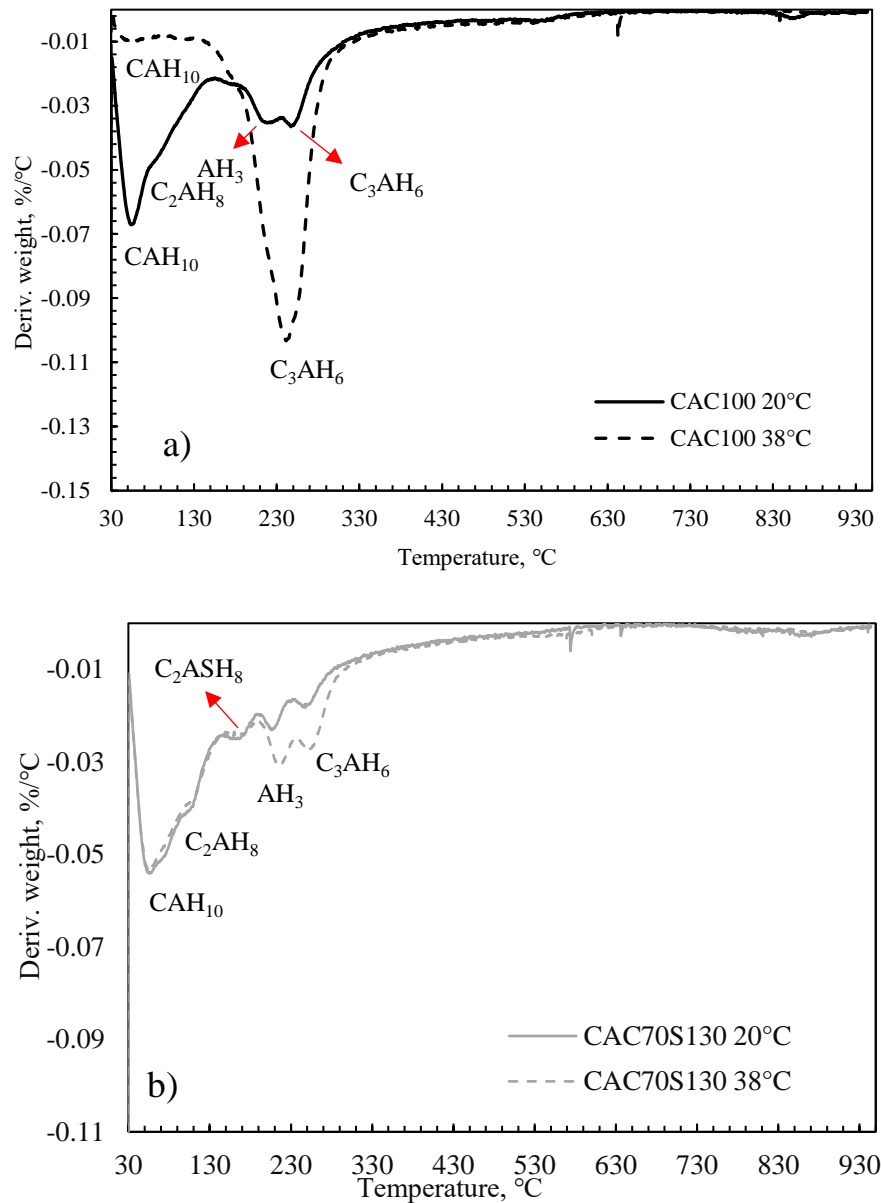


Figure 3.10 DTG for mixes cured at 20°C and 38°C after 28 days: a) CAC100, b) CAC70S130

### X-ray diffraction

Phase composition was also assessed by XRD testing. XRD was performed for all samples after 56 days of curing at 20°C and 38°C. The results are shown in Figure 3.11. The analysis was performed on mortar samples containing siliceous standard sand. Therefore, the peaks of quartz in the XRD analysis results were with greater intensity compared to the peaks of hydrates found in CAC. In the reference sample cured at 20°C (Figure 3.11a), metastable

CAH<sub>10</sub> hydrate was detected (at a diffraction angle between 5 and 15 degrees), as well as stable C<sub>3</sub>AH<sub>6</sub> and AH<sub>3</sub> hydrate. When the same mixture was cured at 38°C, a lower peak intensity was observed for metastable hydrates and a higher peak intensity for the two stable phases (C<sub>3</sub>AH<sub>6</sub> and AH<sub>3</sub>). For the sample with slag (Figure 3.11b), strätlingite hydrate was detected at both curing temperatures. Curing at 20°C showed a higher peak intensity for metastable CAH<sub>10</sub> hydrate and a lower peak intensity for stable hydrates. However, when cured at 38°C, a lower peak was detected for metastable hydrates and a higher peak for stable hydrates, indicating that a conversion process occurred in the sample with slag after 56 days of curing at 38°C.

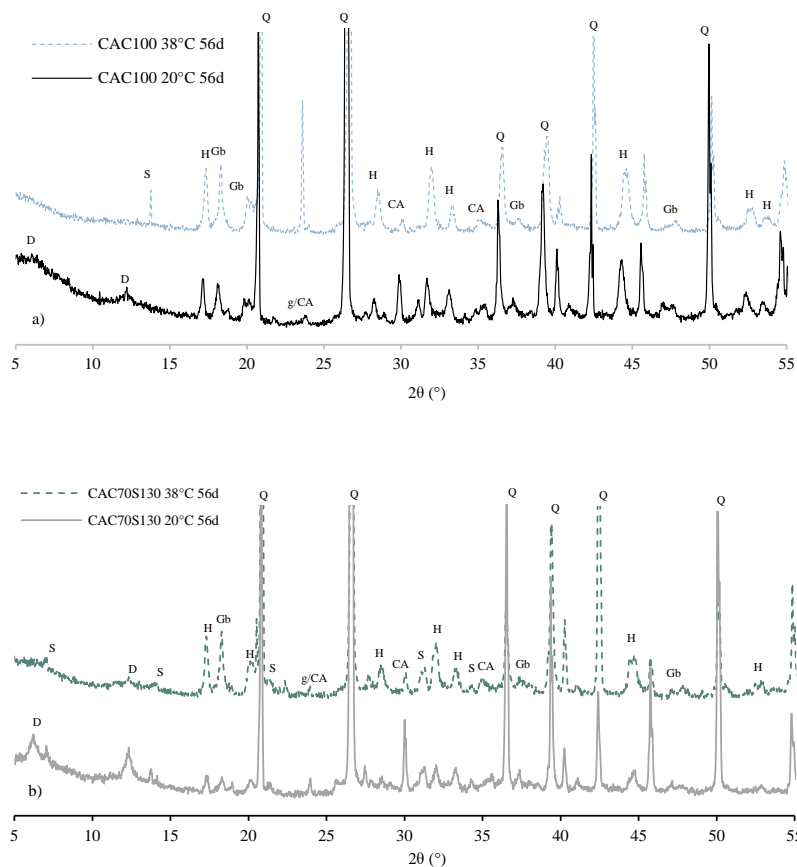


Figure 3.11 Diffractogram for samples cured 56 days at 20°C and 38°C: a) CAC100, b) CAC70S130 (CA=monocalcium aluminate, D=CAH<sub>10</sub>, Gb=AH<sub>3</sub>, G=Gehlenite, H=C<sub>3</sub>AH<sub>6</sub>, O=C<sub>2</sub>AH<sub>8</sub>, S=strätlingite Q=quartz)

*Mercury intrusion porosimetry*

The results of the total accessible porosity are shown in Figure 3.12. The total porosity represents the total accessible pore volume of the connected pores. The samples were tested after 28 days of curing at 20°C and 38°C. The reference mixture CAC100 showed the highest total porosity regardless of the curing temperature: 12.37% when cured at 20°C, and 12.23% when cured at 38°C. The mixture with slag had a lower total porosity compared to the reference mix, namely 8.19% for curing at 20°C and 8.34% for 38°C. Therefore, replacement of CAC cement by 30% of slag impacted the reduction of total accessible porosity for around 4%. The pore volume distribution is shown in Figure 3.13. The maximum mercury intrusion was different for each mixture, but the reference mixture cured at 38°C was the most different. For the reference mixture cured at 38°C, the maximum mercury intrusion was between 500 nm and 1500 nm, and for the other mixtures at a much smaller pore entry diameter. The critical pore entry diameter is shown in Figure 3.14. The critical pore entry diameter is the highest peak in the differential intrusion pore volume curve which corresponds to the maximum intrusion volume. The samples cured at 20°C had a lower critical pore entry than the samples cured at 38°C. Furthermore, sample with slag had a lower critical pore entry than the reference sample at both curing regimes.

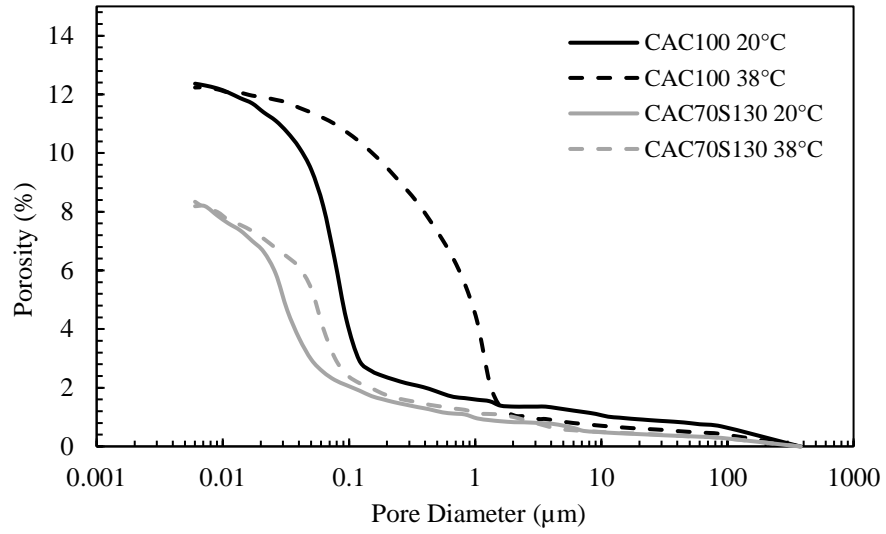


Figure 3.12 Total porosity after 28 days of curing at 20°C and 38°C for CAC100 and CAC70S130 mix

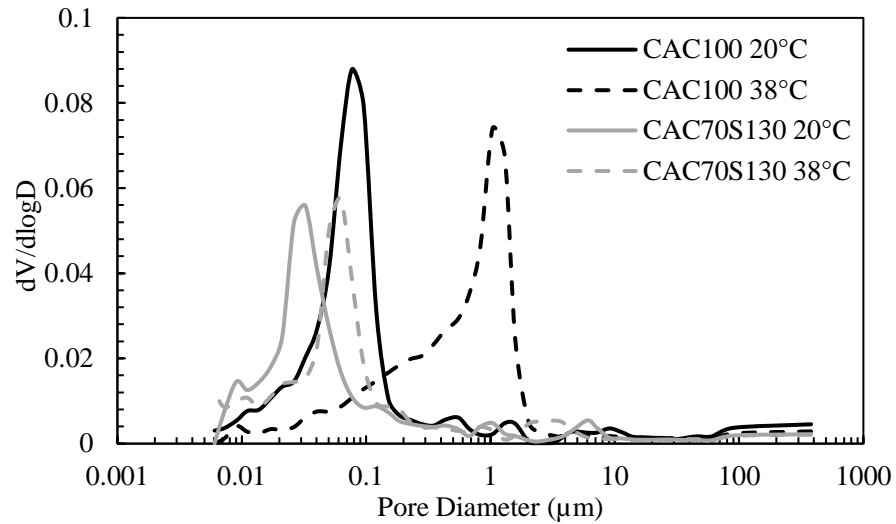


Figure 3.13 Differential intrusion curve after 28 days of curing at 20°C and 38°C for CAC100 and CAC70S130 mix

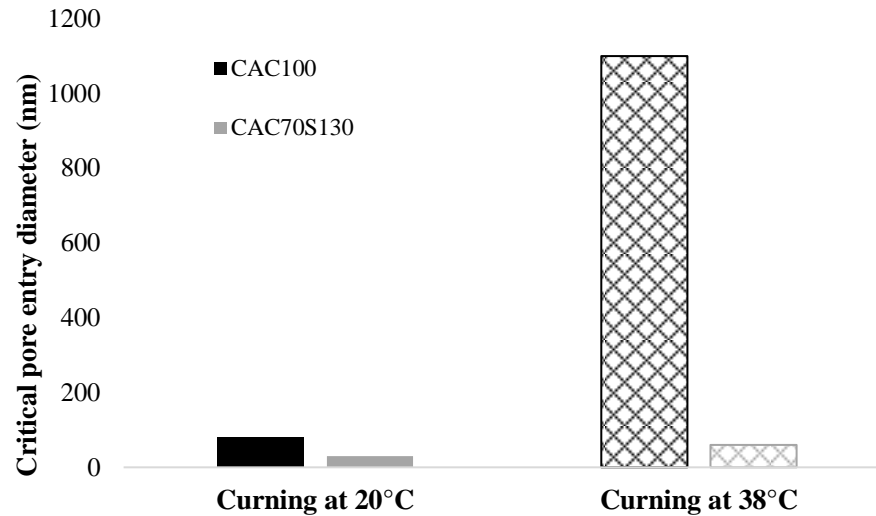


Figure 3.14 Critical pore entry diameter after 28 days of curing at 20°C and 38°C for CAC100 and CAC70S130 mix

### 3.2.4 Impact of slag on basic durability properties of calcium aluminate cement-based concrete

Permeability is one of the most important parameters of concrete, as it defines the resistance of concrete to the penetration of aggressive substances from the environment. To evaluate the changes in durability of CAC cement with and without GGBFS, two concrete mixtures were prepared. A pure CAC mixture (labelled CC100) and one mixture with 30% replacement of CAC cement with slag (labelled CAC70S130). The concrete mixtures were prepared with 420 kg/m<sup>3</sup> CAC, river aggregate and a water to binder ratio of 0.45. The main focus of this part of the research was on the permeability and porosity of the concrete samples. In order to determine the resistance to aggressive substances from the environment, the gas permeability and water permeability, the carbonation resistance and chloride migration as well as freezing and thawing of the concrete with de-icing salts were therefore tested. Additionally, for screening carbonation resistance, microstructure of samples was analysed before and after carbonation.

### Compressive strength

The development of the compressive strength of concrete was analysed for 56 days. The results of the compressive strength measurements are shown in Figure 3.15 and Figure 3.16. It can be seen that the compressive strength of both mixtures increases continuously with prolonged curing. The compressive strength of CAC70S130 mixture after 24 hours and 7 days is 30 % lower compared to the reference mixture. After 28 days and 56 days of curing, the compressive strength of CAC70S130 mixture is 20 % lower than that of CAC100 mixture. It can therefore be concluded that after 28 days of curing slag starts to contribute to the development of compressive strength.

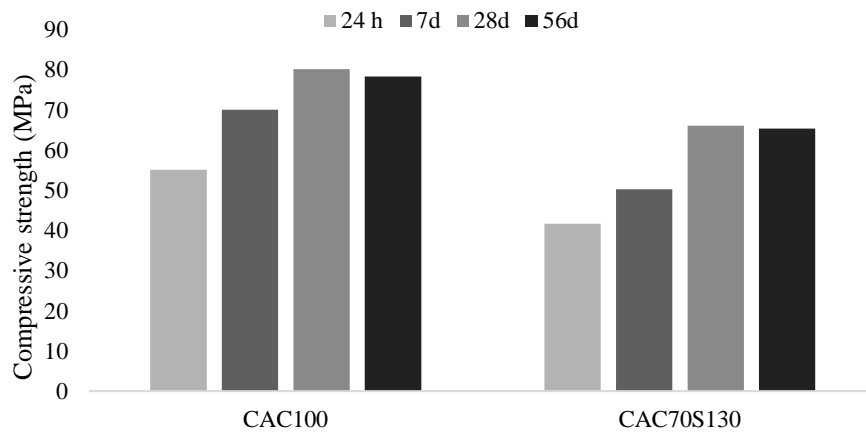


Figure 3.15 Compressive strength of CAC100 and CAC70S130 concrete mix

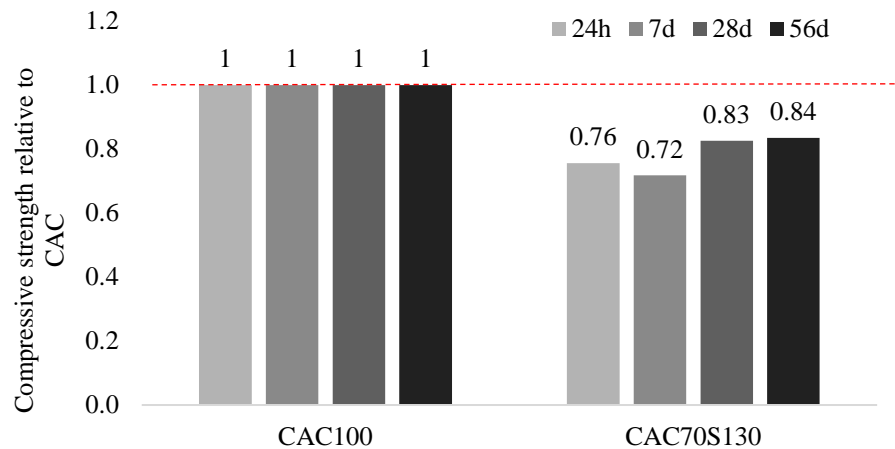


Figure 3.16 Compressive strength relative to CAC100 mix



### *Water permeability*

The results of the water permeability test are shown in Figure 3.17. The measurement was performed according to the standard for OPC (ordinary Portland cement), the Croatian national standard HRN 1128, which is a national annex to standard EN 206-1. The standard defines three quality classes for concrete: a maximum height of water penetration of 50 mm for class 1, 30 mm for class 2, and 15 mm for class 3. It needs to be highlighted that these limiting values are given for OPC and are hereafter used only to reference the values obtained for CAC concrete. The pure CAC mixture, CAC100, has a lower water penetration depth than the mix by 30% replacement of CAC with GGBFS, CAC70S130. However, both mixtures belong to class 2.

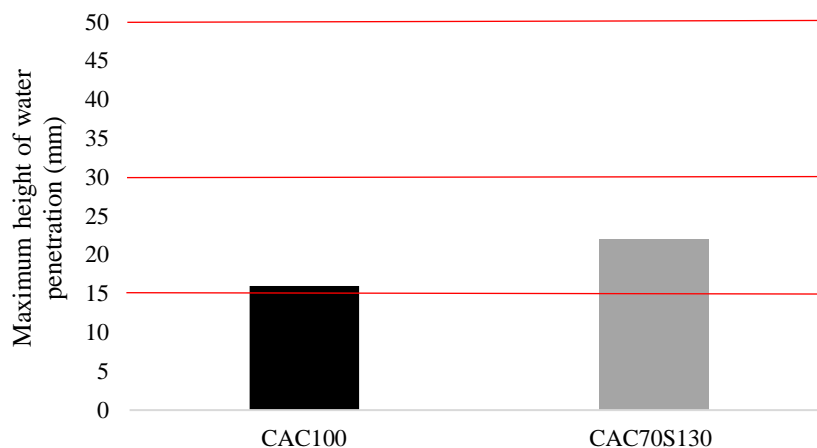


Figure 3.17 Water penetration depth for CAC100 and CAC70S130 mix

### *Gas permeability*

The results of the gas permeability measurements are shown in Figure 3.18. The gas permeability of concrete was also tested according to the standard for OPC. Replacing CAC with 30% GGBFS increases the gas permeability of concrete and thus increases the risk of transport of harmful substances from the environment (e.g. CO<sub>2</sub>, chlorides, sulphates) into the concrete.

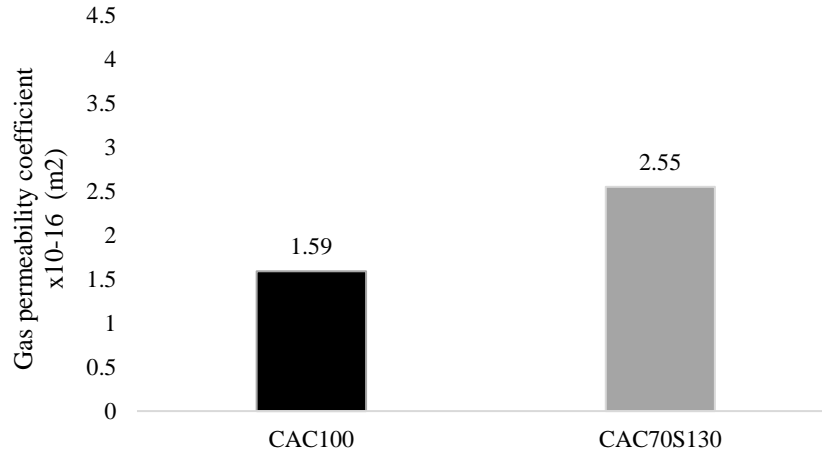


Figure 3.18 Gas permeability coefficient for CAC100 and CAC70S130 mix

### Chloride migration

Samples 28 days and 56 days old were used to investigate the chloride migration coefficient. The results of the chloride migration coefficient for each mixture are shown in Figure 3.19. The usual values for defining OPC concrete quality based on the chloride migration coefficient are listed in Table 2.2. The reference mixture has a lower migration coefficient for both ages of testing compared to mixture with replacement, which means highest resistance to chloride penetration. The replacement of CAC cement with slag reduces the resistance of the concrete to chloride penetration. After 56 days of curing, the coefficient decreases in the case of concrete with slag due to the slow reactivity of the slag.

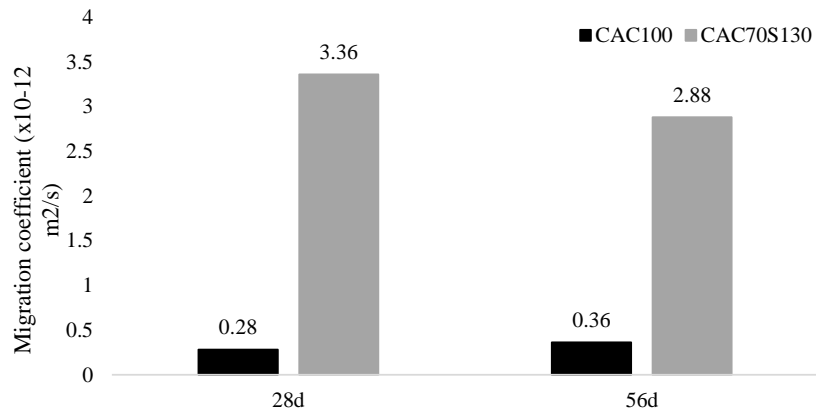


Figure 3.19 Chloride migration coefficient for CAC100 and CAC70S130 mix

### *Freezing and thawing with de-icing slats*

Freezing and thawing with de-icing salts was tested over 56 cycles. The results are shown in Figure 3.20. According to the standard for exposure class XF4, the average weight loss per cycle should be less than 0.5 kg/m<sup>2</sup> and the individual weight loss less than 1 kg/m<sup>2</sup>. Both mixtures did not meet the requirements of the standard. The reference mixture shows a similar behaviour to the classic OPC system without chemical additives. Additionally, the mixture with replacement showed significantly worse behaviour after 7 days compared to reference mixture

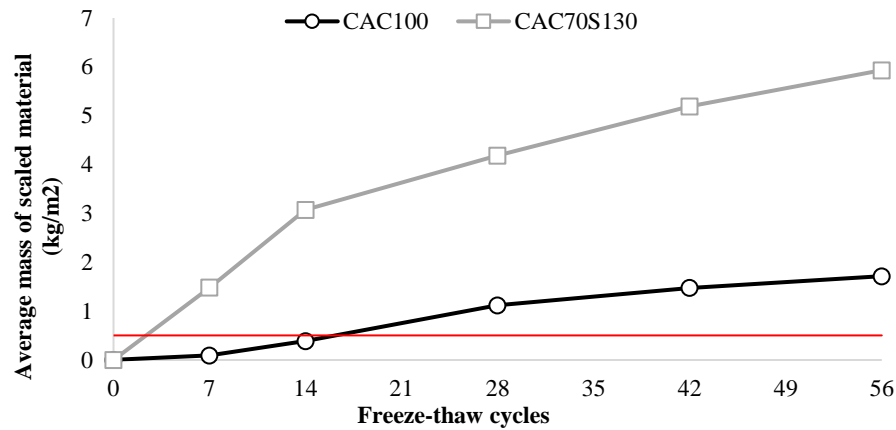


Figure 3.20 Mean value of scaled material per cycle of freezing and thawing

### *Carbonation*

The depth of carbonation was measured after 7 and 28 days of CO<sub>2</sub> exposure. The results of resistance to CO<sub>2</sub> penetration are shown in Figure 3.21. The mixture with replacement by slag showed a slightly faster carbonation rate than the reference mixture on both test days. These results are attributed to the higher gas permeability of the mixture with 30% replacement of CAC by slag. Figure 3.22 shows the samples sprayed with phenolphthalein after 7 days and 28 days of CO<sub>2</sub> exposure. It is noticeable that the CAC70S130 sample shows a higher depth of carbonation after 7 days and after 28 days of exposure.

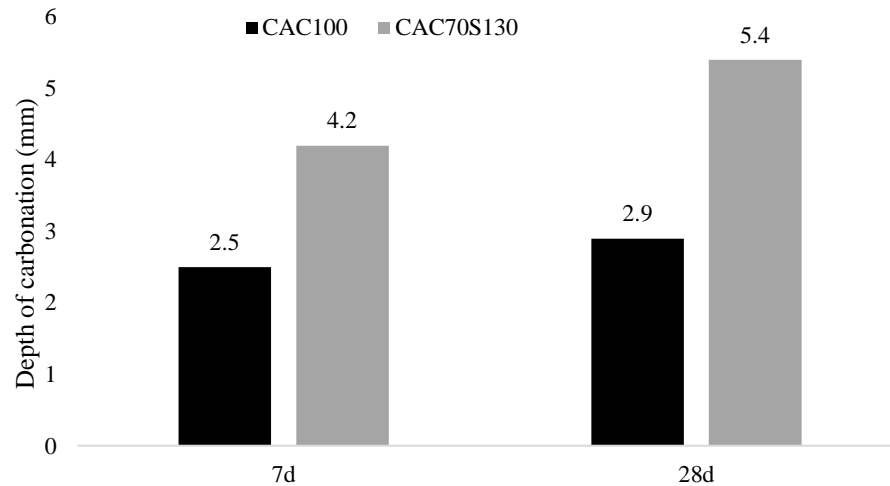


Figure 3.21 Carbonation depth for CAC100 and CAC70S130 mix

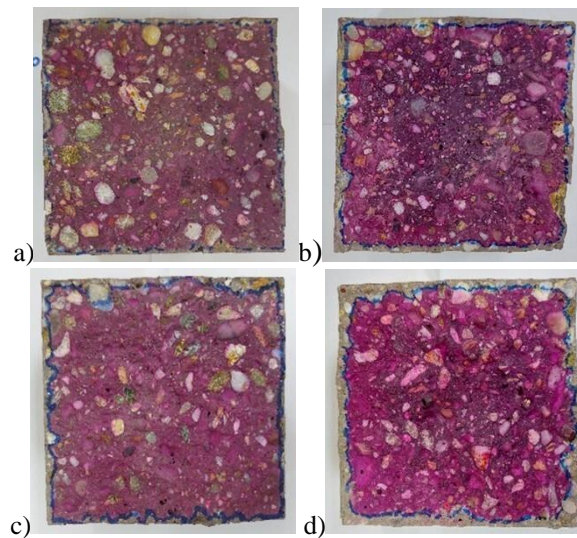


Figure 3.22 Samples sprayed with phenolphthalein after 7 days of carbonation: a) CAC100, b) CAC70S130, and 28 days of carbonation: c) CAC100, d) CAC70S130

### *Microstructural analysis of non-carbonated and carbonated samples*

The Thermogravimetric analysis was tested on non-carbonated and carbonated samples. For this purpose, the powder was extracted from the samples after carbonation. The effects of carbonation on the formation of phases in the cement matrix are shown in Figure 3.23. The carbonation of the pure CAC mixture leads to a decomposition of  $CAH_{10}$  phase into calcium carbonate ( $CaCO_3$ ) and  $AH_3$  gel. With a prolonged carbonation of up to 28 days, a larger amount of the  $CAH_{10}$  phase decomposes. Additionally, with significant decomposition of

CAH<sub>10</sub> phase, decomposition of C<sub>3</sub>AH<sub>6</sub> phase occurs, but the carbonation of that phase is not as significant compared to the carbonation of the CAH<sub>10</sub> phase. Figure 3.23 also shows that the CAH<sub>10</sub> phase decomposes at temperatures below 100 °C, the AH<sub>3</sub> gel and the C<sub>3</sub>AH<sub>6</sub> phase at 230 °C – 280 °C and CaCO<sub>3</sub> at temperatures above 600 °C. The effects of carbonation on the formation of phases for a mixture with a replacement of 30% CAC by slag after 7 and 28 days of carbonation are shown in Figure 3.23b. The metastable phases CAH<sub>10</sub> and C<sub>2</sub>AH<sub>8</sub> carbonate first, followed by strätlingite (C<sub>2</sub>ASH<sub>8</sub>) carbonation. The decomposition of these three phases produces AH<sub>3</sub> gel and CaCO<sub>3</sub>. The formation and decomposition of the C<sub>3</sub>AH<sub>6</sub> phase is similar after 7 and 28 days of carbonation, and the temperatures at which the phases decompose are similar to those of pure CAC cement mixture. The intensity of the peak corresponding to the decomposition of calcium carbonate.

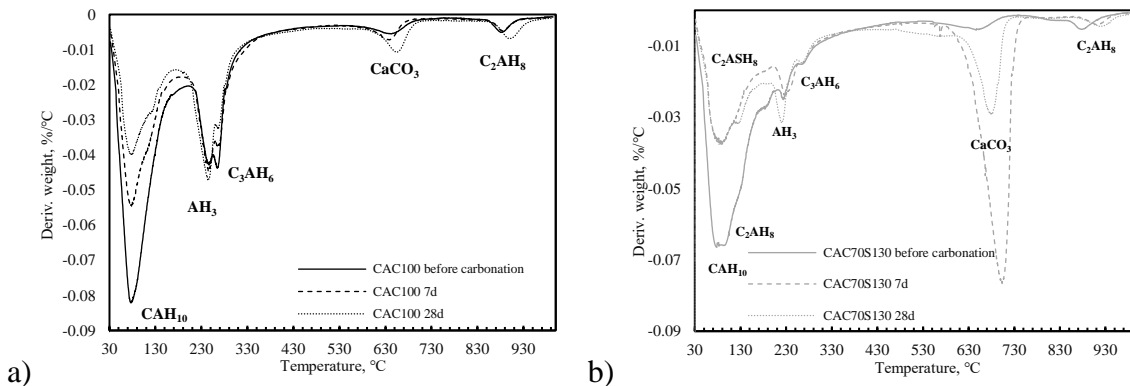


Figure 3.23 dTG curves of non-carbonated and carbonated samples a) CAC100, b) CAC70S130

Mercury intrusion porosimetry was tested on non-carbonated samples and on samples after 7 and 28 days of carbonation. The pore volume distribution measured by MIP for both samples is shown in Figure 3.24. and Table 3.2. The total porosity of both samples decreases after 28 days of carbonation. Figure 3.24a shows that the sample has a significant volume of pores is from 0.07 to 0.4 μm before carbonation. After 7 days and 28 days of carbonation, this volume decreases and divides in two different peaks. For a mixture in which 30% of the

CAC was replaced by slag, carbonation also reduces the capillary porosity, but significantly increases the porosity in the gel pore size range (Figure 3.24b). The CAC70S130 sample has a higher total porosity compared to the pure CAC sample, both for the non-carbonated and carbonated samples but the total porosity of the CAC70S130 sample decreases more after carbonation.

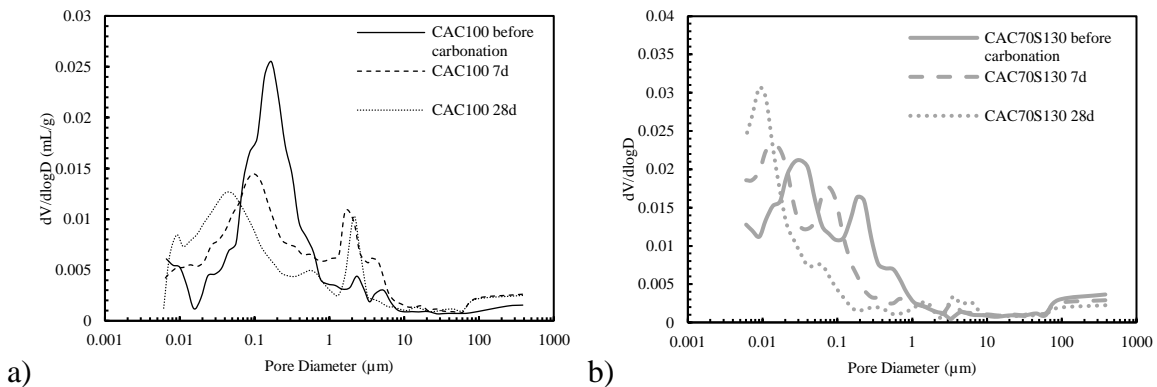


Figure 3.24 Pore size distribution of non-carbonated and carbonated samples a) CAC100, b) CAC70S130

Table 3.2 Total porosity of non-carbonated and carbonated samples

Sample	Porosity (%)		
	Before carbonation	7 days	28 days
CAC100	6.15	6.29	5.26
CAC70S130	7.93	7.16	5.62

The compressive strength was measured after 28 days and 56 days of curing in water for the samples that were not exposed to carbonation. Additionally, the compressive strength was measured on the samples that were exposed to carbonation after 28 days in carbonation chamber. Figure 3.25 shows the results of the compressive strength measurements for non-carbonated and carbonated samples. After 28 days and 56 days of curing in water, the non-carbonated samples of the pure CAC mixture show a 20-25% higher compressive strength than the mixture in which 30% of the CAC was replaced by slag. It is expected that the compressive strength of these samples is higher because there is more cementitious material that reacts with water during the hydration process and contributes to the development of

higher compressive strength. After 28 days of carbonation, the compressive strength values are similar for both mixtures. The 20% increase in compressive strength between the non-carbonated and carbonated CAC70S130 samples is attributed to the faster carbonation rate and higher decrease in total porosity after carbonation.

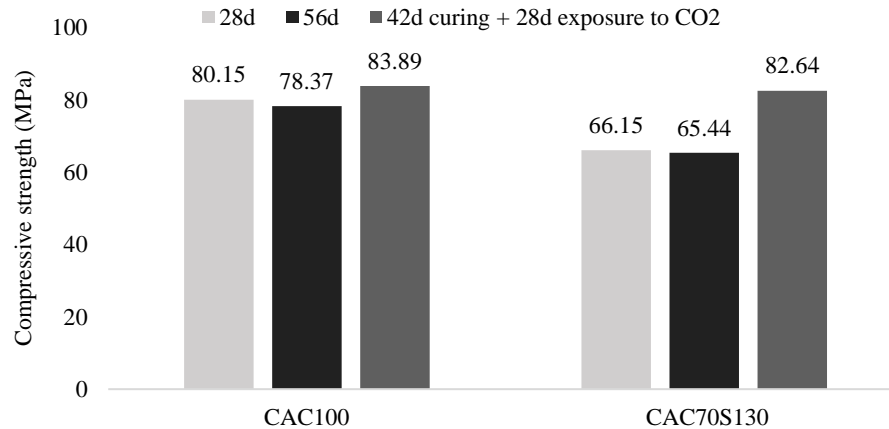


Figure 3.25 Compressive strength of non-carbonated and carbonated samples

### 3.3 Impact of calcined clay

#### 3.3.1 Impact of calcined clay on calcium aluminate-based mortar

Two calcined clays were used to determine their influence on the compressive strength of CAC cement mortar (C1, C2). The oxide composition of the used clay is shown in Table 2.1. The clays were obtained as raw materials. Prior to mixing, both clays were dried, milled (for 90s) in ball mill and calcined at a temperature of 850°C. Figure 2.2 shows the results of the thermogravimetric analysis of the raw clays C1 and C2. The first peak (< 100°C) is related to the moisture content, and the significant mass loss (%) from 350 – 600 °C is related to the dihydroxylation of clay minerals, kaolinite and/or illite. According to the mass loss (%) from 350 – 600 °C, calcined clay had 40% of kaolinite. The kaolinite content, determined from the mass loss curve is 40% for C1, 25.3% for C2. The heat of hydration obtained by the R3 test using calorimetry according to the test developed for the RILEM TC-267 committee

(ASTM C1897-20) is shown in Figure 3.26. Clay 1 showed a higher reactivity compared to clay 2 with a higher amount of heat released through the 7 days. The particle size distribution obtained by laser diffraction of CAC cement and clays C1 and C2 is shown in Figure 3.26.

For the investigation of the influence of calcined clay on the properties of CAC mortar, 2 mixtures were prepared, a reference mixture with 100% CAC, a mixture with a CAC replacement of 30 % by calcined clay C1 and a mixture with a CAC replacement of 30 % by calcined clay C2. The mortar mixtures were prepared from 500 g binder (CAC and/or calcined clay), 200 g water and 1350 g siliceous CEN standard sand. The water to binder ratio was kept constant for all mixtures – 0.4. Additionally, superplasticizer of 0.6 % wt. of binder content was used in mixtures with calcined clay.

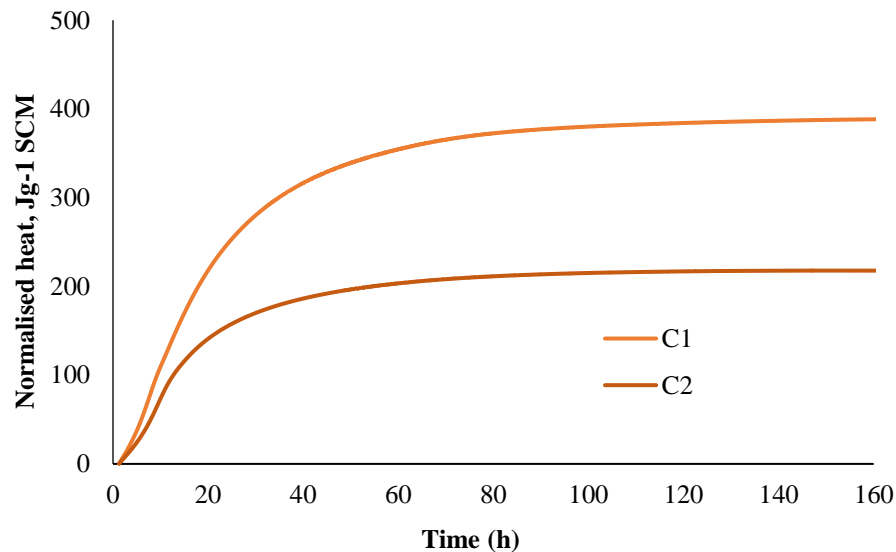


Figure 3.26 Heat of hydration obtained by R3 test using calorimetry for 7 days



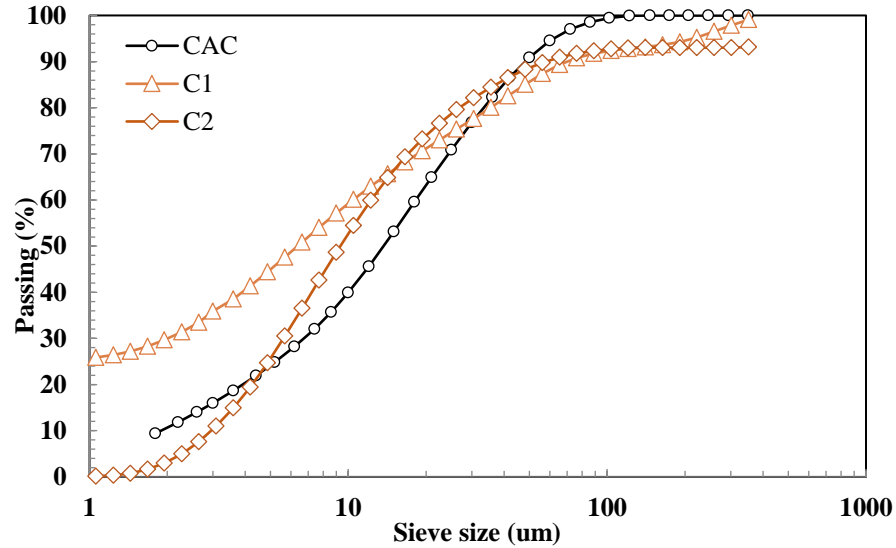


Figure 3.27 Particle size distribution of CAC cement and clay C1, C2

### Compressive strength

Measurements of compressive strength development were conducted after 6h, 24h, 7d and 28 days of curing. Six hours after mixing, the samples were demoulded and tested for 6-hour compressive strength. Other samples were demoulded after 24 hours. The samples for compressive strength testing after 7 and 28 days were stored in water baths at 20°C. The results of the compressive strength measurement are shown in Figure 3.28. All samples showed a continuous increase in compressive strength during 28 days of curing. However, the initial strength (after 6 hours) was the lowest for sample containing clay C2. At the end of the test, the compressive strength of the samples with calcined clays was comparable to that of the reference mixture. The compressive strength of the sample with calcined clay C1 was comparable to the strength of the reference mixture, except after 7 days of curing. The kaolinite content of the used clays is significantly different. The calcined clay C1 has a kaolinite content of 40%, and C2 of 25.3%. It is evident that the kaolinite content has no influence on the strength after 28 days of curing. However, the lower reactivity of C2 clay

has an effect on the early compressive strength. Although 30% of the CAC was replaced by calcined clays C1 and C2, the compressive strength is not compromised..

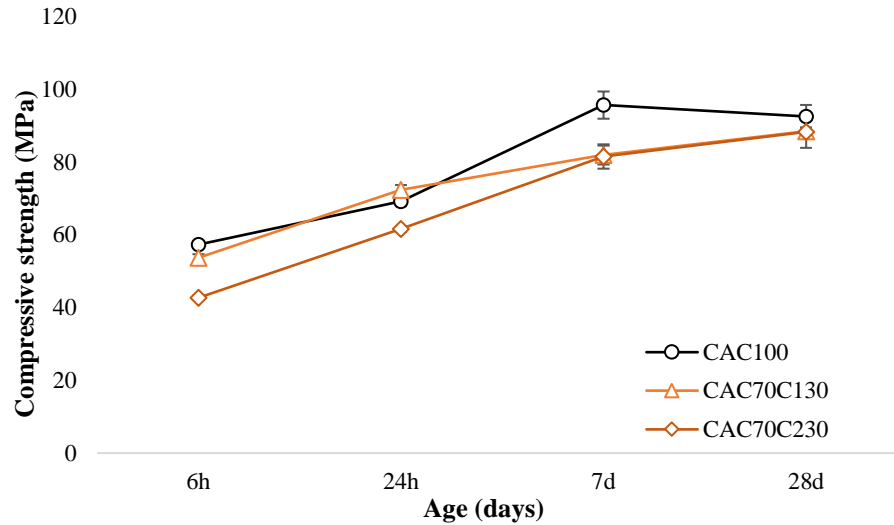


Figure 3.28 Development of compressive strength over 28 days

### 3.3.2 Impact of calcined clay on conversion process of calcium aluminate cement

Based on the initial tests with two different clays and their influence on the compressive strength of CAC mortar, the calcined clay C1 was selected for further investigation of the conversion process. Calcined clay C1 was selected for further testing of the conversion process and microstructural changes due to most optimal development of compressive strength, and availability in the region.

Similar as for initial testing, a special calcium aluminate cement with 52.67%  $\text{Al}_2\text{O}_3$  was used, produced by the Calucem company from Pula, Croatia. Prior to mixing, the clay was first dried at  $60^\circ\text{C}$  for 24 hours to remove moisture, then ground (for 90s) to a Blaine size of  $5980 \text{ cm}^2/\text{g}$  and at the end calcined at  $850^\circ\text{C}$  for one hour. The particle size distribution of CAC and clay is shown in Figure 3.27.

To access conversion process of CAC, two different mixtures were prepared. A reference mixture (labelled CAC100) and a mixture with 30 % replacement of CAC by calcined clay

(labelled CAC70C130). The replacement level of 30% was used to ensure that any changes induced by the addition of SCM are visible in mechanical properties and microstructure. The mixtures were prepared according to EN 14647. The mortar mixtures were prepared from 500 g binder (CAC and/or slag), 200 g water and 1350 g siliceous CEN standard sand. The water to cement ratio was kept constant for all mixtures – 0.4. In addition, for the mixture with clay superplasticizer was used to ensure sufficient and comparable workability to the reference mixture. The amount of superplasticizer was 0.6% by weight of the binder content. The conversion process is highly dependent on the temperature and relative humidity of the environment, therefore before casting, laboratory and all components were conditioned to 20 °C to avoid interference of temperature on early hydration of CAC. For the first 24 hours the samples were covered and stored in a humidity chamber at 20 °C and 95% relative humidity. After 24 hours, the samples were demoulded. To access conversion process, one group of samples was cured in a water bath at 20 °C and one group in a water bath at 38 °C. To evaluate effect of slag on inhibition of conversion process compressive strength, thermogravimetric analysis (TGA), and mercury intrusion porosimetry (MIP) were tested.

#### *Compressive strength*

The development of compressive strength over 56 days for samples cured at 20°C and 38°C is shown in Figure 3.29 a) and b), respectively. When cured at 20°C, the sample with C1 showed a continuous increase in compressive strength. Compared to the reference sample, the compressive strength is lower for 56 days testing period. Although CAC was replaced by 30% C1, the compressive strength did not decrease for 30%, indicating a contribution of the calcined clay to the development of the compressive strength of CAC cement-based mortar. When cured at 38°C, the compressive strength of the reference sample started to decrease

after 5 days of curing, indicating a conversion process from metastable to stable hydrates. After 28 days of curing, the strength of the reference sample is almost stable, implying that almost all metastable hydrates have converted to stable ones. When CAC is replaced by calcined clay and cured at 38°C, the compressive strength is constantly increasing during prolonged curing up to 56 days.

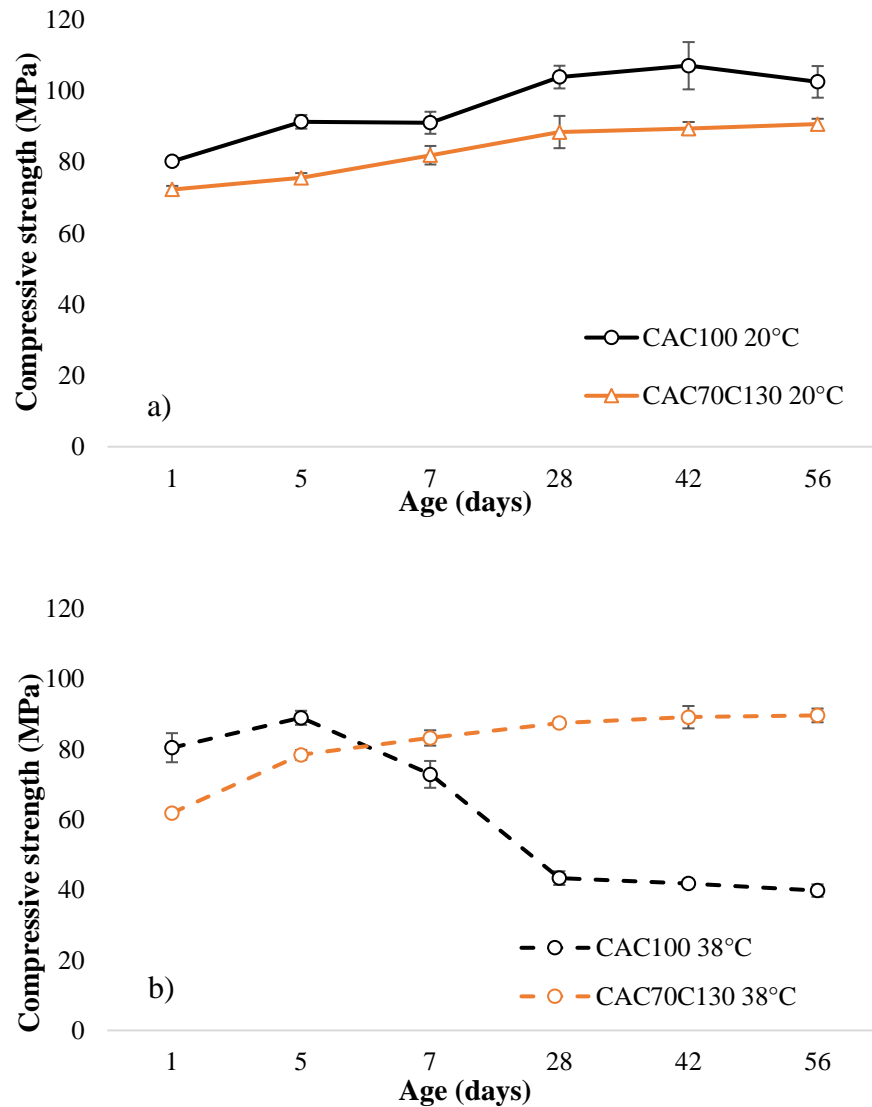


Figure 3.29 Development of compressive strength over 56 days for samples cured at: a) 20°C, b) 38°C

*Thermogravimetric analysis*

Thermogravimetric analysis was conducted on samples cured 28 days at 20°C and 38°C. Obtained derivate of the mass loss curve are shown in Figure 3.30. It can be seen from DTG curves that hydrate dehydration takes place in a similar temperature range for all samples. The decomposition of the metastable hydrate  $CAH_{10}$  was observed in the temperature range of 40-80 °C, the decomposition of  $C_2HA_8$  at 70-130 °C. The dehydration of the stable hydrate  $C_3AH_6$  was observed between 230°C and 300°C, that of the  $AH_3$  hydrate in the temperature range of 170-230 °C. The decomposition of strätlingite in samples with slag and calcined clay was visible from 140°C to 190°C. In the reference sample both metastable and stable hydrates were detected after 28 days of curing. For the same mixture cured at 38°C, a significantly lower peak of metastable hydrates and a significantly higher peak of stable hydrate hydrogarnet was detected. The formation of stable hydrate with higher intensity when cured at 38°C confirmed that the conversion process occurred during curing at 38°C. For sample with calcined clay, metastable and stable hydrates and strätlingite hydrate did occur, but with different peak intensities. The higher peak intensity was observed for metastable hydrates when cured at 38°C and a less intense peak for stable hydrates. Also, when cured at 20°C it showed a higher peak intensity for strätlingite hydrate.

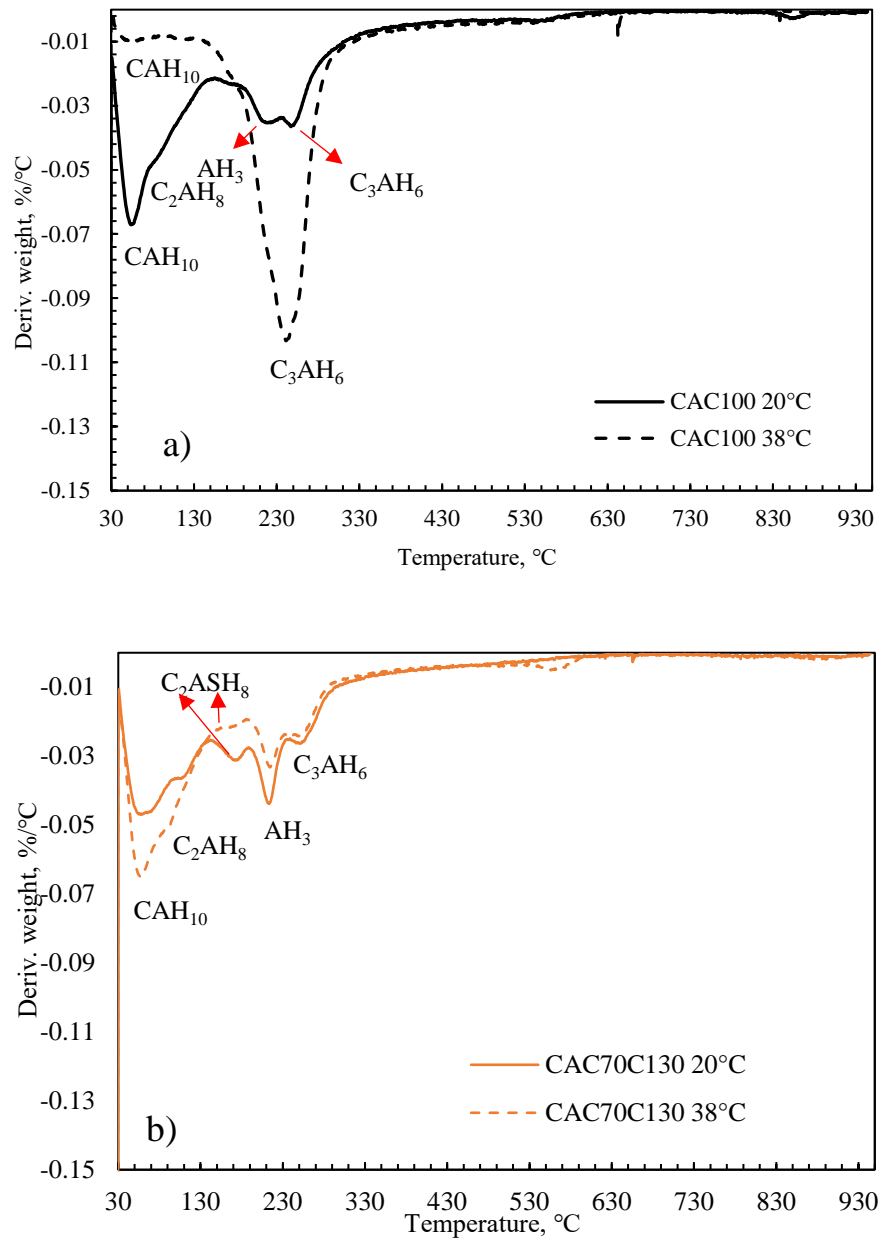


Figure 3.30 DTG for mixes cured at 20°C and 38°C after 28 days: a) CAC100, b) CAC70C130

### X-ray diffraction

The XRD analysis was performed after 56 days of curing at 20°C and 38°C. The results are shown in Figure 3.31. In the reference sample cured at 20°C (Figure 3.31a) metastable CAH<sub>10</sub> hydrate was detected (at a diffraction angle between 5 and 15 degrees) as well as stable C<sub>3</sub>AH<sub>6</sub> and AH<sub>3</sub> hydrate. When the same mixture was cured at 38°C, a lower peak

intensity was observed for metastable hydrates and a higher peak intensity for the two stable phases ( $C_3AH_6$  and  $AH_3$ ). For the calcined clay sample (Figure 3.31b), a higher peak intensity of the metastable hydrate  $CAH_{10}$  was observed, compared to the reference sample, for both curing temperatures. Moreover, lower peaks were observed for stable hydrates compared to the same peaks in the reference sample. Furthermore, strätlingite hydrate was formed during curing at both curing temperatures.

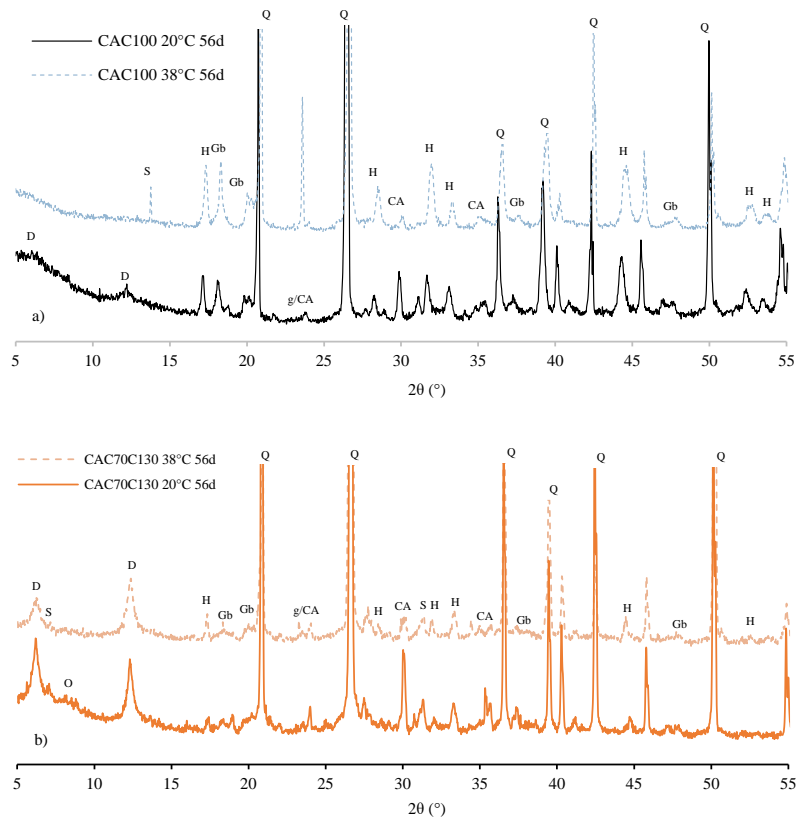


Figure 3.31 Diffractogram for samples cured 56 days at 20°C and 38°C: a) CAC100, b) CAC70C130 (CA=monocalcium aluminate, D=CAH<sub>10</sub>, Gb=AH<sub>3</sub>, G=Gehlenite, H=C<sub>3</sub>AH<sub>6</sub>, O=C<sub>2</sub>AH<sub>8</sub>, S=strätlingite Q=quartz)

### Mercury intrusion porosimetry

The results of the total accessible porosity are shown in Figure 3.32. The total porosity represents the total accessible pore volume of the connected pores. The samples were tested

after 28 days of curing at 20°C and 38°C. The reference sample CAC100 showed the highest total porosity regardless of the curing temperature: 12.37% when cured at 20°C and 12.23% when cured at 38°C. The sample with calcined clay showed a lower total porosity compared to the reference mix: 8.80% when cured at 20°C and 8.19% when cured 38°C. Thus, the replacement of CAC by 30% of calcined clay resulted in a reduction in total accessible porosity of approximately 4%. The pore volume distribution is shown in Figure 3.33. For the reference sample cured at 38°C the maximum mercury intrusion was between 500 nm and 1500 nm, while the samples with calcined clay showed a much smaller pore entry diameter, especially after curing at 38°C. The critical pore entry diameter is shown in Figure 3.34. The critical pore entry diameter is the highest peak in the differential intrusion pore volume curve which corresponds to the maximum volume intrusion. The samples cured at 20°C had a smaller critical pore entry than the samples cured at 38°C. Furthermore, the samples with calcined clay had a lower critical pore entry than the reference sample at both curing regimes.

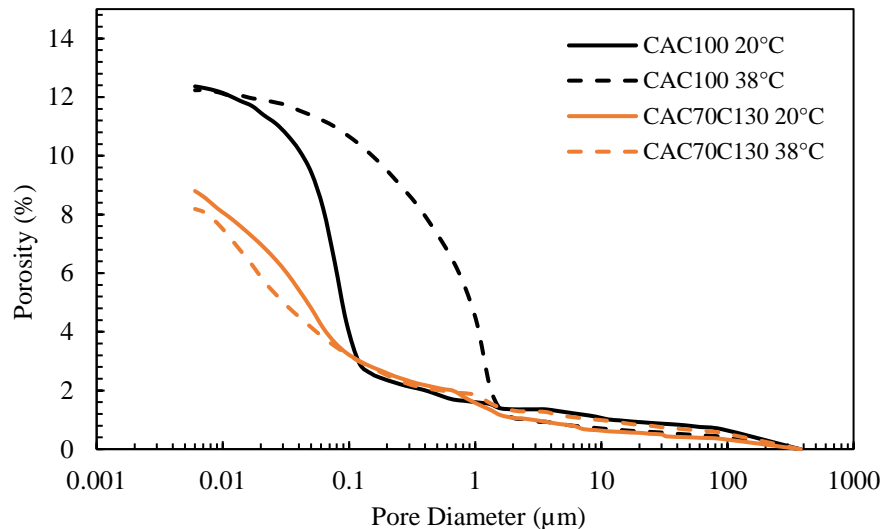


Figure 3.32 Total porosity after 28 days of curing at 20°C and 38°C for CAC100 and CAC70C130 mix



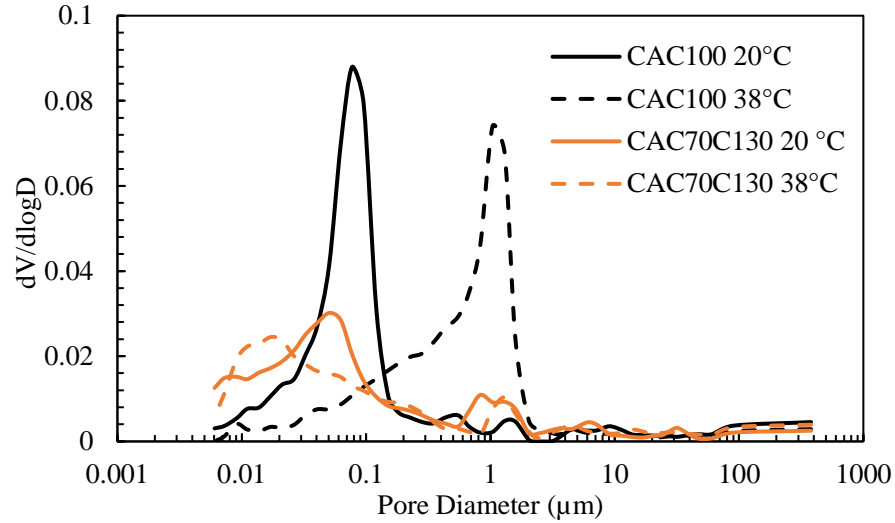


Figure 3.33 Differential intrusion curve after 28 days of curing at 20°C and 38°C for CAC100 and CAC70C130 mix

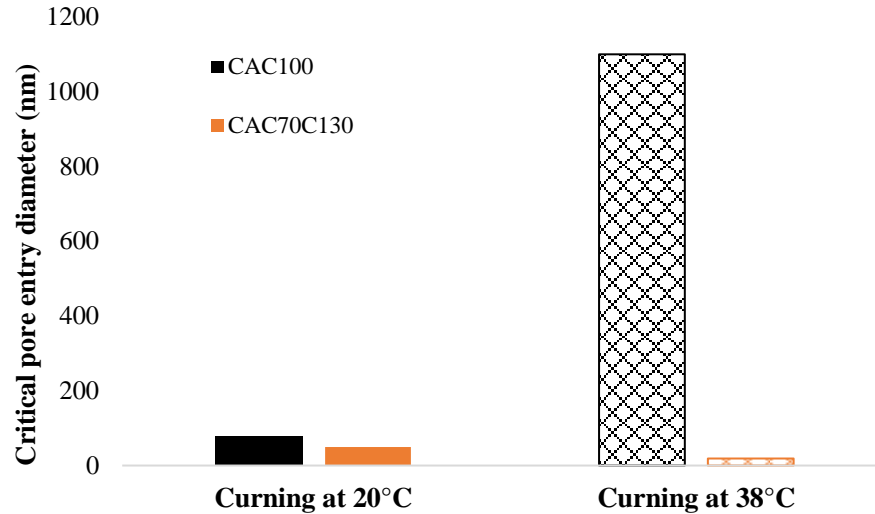


Figure 3.34 Critical pore entry diameter after 28 days of curing at 20°C and 38°C for CAC100 and CAC70S130 mix

### 3.4 Discussion

In the first part of this chapter, it was shown that slag contributes to the development of calcium aluminate cement-based mortar if it is properly treated prior to mixing [70]. In addition to this beneficial effect on the compressive strength of CAC, the durability properties of CAC based concrete are negatively affected by incorporating slag in CAC binder. Higher water and gas permeability enable greater penetration of aggressive substances into the cement matrix [71]. In the second part, the influence of slag and calcined

clay on the conversion process and the changes in the microstructure were investigated. The development of the compressive strength of CAC is closely related to the curing temperature during hydration and hardening of the cement. During curing at 38°C, the transformation of metastable phases into stable phases is accelerated, resulting in a decrease in compressive strength [8]. The compressive strength of the reference sample cured at 38 °C started to decrease after 7 days of curing, and after 28 days of curing, the compressive strength was 60% lower than mix cured at 20 °C. The TGA analysis confirmed that in the case of the pure CAC mixture almost all metastable phases were transformed into stable phases during 28 days of curing at 38 °C, which is directly related to the significant compressive strength decrease. During the conversion process phases of stable hydrates were formed, which have a higher density of cubic phases, increasing the space between the hydrates and therefore overall porosity [5]. The increase in porosity of the cement matrix led to the compressive strength decrease [72]. When cured at 38°C, the pure CAC mixture showed almost complete precipitation of the metastable phases into stable phases until 28 days of curing. However, total porosity of the CAC100 mixture was nearly the same, regardless of the curing temperature. For better understanding of pore structure on the compressive strength, pore classification was carried out. Figure 3.35 shows the pore classification based on their entry diameter according to Kumar et al [73]. It can be seen that there are no significant differences between the reference mix cured at 20°C and 38°C in terms of the percentage of gel pores, capillary pores and macro pores. The compressive strength development is mostly dependant on the formation of capillary pores during cement hydration. Figure 3.36 shows capillary pore classification according to Mehta [74]. In this case, the capillary pores were divided into three groups, micro (0.01 – 0.1 µm), meso (0.1 – 1 µm) and macro (1 – 10 µm) capillary

pores. The reference sample cured at 38°C, where conversion process occurred, has a higher proportion of larger capillary pores than the reference mixture cured at 20°C. Therefore, once metastable phases have transformed into stable phases, the critical pore entry diameter has increased, and the capillary pores have become larger. A pure CAC mixture is inclined to experience reduction in compressive strength at elevated temperatures, but with the addition of materials rich in silica conversion reaction is hindered without reduction in compressive strength. Addition of supplementary cementitious materials in CAC leads to further hydration of CA, resulting in more hydration products [75]. When 30% of the CAC is replaced with slag, the compressive strength becomes more stable during curing at 38°C due to formation of strätlingite hydrate. By curing at lower temperatures (below 20°C), the dominant phase that will form is CAH<sub>10</sub> hydrate. Since the formation of strätlingite is mostly governed by C<sub>2</sub>AH<sub>8</sub> hydrate, strätlingite has no significant influence on the space filling when curing at lower temperatures. On the other hand, by curing at higher temperatures (above 25°C), the formation of C<sub>2</sub>AH<sub>8</sub> and AH<sub>3</sub> hydrate dominates [75]. In this case, more strätlingite hydrate is formed and the decrease in compressive strength is reduced. Despite the formation of strätlingite hydrate, the conversion process still occurs, which can be observed by an increase in the critical pore entry diameter and a slight reduction in compressive strength compared to the same mixture cured at 20°C (Figure 3.9, Figure 3.13). The addition of slag reduces the critical pore entry diameter for both curing regimes, due to the formation of denser hydrate strätlingite [10]. The critical pore entry diameter is higher when cured at 38°C as a result of larger formation of stable hydrates with lower density. The mixture with slag has a lower total intrusion volume than the reference mixture but shows similar behaviour. By curing at higher temperatures, the differential intrusion curve for both

mixture shifts to the right, indicating a coarsening of the pore structure. In the case of mixture where 30% of the CAC was replaced by calcined clay, the formation of strätlingite hydrate was observed at both curing temperatures (Figure 3.30), however compressive strength of this mixture was continuously lower compared to the mixture with slag. The reason for this is the formation of less metastable phases by curing at 20°C, and formation of less strätlingite hydrate by curing at 38°C. Despite that, the compressive strength of the calcined clay mixture neither increased nor decreased when cured at 38°C, so that this mixture was the most stable compared to the other two mixtures. It has been reported that calcined clay in combination with OPC reduces the critical pore entry diameter [64]. When calcined clay was added to CAC, the critical pore entry size was also reduced at both curing temperatures. Moreover, by curing at higher temperatures hydration was faster and there were more finer pores, and the critical pore entry diameter was further reduced (the differential intrusion curve was shifted to the left, Figure 3.33). The mixture with calcined clay forms more hydration products of metastable phases and there is no compressive strength loss or increase in capillary pores size range. Also, the formation of strätlingite hydrate at elevated temperatures contributes to the densification of the structure and the reduction of the critical pore entry diameter.

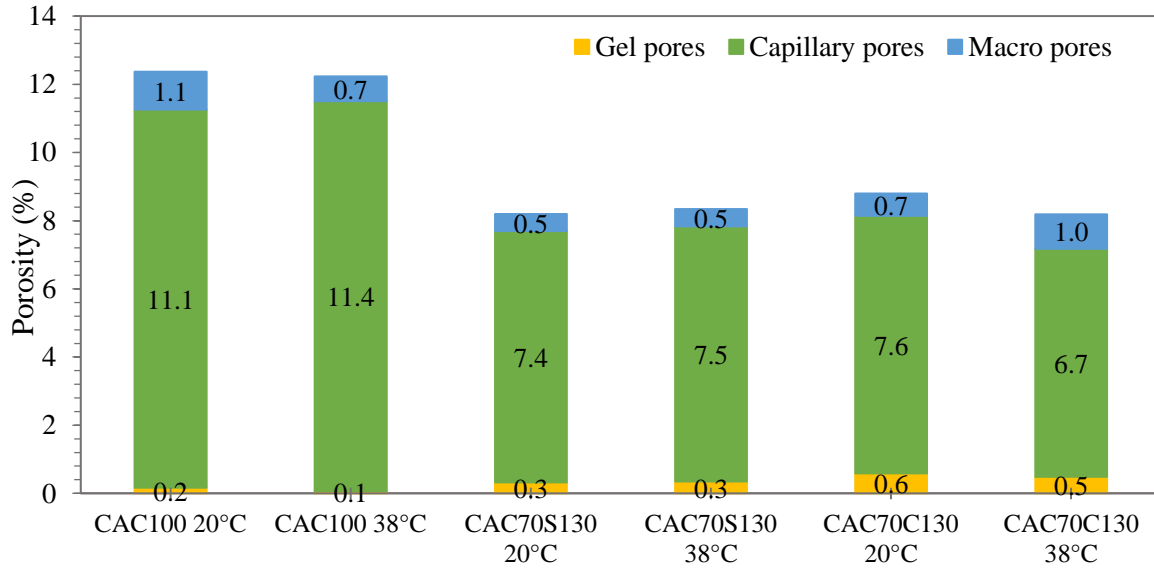


Figure 3.35 Pore classification based on their entry diameter

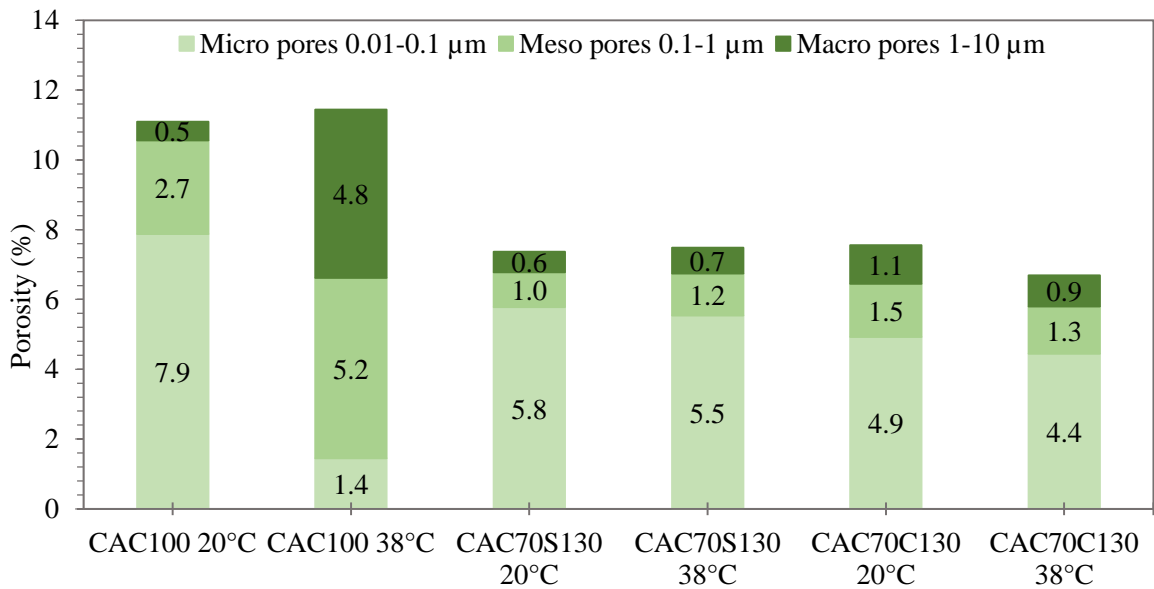


Figure 3.36 Capillary pores classification

### 3.5 Conclusion

The aim of this research was to analyse the influence of slag and calcined clay on the mechanical and durability properties of CAC. The influence of slag on the basic durability properties of CAC based concrete was determined. Furthermore, changes in the

microstructure and their influence on the conversion process of CAC without and with the addition of slag/calcined clay were observed.

The following conclusions are drawn from the study:

- It has been shown that slags of different origin and chemical composition have almost the same influence on the compressive strength of CAC based mortar when cured at 20°C, especially on the 28-day compressive strength.
- The durability properties of CAC based concrete cured at 20°C were reduced when CAC was replaced by 30% of slag. Also, the compressive strength of concrete with slag was lower than that of the pure CAC concrete.
- A positive influence on the compressive strength of CAC concrete with the addition of slag was observed during carbonation of the CAC concrete. In this case, the strength increased by 20% after 56 days of carbonation.
- Curing CAC at 38°C resulted in the compressive strength decrease of 60%, due to the conversion of metastable hydrates to stable hydrates, and consequently an increase in the critical pore entry diameter and the formation of larger capillary pores.
- The formation of strätlingite  $C_2ASH_8$  hydrate was confirmed for CAC with the addition of slag as well as for calcined clay.
- In the presence of  $C_2ASH_8$  hydrate, the structure of the cement matrix was densified which contributed to a lower total intrusion volume and a lower total accessible porosity compared to a mixture without the addition of slag and calcined clay.
- The addition of slag reduced the conversion process rate, however with prolonged curing at 38°C, a decrease in compressive strength was observed, as well as the

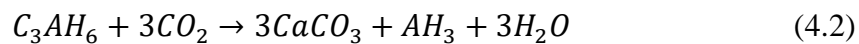
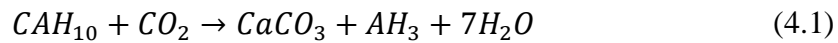
formation of a larger amount of stable hydrates, which indicates occurrence of the conversion process.

- The addition of calcined clay to CAC slightly reduced overall compressive strength compared to the CAC system, however a decrease in compressive strength was avoided when cured at 38°C, making this mixture the most stable.
- Despite reduced overall compressive strength, the addition of calcined clay to CAC contributed to the avoidance of the conversion process even after 56 days of curing at 38°C
- The formation of strätlingite in the calcined clay mixture densified the structure and reduced the critical pore entry diameter particularly when the mixture was cured at 38°C.

## Chapter 4 Carbonation of CAC with slag/calced clay

### 4.1 Introduction

The durability of calcium aluminate cement is often cited as the greatest advantage of this material [4][5][22]. One of the durability properties raising additional attention in concrete research is resistance to carbonation, due to the implication concrete based materials as carbon sinks have in the carbon neutrality strategy [33][34]. The reaction of carbon dioxide with hydrates within cement matrix leads to the formation of calcium carbonate polymorphs. In CAC cement, according to the literature, the reaction with CO<sub>2</sub> leads to the formation of CaCO<sub>3</sub> and AH<sub>3</sub> gel, irrespective of the hydrates present [5]. The carbonation reactions of CAC hydrates are shown in equations below [35][36].



Alapati and Kurtis [37] demonstrated that CAC concrete exhibits a faster carbonation rate in comparison to OPC concrete. Additionally, they showed that the decomposition of primary hydration products due to carbonation can lead to a considerable decrease in compressive strength and capillary porosity. On the contrary, studies of CAC exposure to carbon dioxide as curing during early age showed that it is possible to overcome conversion process by exposing samples to critical carbonation (100 % of CO<sub>2</sub>) or by early carbonation curing [38][39]. Studies showed formation of stable hydrates without causing an increase in the porosity of the cement matrix. As can be seen, there is an absence of uniform conclusion on the effect of carbonation on CAC. Furthermore, there is limited knowledge about how SCMs impact the carbonation process of calcium aluminate cement.



This research is focused on evaluating the carbonation resistance of mortar based on CAC without and with the addition of slag and calcined clay. For this purpose, three mixes were made. One reference mixture with 100% of CAC, and two mixes with 30% replacement of CAC by slag and calcined clay respectively. Prior to placement in the carbonation chamber, one set of mixtures was cured at 20°C while the other set was cured at 38°C to accelerate the conversion process. Influence of carbonation was evaluated on non-converted (cured at 20°C) and converted samples (cured at 38°C). Depth of carbonation was measured with phenolphthalein indicator. To assess the impact of carbonation on the mechanical properties, the compressive strength of the samples was tested before and after 56 days of carbonation. Microstructure studies were performed by thermogravimetric analysis (TGA), mercury intrusion porosimetry (MIP), and X-ray diffraction (XRD).

## **4.2 Results**

### 4.2.1 Depth of carbonation

Carbonation ingress was monitored over 56 days of exposure to CO<sub>2</sub>. Results obtained from carbonation depth measurement are shown in Figure 4.1. Mixture CAC70C130 20°C exhibited the highest carbonation ingress throughout all testing periods. Mixtures cured at 38°C before carbonation have an overall lower carbonation depth than mixtures cured at 20°C. This difference also can be seen in, Figure 4.2, where samples sprayed with phenolphthalein after 56 days of exposure to CO<sub>2</sub>. Phenolphthalein is used as an indicator of uncarbonated, partially carbonated, or fully carbonated concrete. The purple colour indicates that the concrete has not carbonated, and if part of the sample is colourless, it implies that carbonation occurred. Both slag and calcined clay samples show smaller carbonation depth in the case of samples cured at higher temperature which also can be seen from samples sprayed with phenolphthalein. If all samples sprayed with phenolphthalein are compared, a

different colour of the reference mixture cured at 38°C is visible. The colour of this sample is pale purple, potentially due to the differences in the phase assemblage of this mix during carbonation, causing weaker reaction of phenolphthalein with the surface of the sample.

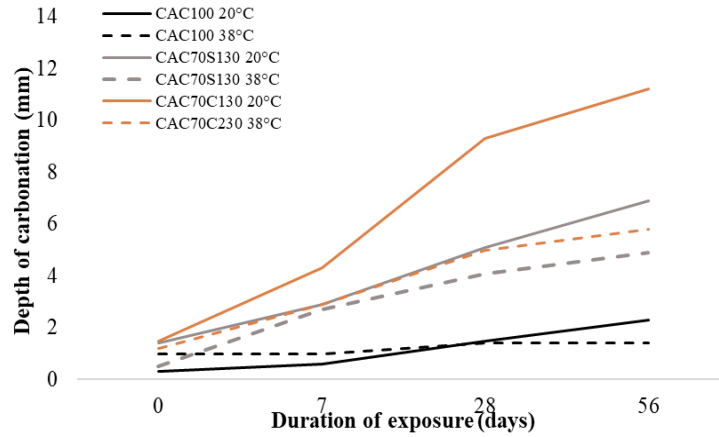


Figure 4.1 Carbonation depth values for all mixes

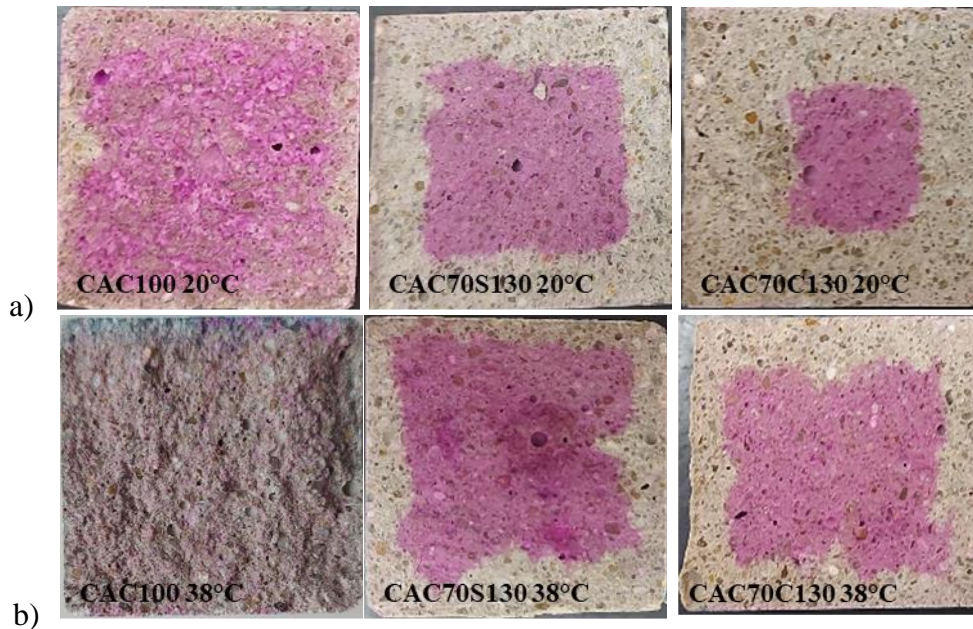


Figure 4.2 Samples sprayed with phenolphthalein after 56 days of exposure for CAC70S130 mix: a) 20°C, b) 38°C

#### 4.2.2 Compressive strength development

The compressive strength was tested after 28 days and 56 days of curing at 20°C and 32°C, Figure 4.3. The compressive strength of the reference mixture cured at 20°C remained the

same after 56 days of curing compared to the 28 days cured samples. A similar trend can be noticed for the reference mixture cured at 38°C. Although this mixture already had a lower compressive strength after 28 days of curing compared to the mixture cured at 20°C, the strength continued to decrease, indicating that not all metastable hydrates were transformed into stable hydrates during first 28 days of curing. Mixtures where 30% of CAC was replaced by slag or calcined clay had increased compressive strength after 56 days of curing, potentially implying that the conversion process did not occur in these samples after 56 days of curing, or that due to the higher temperature of curing, there is a higher degree of hydration.

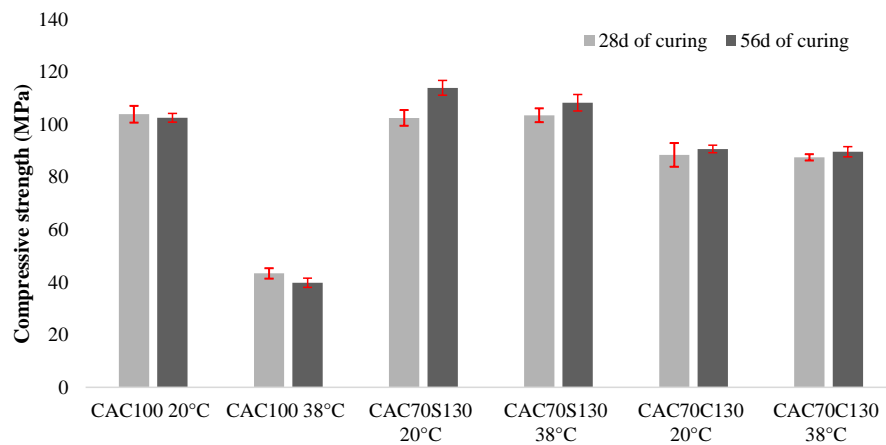


Figure 4.3 Compressive strength values after 28 days and 56 days of curing at 20°C and 38°C

Additionally, compressive strength measurements were conducted after 56 days of carbonation compared to compressive strength of samples prior to carbonation, Figure 4.4. Accelerated carbonation had the greatest impact on the change in the compressive strength of the reference mixture for both curing temperatures. While the compressive strength of non-converted reference mixture cured at 20°C decreased for almost 30% after 56 days of carbonation, the same mix converted due to the curing at 38°C experienced increase in compressive strength for almost 40% after carbonation. In the case of mixtures with slag and

calcined clay, a slight increase in strength was recorded for all mixtures after 56 days of carbonation, regardless of curing conditions prior to carbonation.

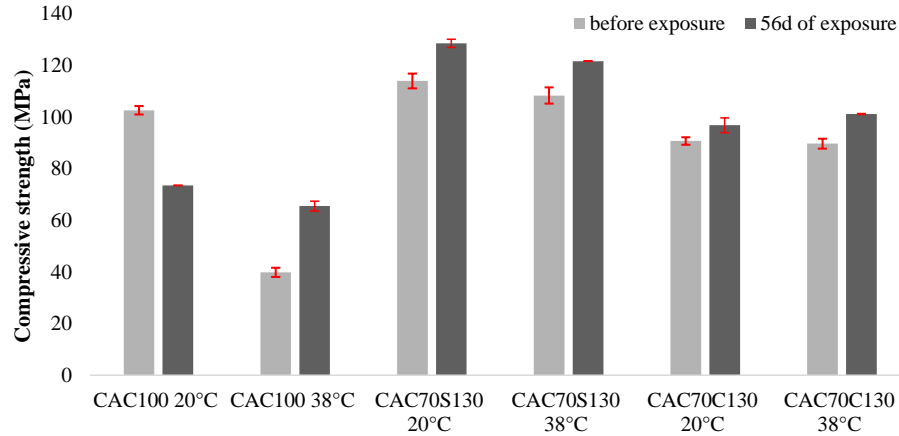


Figure 4.4 Compressive strength values before and after 56 days of carbonation compared to compressive strength prior to carbonation

#### 4.2.3 Microstructural changes during carbonation

##### *Calcium aluminate cement*

Figure 4.5 shows dTG curves for CAC100 mix cured at 20°C (a) and 38°C (b) after 28 days and 56 days of curing, as well as after 28 days and 56 days of carbonation. On Figure 4.5a) metastable hydrates  $CAH_{10}$  and  $C_2AH_6$  were identified decomposing on temperatures from 40°C to 130°C, and stable hydrates  $AH_3$  and  $C_3AH_6$  on temperatures from 210°C to 290°C. Also, metastable hydrate  $C_2AH_8$  can be noticed at temperatures higher than 800°C. This hydrate decomposes in several steps; an amorphous phase of  $C_2AH_8$  hydrate decomposes at lower temperatures (up to 320°C), but this phase crystallizes again and decomposes at higher temperatures [76]. CAC cement hydrates occur at similar temperatures both after 28 days, and 56 days of curing, but with different peak intensities. With prolonged curing of 56 days at 20°C, more stable hydrates were formed, indicating conversion process started to occur.

By curing at 38°C CAC experienced almost complete conversion of metastable hydrates to stable hydrates after 28 and 56 days of curing, as evident from Figure 4.5b).

After 28 days of carbonation in the case of CAC cured at 20°C peak intensity for metastable hydrates was lower, and peak intensity for stable hydrates slightly higher. Also, decomposition of  $\text{CaCO}_3$  phase can be noticed in temperature range from 430°C to 630°C. However, after 56 days of carbonation higher peak intensity was detected from 30°C to 130°C for both curing regimes. Therefore, after a prolonged period of exposure to  $\text{CO}_2$ , metastable hydrates begin to form again. Additionally, higher peak intensity of  $\text{C}_2\text{AH}_8$  hydrate was detected after 28 days, and 56 days of carbonation.

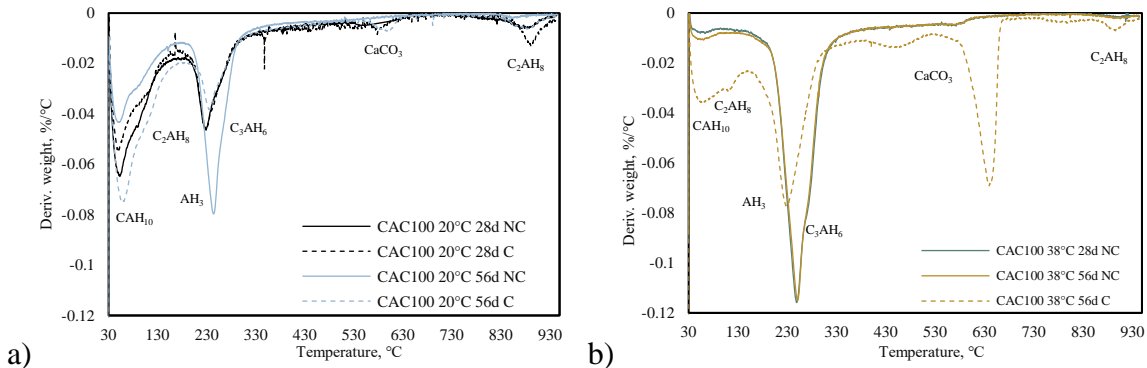


Figure 4.5 DTG curves of carbonated CAC100 mix cured at (a) 20°C and at (b) 38°C after 28 days and 56 days of exposure

In the case of CAC100 mix cured at 38°C after 28 days and 56 days of carbonation, it is visible that during carbonation the peak of stable hydrates was decreasing. After 56 days of carbonation there was no  $\text{C}_3\text{AH}_6$  hydrate detected, while metastable hydrates and calcium carbonate occurred. Also, formation of more  $\text{AH}_3$  hydrate was detected after 56 days of carbonation in sample cured at 38°C.

XRD was performed on the reference mixture subjected to carbonation for 56 days. The results for mixture CAC100 20°C, and CAC100 38°C are shown in Figure 4.6 and Figure

4.7, respectively. The testing was conducted on mortar samples containing silicious standard sand. Given that quartz has high crystallinity, the peaks of quartz in the XRD analysis results are much larger compared to the peaks of the hydrates found in CAC. In the case of CAC100 20°C sample, at the diffraction angle between 5 and 15 degrees, metastable hydrates,  $CAH_{10}$  and  $C_2AH_8$  were detected. Moreover, higher peak intensity for these hydrates was detected in carbonated sample, indicating metastable hydrates formed during carbonation. In both non-carbonated and carbonated samples stable hydrogarnet and  $AH_3$  hydrate were detected. In the reference sample cured at 38°C very low peak intensity was detected for metastable hydrate  $CAH_{10}$  in non-carbonated part of the sample. This indicates that the conversion process was nearly complete. Similarly, as for the sample cured at 20°C, higher peak intensities were detected for both metastable hydrates  $CAH_{10}$  and  $C_2AH_8$  in carbonated sample, compared to non-carbonated sample, indicating formation of metastable phases during carbonation. In carbonated sample traces of calcite and vaterite polymorph of calcium carbonate were detected, and the third polymorph of calcium carbonate, aragonite, predominantly formed.

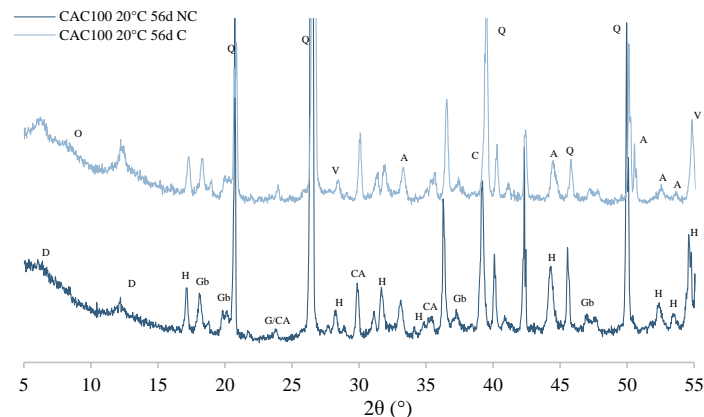


Figure 4.6 Diffractogram for non-carbonated and carbonated CAC100 20°C mix (CA=monocalcium aluminate, D= $CAH_{10}$ , Gb= $AH_3$ , G=Gehlenite, H= $C_3AH_6$ , O= $C_2AH_8$ , Q=quartz, A=aragonite, C=calcite, V=vaterite)

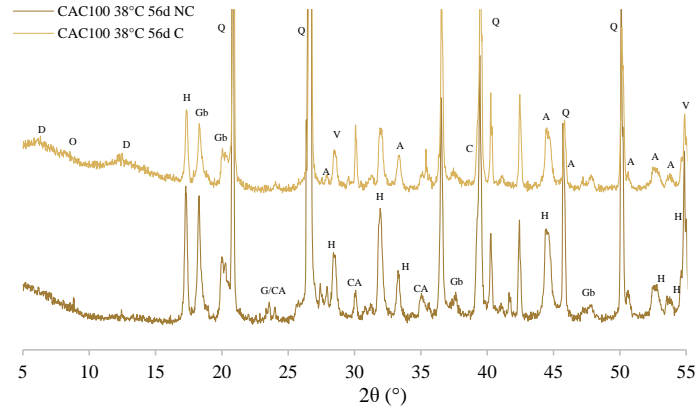


Figure 4.7 Diffractogram for non-carbonated and carbonated CAC100 38°C mix (CA=monocalcium aluminat, D=CAH<sub>10</sub>, Gb=AH<sub>3</sub>, G=Gehlenite, H=C<sub>3</sub>AH<sub>6</sub>, O=C<sub>2</sub>AH<sub>8</sub>, Q=quartz, A=aragonite, C=calcite, V=vaterite)

### Calcium aluminat cement with slag

Figure 4.8 shows dTG curves for mix where 30% of CAC is replaced by slag cured at 20°C (a) and 38°C (b) after 28 days and 56 days of curing, as well as after 28 days and 56 days of carbonation. Except for the hydrates that occur in CAC, formation of strätlingite (C<sub>2</sub>ASH<sub>8</sub>) hydrate, which decomposes at the temperature range from 150°C to 190°C, was detected in non-carbonated samples both cured at 20 and 38°C. With prolonged curing, up to 56 days, slightly more metastable hydrates and stable hydrates were formed in non-carbonated samples.

After carbonation, peak intensity for CAH<sub>10</sub> hydrate was lower. After 28 days and 56 days of carbonation a clear formation of C<sub>2</sub>AH<sub>8</sub> at higher temperatures was detected. For samples first cured at 38°C, lower peak intensity was detected for CAH<sub>10</sub> after both days of exposure, while more C<sub>2</sub>AH<sub>8</sub> hydrate at lower and higher temperatures was detected after carbonation. Furthermore, by the carbonation of CAH<sub>10</sub> and C<sub>3</sub>AH<sub>6</sub> hydrate formation of CaCO<sub>3</sub> and AH<sub>3</sub> hydrate was detected.

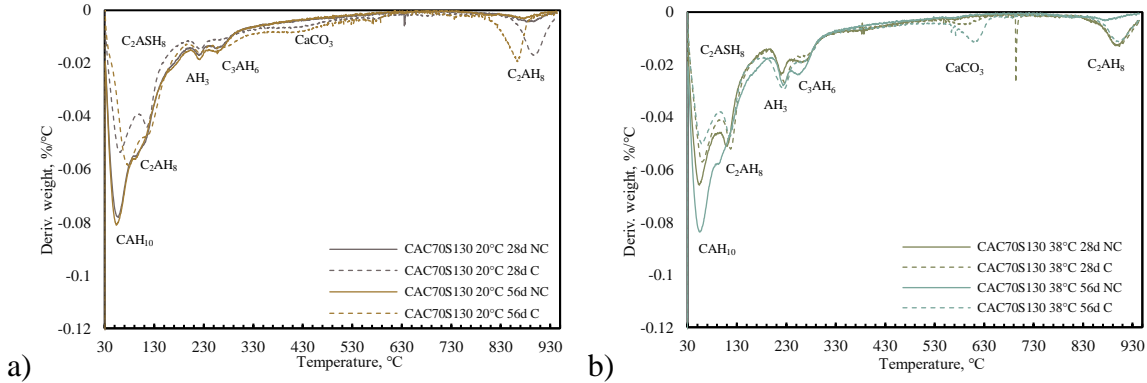


Figure 4.8 DTG curves of carbonated CAC70S130 (a) 20°C and (b) 38°C mix after 28 days and 56 days of exposure

XRD analysis was conducted on non-carbonated and carbonated sample cured at 20°C and 38°C, to confirm phases identified using TGA. The results are shown in Figure 4.9 and Figure 4.10. At the diffraction angle between 5 and 15 degrees metastable hydrate CAH<sub>10</sub> was detected. Also, strätlingite hydrate was detected at lower and higher diffraction angles. In the carbonated part of the sample, lower peak intensity was detected for metastable CAH<sub>10</sub> hydrate indicating that this hydrate decomposes during carbonation. In both samples stable hydrogarnet and AH<sub>3</sub> hydrate were detected. No calcite was detected in the carbonated sample; however, the other two polymorphs of calcium carbonate, vaterite and aragonite, were present. As in the reference sample, aragonite was predominantly formed. Similar behaviour can be noticed for sample with slag cured at 38°C. In the non-carbonated sample higher peak intensity for metastable hydrate was detected, however after 56 days of carbonation peak intensity for this hydrate was lower. A higher peak intensity was detected for stable hydrogarnet and AH<sub>3</sub> hydrate after carbonation. In this sample, aragonite was mostly formed after 56 days of carbonation.



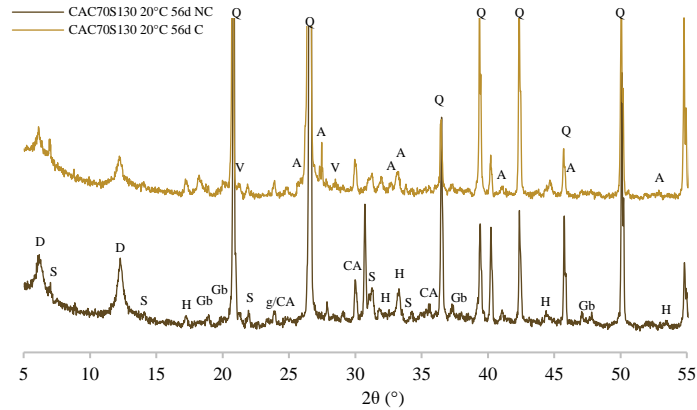


Figure 4.9 Diffractogram for non-carbonated and carbonated CAC70S130 20°C mix (CA=monocalcium aluminate, D=CAH10, Gb=AH3, G=Gehlenite, S=Strätlingite, H=C3AH6, O=C2AH8, Q=quartz, A=aragonite, C=calcite, V=vaterite)

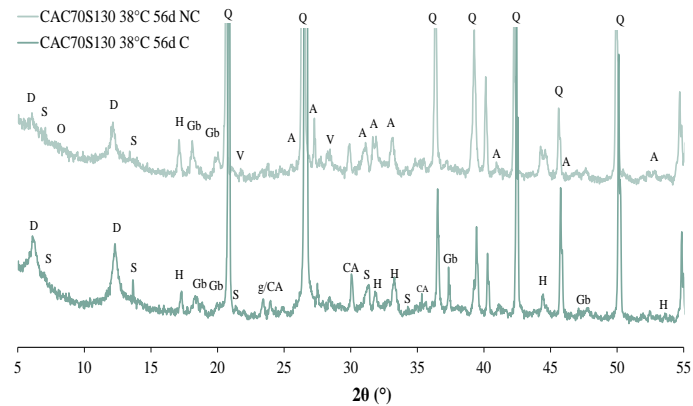


Figure 4.10 Diffractogram for non-carbonated and carbonated CAC70S130 38°C mix (CA=monocalcium aluminate, D=CAH10, Gb=AH3, G=Gehlenite, S=Strätlingite, H=C3AH6, O=C2AH8, Q=quartz, A=aragonite, C=calcite, V=vaterite)

#### Calcium aluminate cement with calcined clay

Figure 4.11 shows dTG curves for mix where 30% of CAC is replaced by calcined clay cured at 20°C (a) and 38°C (b) after 28 days and 56 days of curing, as well as after 28 days and 56 days of carbonation. By prolonged hydration lower peak intensity is detected for metastable hydrates and higher for stable hydrates. Formation of  $C_2AH_8$  at higher temperatures is detected for both curing periods, as well as strätlingite hydrate. When CAC70C130 mix is cured at 38°C, more metastable hydrates are formed with prolonged curing, up to 56 days

(Figure 4.11b). Also, slight peak intensity is detected for  $C_2AH_8$  hydrate at higher temperatures, and for strätlingite hydrate.

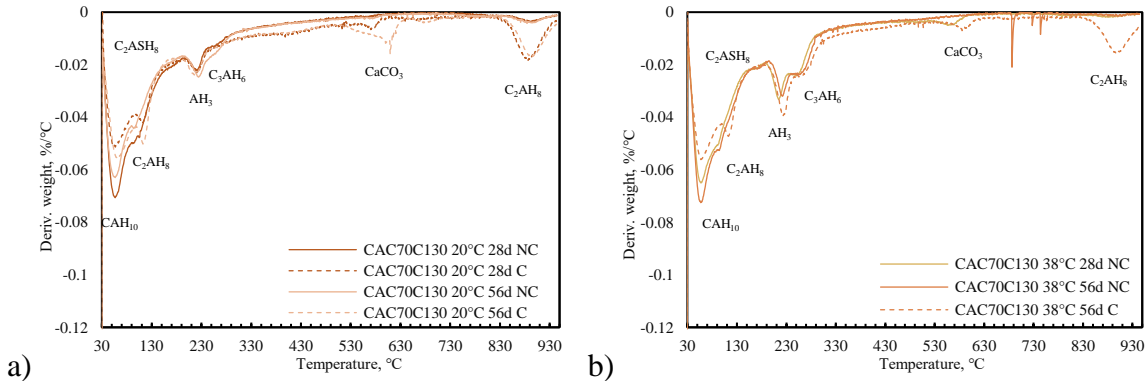


Figure 4.11 DTG curves of carbonated CAC70C130 (a) 20°C and (b) 38°C mix after 28 days and 56 days of exposure

When samples are exposed to  $CO_2$ , lower peak intensity was detected for  $CAH_{10}$  hydrate, while higher peak intensities were detected for  $AH_3$ ,  $CaCO_3$  and high crystallinity  $C_2AH_8$ . The same can be noticed for  $C_3AH_6$  hydrate. Similarly, for samples cured at 38°C, lower peak intensity was detected for  $CAH_{10}$  after exposure to  $CO_2$ , while more  $C_2AH_8$  hydrate at lower and higher temperatures was detected after carbonation. In this case, more  $C_3AH_6$  hydrate was also detected after carbonation. Furthermore, by the carbonation of  $CAH_{10}$  formation of  $CaCO_3$  and  $AH_3$  hydrate was detected.

XRD analysis was performed on non-carbonated and carbonated samples cured at 20°C and at 38°C. The results are shown in Figure 4.11 and Figure 4.13. Similarly, as for sample with slag, higher peak intensity of metastable hydrate  $CAH_{10}$  was detected in non-carbonated sample and lower peak intensity in carbonated sample. The lower peak intensity indicates carbonation of metastable  $CAH_{10}$  hydrate. Also, strätlingite hydrate was detected in both samples, at lower and higher diffraction angles. In both samples stable hydrogarnet and  $AH_3$  hydrate were detected. Two polymorphs of calcium carbonate were found: aragonite and vaterite. For the sample with calcined clay cured at 38°C, a higher peak intensity was

detected for metastable hydrate  $CAH_{10}$  before carbonation compared to the carbonated sample. Furthermore, similarly as in the carbonated sample cured at  $20^{\circ}\text{C}$ , polymorphs of calcium carbonate, aragonite and vaterite were detected.

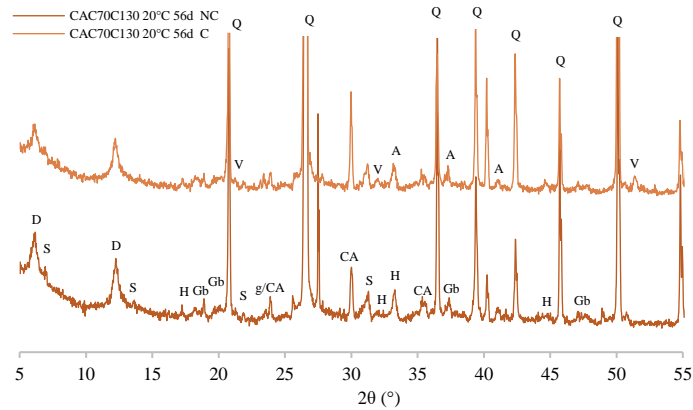


Figure 4.12 Diffractogram for non-carbonated and carbonated CAC70C130  $20^{\circ}\text{C}$  mix (CA=monocalcium aluminate, D= $CAH_{10}$ , Gb=AH3, G=Gehlenite, S=Strätlingite, H= $C_3AH_6$ , O= $C_2AH_8$ , Q=quartz, A=aragonite, C=calcite, V=vaterite)

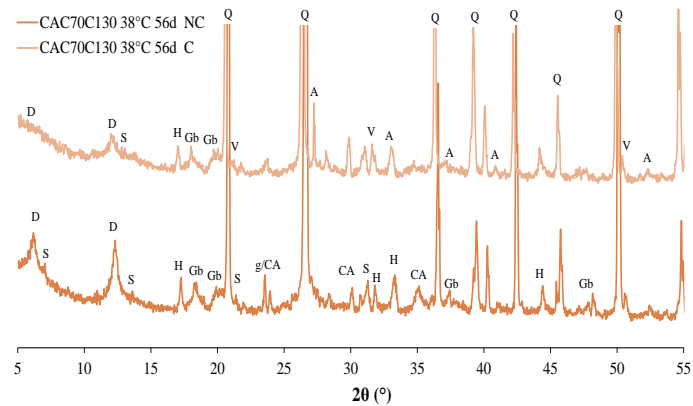


Figure 4.13 Diffractogram for non-carbonated and carbonated CAC70C130  $38^{\circ}\text{C}$  mix (CA=monocalcium aluminate, D= $CAH_{10}$ , Gb=AH3, G=Gehlenite, S=Strätlingite, H= $C_3AH_6$ , O= $C_2AH_8$ , Q=quartz, A=aragonite, C=calcite, V=vaterite)

#### 4.2.4 Pore structure changes during carbonation

The porosity measurements were conducted on non-carbonated samples and carbonated samples after 56 days of carbonation. The results of total porosity and pore volume distribution of reference CAC100 mix are shown in Figure 4.14. The non-carbonated part of

CAC100 sample cured at 20°C had lower total accessible porosity after 56 days of curing (11.35 %) compared to same mix cured at 38°C (12.92 %). Porosity of non-carbonated and carbonated samples, as well as average pore diameter are shown in Table 4.1. The carbonated part of both samples has a lower total porosity after 56 days of carbonation. Maximum intrusion volume significantly decreased for CAC100 20°C sample after carbonation. Also, the average pore diameter of this sample decreased after carbonation. In the case of CAC100 38°C sample two peaks are visible in non-carbonated sample, and after carbonation the pore volume decreases, and one peak remains. Figure 4.15 shows the results of total porosity and pore volume distribution of CAC70S130 mix. Replacement of 30% of CAC with slag decreases total porosity of non-carbonated samples for around 4 % for both curing regimes. Also, after carbonation only minor changes can be noticed. Furthermore, replacement of CAC with 30% of calcined clay also decreases total porosity of CAC based mortar. Figure 4.16 shows the results of total porosity and pore volume distribution of CAC70C130 mix. Mixes with calcined clay have higher porosity compared to mixes with slag for both non-carbonated and carbonated samples. However, the porosity of these mixtures is still lower compared to the reference mixture.

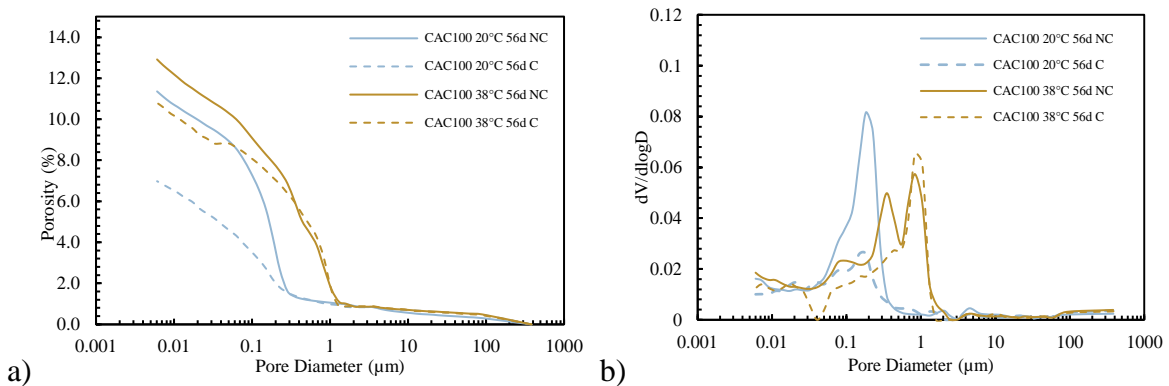


Figure 4.14 CAC100 mix: a) Total porosity for non-carbonated and carbonated samples, b)  $dV/d\log D$

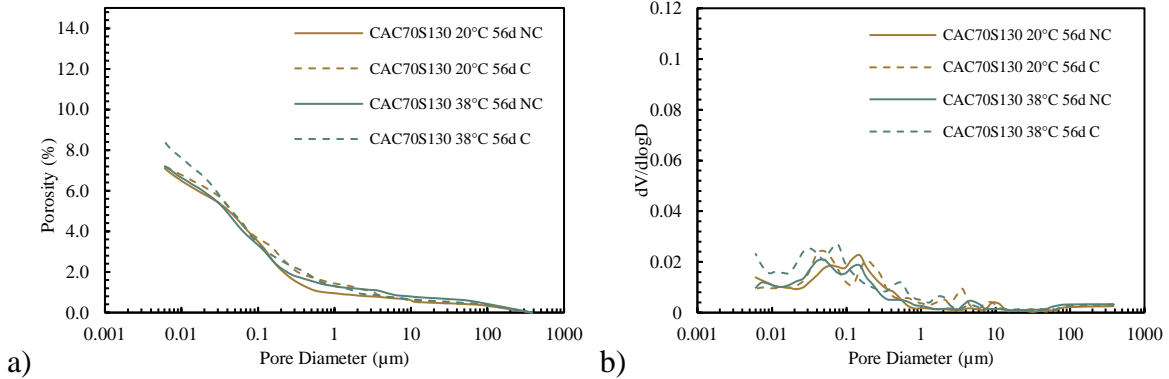


Figure 4.15 CAC70S130 mix: a) Total porosity for non-carbonated and carbonated samples, b)  $dV/d\log D$

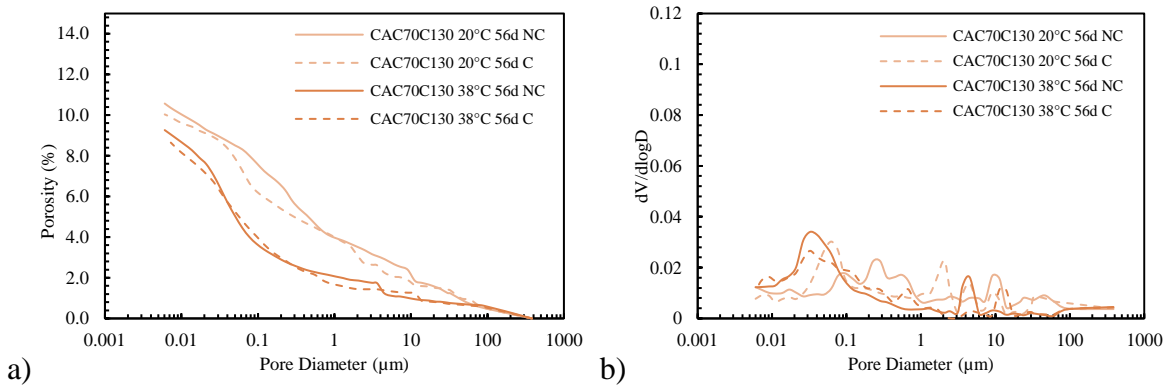


Figure 4.16 CAC70C130 mix: a) Total porosity for non-carbonated and carbonated samples, b)  $dV/d\log D$

Table 4.1 Total porosity and average pore diameter values of non-carbonated and carbonated samples

Mix	Porosity (%)	Average pore diameter (nm)
CAC100 20°C	NC 11.35	49.67
	C 6.98	38.72
CAC100 38°C	NC 12.92	55.62
	C 10.8	57.07
CAC70S130 20°C	NC 7.1	36.65
	C 7.22	42.96
CAC70S130 38°C	NC 7.19	37
	C 8.41	31.97
CAC70C130 20°C	NC 10.57	60.68
	C 10.03	62.63
CAC70C130 38°C	NC 9.27	35.74
	C 8.83	35.9

### 4.3 Discussion

Once CAC100 20°C was exposed to prolonged curing between 28 and 56 days the average compressive strength decreased from 104 MPa to 102.5 MPa, however, the error bars indicate that this may not be a statistically significant difference. Once CAC was exposed to significant levels of CO<sub>2</sub>, carbonation started to occur. It was reported in the literature

[3][39][77] that  $CAH_{10}$  hydrate reacts with carbon dioxide to form  $AH_3$  and  $CaCO_3$ . Metastable hydrate  $CH_{10}$  has significant influence on carbonation process of CAC; the more  $CAH_{10}$  is in the system, the system is more resistant to carbonation [4]. Since in the case of CAC cured at  $20^\circ\text{C}$ , there is a significant availability of metastable  $CAH_{10}$  hydrate, it reacts first, leading to formation of  $AH_3$  and carbonates. When most of this hydrate carbonates, the remaining hydrates participate in the carbonation process. In that case, TGA results as well as XRD indicate that metastable hydrates reform, together with  $AH_3$  and carbonates. Nevertheless, despite the visible carbonation and formation of metastable hydrates and carbonates, the compressive strength of the CAC100  $20^\circ\text{C}$  mix significantly decreased after 56 days of carbonation (Figure 4.4).

In previous studies it was confirmed that CAC carbonates in the presence of  $CO_2$ , however it was not investigated how CAC in which conversion process occurred behaves under the influence of  $CO_2$ . During curing at  $38^\circ\text{C}$ , conversion process is accelerated, which is evident from the phase transformation and significant loss in compressive strength of CAC cured at  $38^\circ\text{C}$  compared to the compressive strength at  $20^\circ\text{C}$ . After 56 days of exposure to  $CO_2$ , higher carbonation depth was detected for CAC cured at  $20^\circ\text{C}$  compared to the same mix cured at  $38^\circ\text{C}$ , which underwent conversion. Table 4.2 shows parameters quantified from thermogravimetric analysis before and after 56 days of accelerated carbonation. Before carbonation sample cured at  $20^\circ\text{C}$  had higher amount of metastable hydrates (3.14 %), and sample cured at  $38^\circ\text{C}$  has higher amount of stable hydrates (8.36 %). It was expected that metastable hydrate  $CAH_{10}$  will react first because of its high solubility ( $K_s=10^{-7.6}$ ), and then stable hydrogarnet with lower solubility ( $K_s=10^{-22.3}$ ) would react [35]. A higher proportion of cubic phases ( $AH_3$  and  $C_3AH_6$ ) before carbonation provides higher carbonation resistance

due to its better crystalline symmetry compared to hexagonal phases ( $\text{CAH}_{10}$  and  $\text{C}_2\text{AH}_8$ ) [78]. Further, a higher amount of water is produced by the carbonation of metastable hydrates, and higher amount of  $\text{CO}_2$  can react, which makes carbonation reaction faster [78]. Sample cured at  $38^\circ\text{C}$  experienced almost complete conversion from metastable to stable hydrates before carbonation, which means there were no available metastable hydrates for carbonation. In this case, it seems stable hydrogarnet carbonated to form metastable hydrates ( $\text{CAH}_{10}$  and  $\text{C}_2\text{AH}_8$ ) and calcium carbonate. The formation of calcium carbonate polymorphs is influenced by the kinetics of carbonation. Goni et al. [35] reported that under accelerated carbonation conditions, vaterite and aragonite are the predominant polymorphs formed in CAC samples. Also, predominantly aragonite was formed in carbonated part of the sample, however with higher peak intensities than in the same mix cured at  $20^\circ\text{C}$ . Quantitative TG analysis determined that the formed  $\text{CaCO}_3$  for CAC mixture cured at  $38^\circ\text{C}$  was 5.96 %, significantly higher than for other mixes with less than 2 % (Table 4.2). Park et al. [39] observed that during carbonation curing of CAC paste, metastable hydrates are mostly absent, and water is produced during carbonation. However, in present study XRD analysis confirmed that carbonation of CAC based mortar led to the reformation of metastable hydrates. Also, when images of samples sprayed with phenolphthalein are compared (Figure 4.2) it can be noticed that only for CAC mixed cured at  $38^\circ\text{C}$  the colour of the indication of the non-carbonated part is pale purple. The reason for this could be formation of higher amount of  $\text{AH}_3$  and  $\text{C}_3\text{AH}_6$  phase after curing at  $38^\circ\text{C}$ . These two hydrates have a lower initial pH of 11.97, compared to the metastable hydrates with pH from 12.5 to 12.7 [4]. After exposure to  $\text{CO}_2$  pH of dissolution of metastable phases will be 11.35, and for stable phases 10.8 [35]. Hence, a sample where stable hydrates additionally carbonate could have a weaker

reaction to the phenolphthalein indicator. For reference mixtures cured at both curing regimes, total accessible porosity decreased after 56 days of carbonation. The faster development of the conversion process in the sample cured at 38°C caused greater porosity and average pore diameter in the non-carbonated part of the sample. By carbonation, new hydrates that are forming likely fill some pores created during conversion in cement matrix lowering the total accessible porosity.

Further supporting this, the reference mixture cured at 38°C showed an increase in compressive strength from 40 MPa before to 65 MPa after carbonation likely due to the formation of calcium carbonate polymorphs that were filling the pores. There is also potential for reformation of metastable hydrates during carbonation as evidenced by XRD. On the contrary, reference mixture cured at 20°C experienced a decrease in compressive strength after carbonation although the total porosity only slightly decreased. The reason for the loss in strength could therefore be attributed to the carbonation of metastable hydrates and reduced formation of calcium carbonate compared to the mixture cured at 38°C.

It was reported that in combination with OPC, carbonation rate increases with increasing slag content [79], however no information is available on the influence of slag on the carbonation rate of CAC. Both samples with slag in the present study had higher depth of carbonation regardless of curing temperature compared to the reference sample without slag. Similarly to reference mixture, after 56 days of carbonation samples cured at 20°C had higher carbonation depth. However, more calcium carbonate was detected for samples cured at 38°C. Also, in system with slag after curing at 38°C more stable hydrates are formed before carbonation, and this system had slower carbonation rate. The formation of strätlingite hydrate was detected for both curing regimes before carbonation, but after 56 days of



carbonation higher peak intensity for strätlingite hydrate was detected for sample cured at 20°C. Exposure of CAC with slag substitution to CO<sub>2</sub> therefore led to carbonation of metastable hydrate CAH<sub>10</sub> and stable hydrogarnet, and formation of calcium carbonate polymorphs as well as formation of C<sub>2</sub>AH<sub>8</sub> at higher temperatures. Accelerated carbonation of mixes with 30% slag has minimal impact on total porosity. The total porosity slightly decreases, whereas compressive strength slightly increases. Overall, these minor changes in the microstructure enhance the stability of these mixes compared to the reference. The compressive strength of both mixtures increased for 10 % after 56 days of carbonation. Therefore, during carbonation of CAC with the addition of slag, transformation from metastable to stable hydrates occurred, which was not accompanied by the loss of compressive strength.

Similarly as for slag, with increasing replacement percentage of OPC with calcined clay, carbonation rate increases [80]. This present study confirmed that carbonation rate also increased in CAC systems when cement is replaced by calcined clay. Sample with calcined clay cured at 20°C had the highest carbonation depth compared to all samples studied. It can be noticed that sample with the highest carbonation depth also has the lowest amount of stable hydrogarnet before carbonation. As already mentioned, larger quantities of C<sub>3</sub>AH<sub>6</sub> hydrate increases carbonation resistance due to its lower solubility. Carbonation of CAH<sub>10</sub> and C<sub>3</sub>AH<sub>6</sub> hydrate for sample cured at 20°C leads to the formation of AH<sub>3</sub>, CaCO<sub>3</sub>, and C<sub>2</sub>AH<sub>8</sub> at higher temperatures. Carbonation of CAH<sub>10</sub> hydrate for sample cured at 38°C resulted in formation of AH<sub>3</sub> and C<sub>3</sub>AH<sub>6</sub>, as well as CaCO<sub>3</sub> and C<sub>2</sub>AH<sub>8</sub> at higher temperatures. Similar to the samples with slag, there were slight changes in total porosity evident during carbonation. The average pore diameter was significantly higher for the

sample cured at 20°C, than the sample cured at 38°C. The probable reason for this is that curing at 20°C slows down the hydration process of the clay, while curing at 38°C accelerates hydration, promotes a higher degree of reaction and leads to a smaller average pore diameter. The compressive strength is increased after carbonation, but in slower rate than mix where 30% of CAC is replaced by slag. Therefore, during carbonation transformation from metastable  $CAH_{10}$  to stable hydrates occurred, which was not accompanied by the loss of compressive strength.

Table 4.2 Parameters quantified from thermogravimetric analysis before and after 56 days of accelerated carbonation

Hydrate		CAC100	CAC100	CAC70S130	CAC70S130	CAC70C130	CAC70C130
		20°C	38°C	20°C	38°C	20°C	38°C
<b>Metastable hydrates (<math>CAH_{10}</math>, <math>C_2AH_8</math> (lt)) (%)</b>	NC	3.14	0.85	6.04	6.22	4.70	5.25
	C	6.38	4.3	4.39	4.25	4.67	4.66
<b>Strätlingite (<math>C_2ASH_8</math>) (%)</b>	NC	/	/	1.26	1.33	1.14	1.28
	C	/	/	0.94	1.15	1.13	1.29
<b>Stable hydrates (<math>AH_3</math>, <math>C_3AH_6</math>) (%)</b>	NC	5.39	8.36	2.11	2.82	2.33	2.81
	C	3.71	6.28	1.70	2.63	2.30	3.20
<b>Carbonates (%)</b>	NC	0.57	0.95	0.43	0.55	0.56	0.54
	C	0.95	5.96	1.33	1.70	2.10	1.44
<b><math>C_2AH_8</math> (ht) (%)</b>	NC	0.16	0.21	0.32	0.35	0.43	0.20
	C	0.55	0.76	1.10	0.82	1.27	1.23
<b>Total (%)</b>	NC	9.26	10.38	10.16	11.27	9.16	10.08
	C	11.59	17.30	9.46	10.56	11.48	11.83
<b>Aggregate (%)</b>	NC	89.93	89.41	88.88	87.62	89.91	89.16
	C	87.63	82.04	88.66	88.83	87.88	87.53
<b><math>\Sigma</math> (%)</b>	NC	99.19	99.79	99.04	98.88	99.07	99.24
	C	99.22	99.34	98.12	99.39	99.36	99.35

## 4.4 Conclusion

The objective of this study was to estimate the impact of accelerated carbonation on compressive strength development and changes in microstructure of CAC based mortar where part of the cement is substituted with slag or with calcined clay. The compressive strength was tested before and after carbonation, while microstructural changes due to carbonation were analysed using thermogravimetric analysis (TGA), mercury intrusion porosimetry (MIP), and X-ray diffraction (XRD).

Based on the results, several conclusions were drawn:

- Incorporating slag and calcined clay to CAC based mortar decreased resistance of mortar to carbonation compared to the reference sample cured at 20°C.
- Curing at 38°C for mixtures incorporating slag and calcined clay to CAC based mortar improved resistance to carbonation compared to those samples cured at 20°C. However, the carbonation depth was still greater in these samples compared to plain CAC mixtures cured at 20 or 38°C.
- Results of compressive strength showed that only a plain CAC reference sample cured at 20°C experienced decrease in compressive strength after 56 days of carbonation.
- Compressive strength of samples with slag and calcined clay increased after 56 days of exposure to CO<sub>2</sub>.
- Total accessible porosity of plain CAC mixture significantly decreased after carbonation, for both curing regimes, due to the formation of metastable hydrates and carbonates.

- Aragonite was the most prevalent polymorph of calcium carbonate formed in both plain CAC (reference samples) cured at 20°C and 38°C.
- Mixtures with slag and calcined clay addition did not experience major changes in microstructure after carbonation, which makes these mixtures more stable, in relation to compressive strength, compared to the reference mixture.
- During carbonation, transformation from metastable CAH10 to stable hydrates occurred in mixtures with slag and calcined clay, which was not accompanied by the loss of compressive strength.

## Chapter 5 Chloride transfer in CAC with slag/calced clay

### 5.1 Introduction

The durability of concrete can be compromised by the penetration of chlorides in marine environments or from de-icing salts. Chloride ions in the concrete structure can be free in the pore solution, adsorbed on surfaces, or react with hydration products to form new compounds [40]. Only the free ions in the pore solution are considered in the mechanism of chloride movement in concrete, as they are the only ones that affect corrosion processes [41]. The pore structure (e.g. size and tortuosity) and phase assemblage are the most important factor in chloride-induced corrosion [81][82]. The chloride binding capacity is an important parameter for evaluating the resistance of concrete to chloride penetration. A higher chloride binding capacity by the hydration products slows down the chloride transport through the concrete and leads to a lower degree of chloride-induced corrosion [42]. The chloride binding capacity of concrete depends on the phases containing aluminum. A high content of aluminum oxide ( $\text{Al}_2\text{O}_3$ ) in the chemical composition of calcium aluminate cement (more than 30%) enables the binding of chlorides in the concrete pores and reduces the degree of concrete corrosion. Chlorides react with the hydration products of CAC and form a new product in the form of Friedel's salt ( $3\text{CaO}\cdot\text{Al}_2\text{O}_3\cdot\text{CaCl}_2\cdot 10\text{H}_2\text{O}$ ) [43]. Friedel's salt is generally considered the most effective product formed that leads to chloride binding.

The pore structure of CAC cement is greatly influenced with the rate of the conversion process [83]. During initial hydration, metastable hydrates ( $\text{CAH}_{10}$  and  $\text{C}_2\text{AH}_8$ ) are formed. However, with prolonged hydration and especially at temperatures above  $30^\circ\text{C}$ , the metastable hydrates are transformed into stable hydrates ( $\text{C}_3\text{AH}_6$  and  $\text{AH}_3$ ) [84]. The

conversion process increases the porosity of the cement matrix, allowing a greater amount of different ions to penetrate it [85]. It is known that incorporating materials with high silica content can inhibit conversion process and prevent or reduce this increase in porosity[75][86]. Also, it was already established that both slag and calcined clay can increase the resistance of OPC to chloride penetration [87][88]. However, the influence of slag and calcined clay on the resistance of CAC to chlorides, especially when the conversion process occurs, has not yet been investigated in detail.

The main objective of this study was to determine the influence of slag and calcined clay on the chloride resistance of CAC based mortar before and after the conversion process. The replacement percentage of CAC with slag or calcined clay was 30%. Three mixtures were prepared: a reference mixture (labelled CAC100), a mixture with slag (labelled CAC70S130) and a mixture with calcined clay (labelled CAC70C130). Prior to exposure to a 16.5% sodium chloride solution, part of the samples was cured at 20°C and the rest of the samples at 38°C to accelerate the conversion process. The chloride resistance was determined using titration method. In addition, compressive strength and microstructural analysis (TGA, MIP) were investigated prior to exposure to chlorides.

## **5.2 Results**

### **5.2.1 Compressive strength**

The compressive strength was measured after 7 and 28 days of curing at two different temperatures. The results of the compressive strength measurements are shown in Figure 5.1. The compressive strength of the reference mixture cured at 20°C increased after 28 days of curing. The reference mixture cured at 38°C showed a lower compressive strength after 7 days of curing than the same mix cured at 20°C. A lower compressive strength indicates the

beginning of the conversion process. Furthermore, the compressive strength of the same mixture cured at 38°C decreased significantly after 28 days, which is due to the complete conversion of the metastable hydrates into stable hydrates (conversion process). The compressive strength of the mixture with slag replacement was constantly higher than that of the reference mixture cured at 20°C regardless of curing temperature. Although, by curing at 38°C, the strength slightly decreased after 28 days of curing. The mixture with calcined clay replacement exhibited a lower compressive strength for both testing periods compared to reference mixture cured at 20°C, for both curing regimes. A slight increase in compressive strength was observed for this mixture after 28 days of curing, at 20°C and 38°C. For both mixtures incorporating SCM, the strength at 28 days was 80 MPa or higher. The stable compressive strength of the slag and calcined clay mixtures indicates that the conversion process did not start during the 28-day curing period.

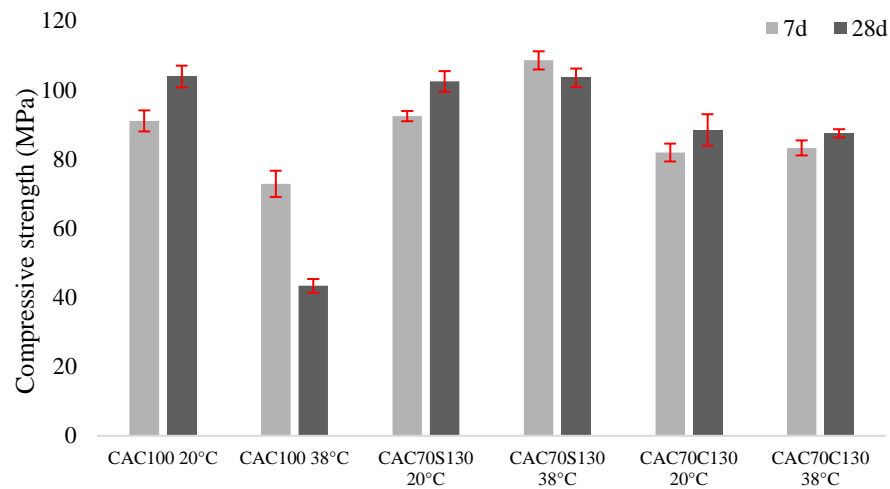


Figure 5.1 Compressive strength of each mixture after 7 and 28 days of curing

### 5.2.2 Thermogravimetric analysis

The thermogravimetric analysis was conducted after 28 days of curing at 20°C and 38°C. Figure 5.2 shows the DTG curves for all mixtures cured for 28 days at 20°C (a), and 38°C (b). For all mixtures cured at 20°C, metastable hydrates  $CAH_{10}$  and  $C_2AH_8$  were identified

at temperatures from 40°C to 130°C. Also, stable hydrates  $C_3AH_6$  and  $AH_3$  were observed at temperatures from 210°C to 290°C. In samples with slag and calcined clay, the formation of strätlingite hydrate was observed at temperatures from 150°C to 190°C. The highest peak intensity of metastable  $CAH_{10}$  was observed in the reference sample. The formation of this hydrate is related to the highest compressive strength of this mixture after 28 days of curing. Although less  $CAH_{10}$  was formed in the sample with slag, the compressive strength is the same as the reference sample. The reason for this is likely the formation of strätlingite, which densifies the cement matrix and contributes to the development of high compressive strength. The highest peak intensity for stable  $AH_3$  hydrate was detected in the sample with calcined clay, which may be the result of the slightly lower compressive strength after 28 days of curing at 20°C. The reference sample cured at 38°C, experienced almost complete conversion from metastable to stable hydrates for 28 days curing period (Figure 5.2b). Hence, the compressive strength of this sample is the lowest after 28 days of curing. The samples containing slag and calcined clay undergo the conversion process, but with a much lower intensity than the reference sample. This lower intensity is primarily due to the formation of stable strätlingite, which is stable at 38°C.

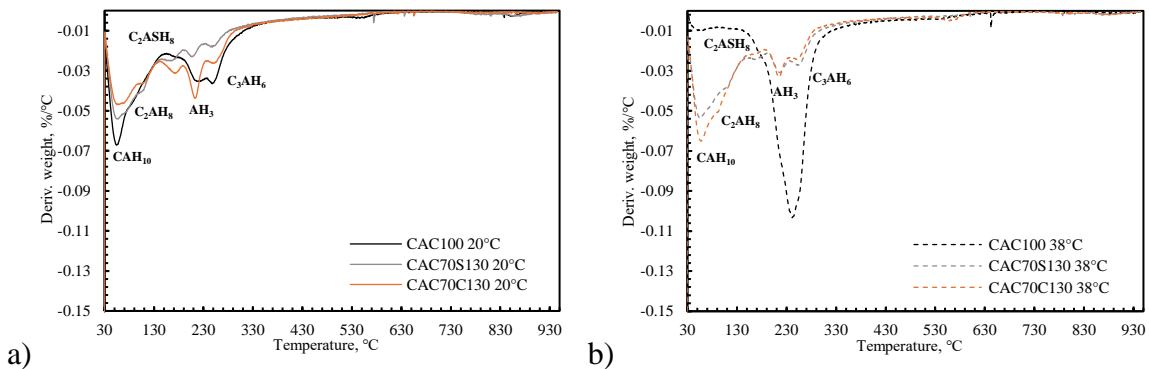


Figure 5.2 DTG curves of all mixes after 28 days of curing at (a) 20°C and at (b) 38°C



### 5.2.3 Mercury intrusion porosimetry

The porosity measurements were conducted after 28 days of curing at 20°C and 38°C. The results of the total porosity and pore volume distribution for all samples are shown in Figure 5.3. The values of total porosity, critical pore entry diameter and average pore entry diameter are shown in Table 5.1. The highest total porosity was detected for the reference mixture regardless of the curing regime. For the reference mixture cured at 20°C, the porosity was 12.37%, and for curing at 38°C, the porosity was 12.23 %. The reference mixture cured at 38°C, shows the highest mercury intrusion in the pore size range of 500 nm to 1500 nm, indicating significantly larger pore openings compared to other mixtures. Moreover, the critical pore entry diameter is significantly higher for reference mixture cured at 38°C compared to the other mixtures. By curing at 38°C, the plain calcium aluminate cement mixture undergoes a conversion process that increases the porosity of the cement matrix. The mixture with slag showed a lower total porosity compared to the reference mixture, namely 8.19% for curing at 20°C and 8.34% for 38°C. The same can be noticed for the mixture with calcined clay with porosity of 8.80% at 20°C, and 8.19% at 38°C. Furthermore, by curing at 38°C, critical pore entry diameter increases for mix with slag, and decreases for mix with calcined clay compared to curing at 20°C. Therefore, replacement of CAC by 30% of slag or calcined clay resulted in a reduction of the total accessible porosity by approximately 4%. Each mixture shows a different maximum of mercury intrusion depending on the curing regime.

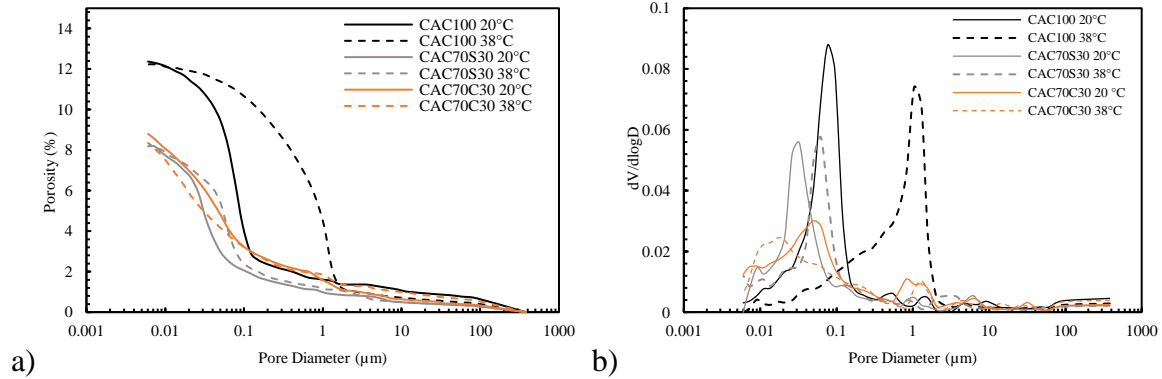


Figure 5.3 Results of a) Total porosity, b)  $dV/d\log D$

Table 5.1 Total porosity and average pore diameter values of non-carbonated and carbonated samples

	Total porosity (%)	Critical pore entry diameter (nm)	Average pore diameter (nm)
CAC100 20°C	12.37	79	54.82
CAC100 38°C	12.23	1100	162.56
CAC70S130 20°C	8.19	30	31.16
CAC70S130 38°C	8.34	60	38.29
CAC70C130 20°C	8.80	50	32.68
CAC70C130 38°C	8.19	19	29.4

#### 5.2.4 Chloride diffusion results

Chloride diffusion measurements were conducted after 28 days of curing at 20°C and 38°C. The samples were exposed to a sodium chloride solution for 35 days. Figure 5.4 shows the apparent diffusion coefficient of samples cured at 38°C relative to the apparent diffusion coefficient of samples cured at 20°C. Curing at 38°C increased the diffusion coefficient for all samples. However, the highest increase in diffusion coefficient was observed for the reference sample, while the smallest change occurred for the sample with calcined clay. Figure 5.5 shows the total (acid soluble), bound and free (water soluble) chloride content for the samples cured at 20°C and Figure 5.6 for the samples cured at 38°C. Bound chlorides were calculated as the difference between the total and free chloride content. The results

show that the total chloride content is significantly lower for reference sample initially cured at 20°C for every depth except for a depth of 2 mm below the exposed surface. The highest chloride content was detected for the mixture with calcined clay replacement. However, this sample had a higher amount of bound chlorides compared to the reference sample and the sample with slag replacement. When cured at 38°C, the reference sample had the lowest total chloride content compared to the samples with slag and calcined clay replacement. However, the samples with slag and calcined clay replacement showed a higher amount of bound chlorides. Figure 5.7 shows bound chloride content in relation to the total chloride content for CAC100 (a), CAC70S130 (b), and CAC70C130 (c) samples. The reference sample cured at 20°C had a higher percentage of bound chlorides than the samples that were cured at 38°C. The same can be noticed for samples with slag, but at a depth higher than 6.5 mm. However, samples with calcined clay replacement had a similar relation between bound and the total chlorides content for both curing regimes. The reference mixture cured at 20°C showed the highest percentage of bound chlorides from a depth of 6.5 mm below the surface. From this depth, all chlorides that penetrated the sample were bound. During curing at 20°C, predominantly metastable hydrates  $CAH_{10}$  and  $C_2AH_8$  are formed, which contribute to the higher chloride binding in the case of reference sample.

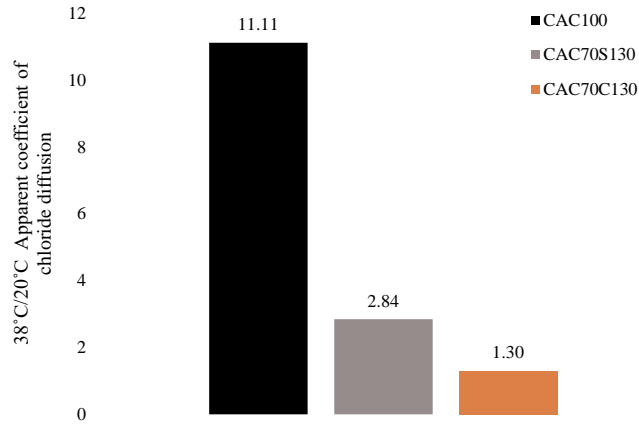


Figure 5.4 Apparent diffusion coefficient: relation between curing at 38°C and 20°C

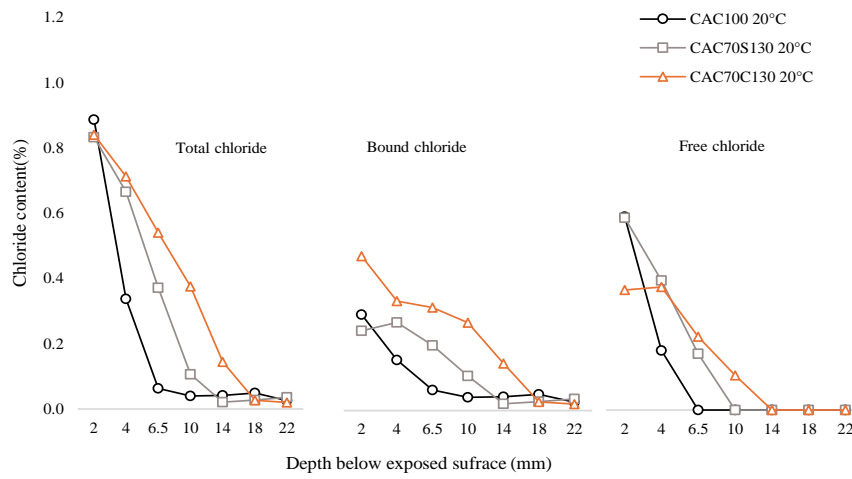


Figure 5.5 Total chloride content of each mixture cured at 20°C categorized into bound and free chloride content

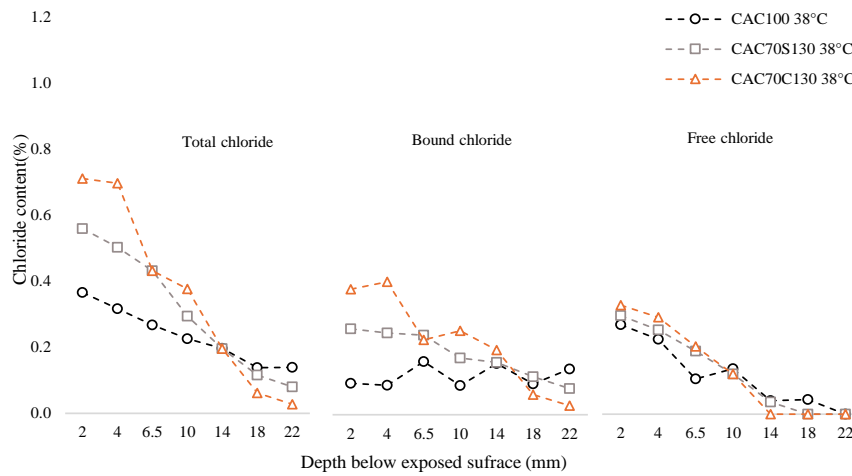


Figure 5.6 Total chloride content of each mixture cured at 38°C categorized into bound and free chloride content

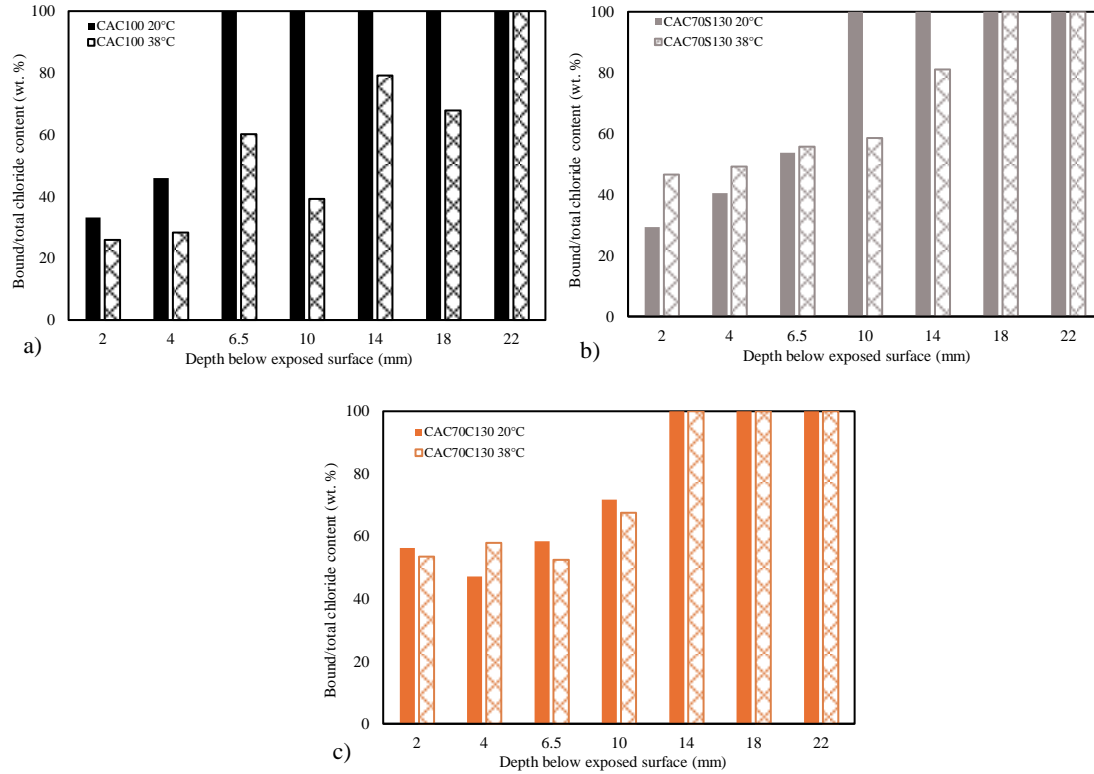


Figure 5.7 Bound chlorides in relation to total chlorides for: a) CAC100, b) CAC70S130, and c) CAC70C130 mixes

### 5.2.5 X-ray diffraction

Qualitative XRD analysis was performed on samples cured at 20°C and 38°C for 56 days and on samples exposed to NaCl for 35 days. For the samples exposed to sodium chloride, a depth of 10 mm below the exposed surface was chosen as the relevant measurement point. The results for the CAC100 sample cured at 20°C and 38°C are shown in Figure 5.8 and Figure 5.8b, respectively. The measurements were conducted on mortar samples containing siliceous standard sand. Since quartz has a high crystallinity, the peaks of the quartz in the XRD analysis results are much larger than the peaks of the hydrates found in CAC. In the sample CAC100 cured at 20°C, at the diffraction angles from 5° to 15°, the metastable hydrate CAH<sub>10</sub> was detected. Also, stable hydrogarnet and AH<sub>3</sub> hydrate were detected in the sample cured 56 days at 20°C. After exposure for 35 days in sodium chloride solution, the peak intensity for the metastable hydrate CAH<sub>10</sub> decreased and the peak intensity for the

stable hydrate increased. It should be noted that no Friedel's salt was detected after exposure of CAC mortar to sodium chloride solution. When CAC cement is exposed to NaCl solution, the chloride ions are mainly bound in Friedel's salt [43][89][90]. However, some researchers have pointed out that Friedel's salt is unstable and decomposes with an increasing of curing period [43][91]. The influence of carbonation should also be considered in the decomposition of Friedel's salt. Under the influence of carbonation, Friedel's salt is destabilized, which leads to the release of chlorides over time [92]. For sample CAC100 cured at 38°C, a very low peak intensity for metastable  $CAH_{10}$  hydrate was detected after 56 days of curing. This indicates that most of the metastable hydrates transformed into the stable ones. After exposure to sodium chloride solution, Friedel's salt was not detected, however a slight increase in peak intensity for metastable hydrate  $CAH_{10}$  was observed.

The XRD results for sample CAC70S130 cured at 20°C and 38°C<sub>b</sub> are shown in Figure 5.9a and Figure 5.9b, respectively. After 56 days of curing at 20°C, metastable hydrate  $CAH_{10}$  and strätlingite hydrate were detected at diffraction angles ranging from 5° to 15°. Also, a low peak intensity was detected for stable hydrogarnet and  $AH_3$  hydrate. After 35 days of exposure to NaCl, a lower peak intensity was detected for  $CAH_{10}$  hydrate, and no strätlingite hydrate was detected. In the sample with slag cured at 38°C, both  $CAH_{10}$  and strätlingite were detected after 56 days of curing, but with lower peak intensity than in the sample cured at 20°C. After exposure to NaCl solution,  $CAH_{10}$  was no longer detected, while the peak intensity for strätlingite was higher than before exposure. A lower peak intensity was also detected for hydrogarnet and  $AH_3$  after exposure to NaCl.

The XRD results for sample CAC70S130 cured at 20°C and 38°C<sub>b</sub> are shown in Figure 5.10a and Figure 5.10b, respectively. After 56 days of curing at 20°C, a high peak intensity was

detected for the metastable hydrate  $CAH_{10}$ . Also, the metastable hydrate  $C_2AH_8$  was detected, which was not the case for the other samples. After 35 days of exposure to NaCl, almost all the  $CHA_{10}$  hydrate decomposed, but the peak for strätlingite was detected as before exposure. The sample with calcined clay cured at  $38^\circ\text{C}$  also showed a very high peak for  $CAH_{10}$  hydrate. However, after exposure to the sodium chloride solution, no peaks were detected for either  $CAH_{10}$  hydrate or strätlingite.

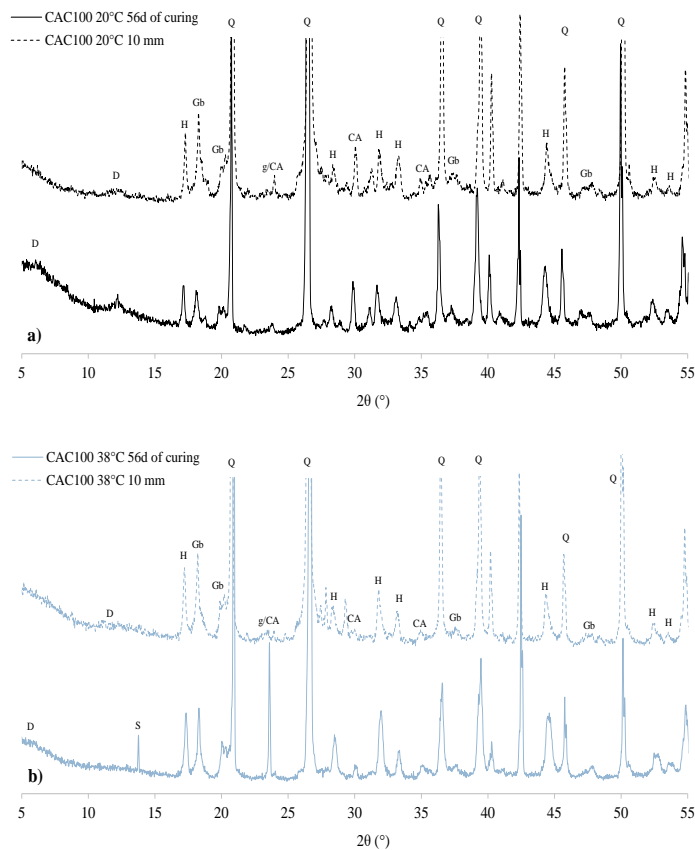


Figure 5.8 Diffractogram of samples cured 56 days in water and after exposure to NaCl: a) CAC100 20°C, b) CAC100 38°C (CA=monocalcium aluminate, D= $CAH_{10}$ , Gb=AH3, G=Gehlenite, H= $C_3AH_6$ , O= $C_2AH_8$ , Q=quartz, S=Strätlingite)

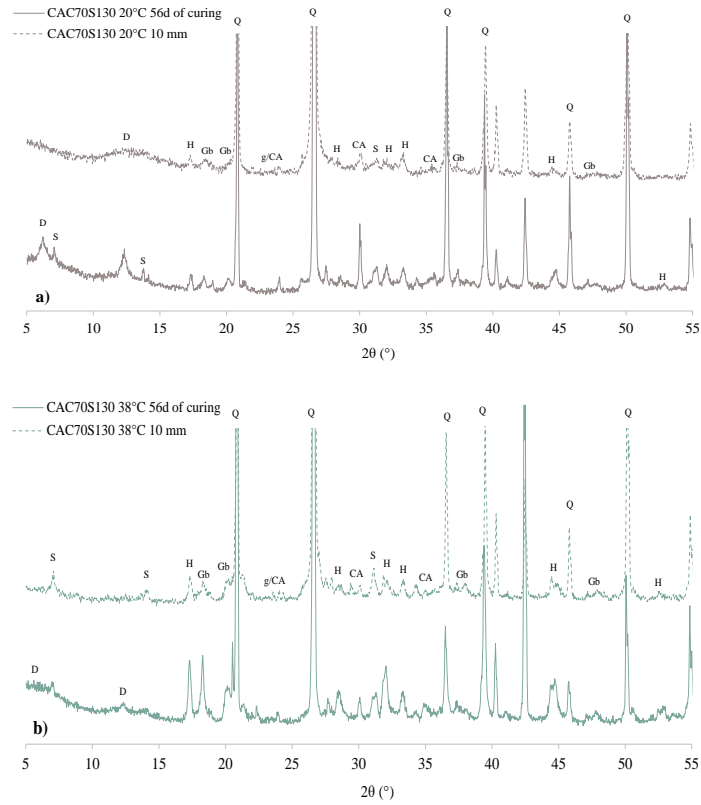
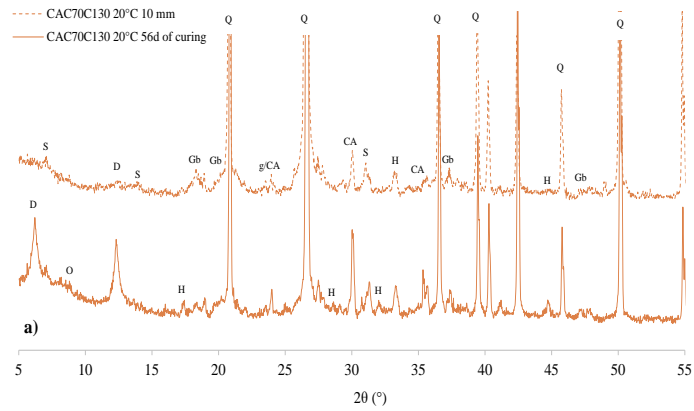


Figure 5.9 Diffractogram of samples cured 56 days in water and after exposure to NaCl: a) CAC70S130 20°C, b) CAC70S130 38°C (CA=monocalcium aluminate, D=CAH10, Gb=AH3, G=Gehlenite, H=C3AH6, O=C2AH8, Q=quartz, S=Strätlingite)





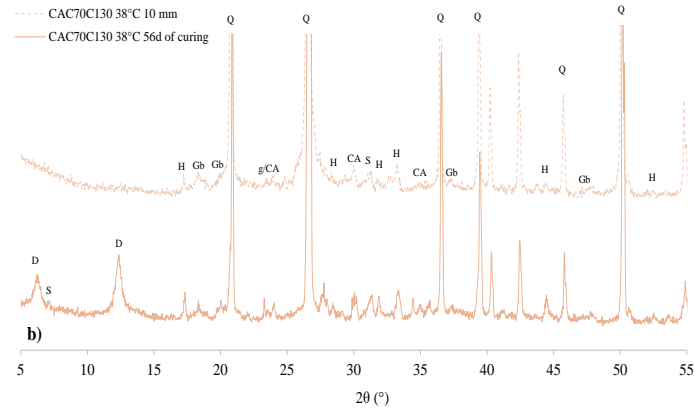


Figure 5.10 Diffractogram of samples cured 56 days in water and after exposure to NaCl: a) CAC70C130 20°C, b) CAC70C130 38°C (CA=monocalcium aluminate, D=CAH<sub>10</sub>, Gb=AH<sub>3</sub>, G=Gehlenite, H=C<sub>3</sub>AH<sub>6</sub>, O=C<sub>2</sub>AH<sub>8</sub>, Q=quartz, S=Strätlingite)

### 5.3 Discussion

The curing of calcium aluminate cement mortar at ambient temperatures (20°C) resulted in an increased compressive strength from the 7 to 28 days of curing. Increase in the compressive strength was detected both for samples without and with slag and calcined clay replacement. On the contrary, by curing at elevated temperatures (38°C) compressive strength of the reference sample decreased almost 60% between 7 and 28 days of curing. The compressive strength decrease indicated that a transformation from metastable hydrates to stable hydrates occurred. The replacement of slag resulted in a slight decrease in compressive strength, indicating that the conversion process occurred, but the effect was negligible. Furthermore, with the addition of calcined clay, a slight increase in compressive strength was observed when cured at 38°C. The stability of the compressive strength under 38°C indicated the formation of strätlingite hydrate. The metastable hydrates CAH<sub>10</sub> and C<sub>2</sub>AH<sub>8</sub> are predominantly formed during curing at 20°C in both samples without and with SCM replacement (Figure 5.2a). However, by curing at 38°C, the metastable hydrates were very rapidly converted to stable C<sub>3</sub>AH<sub>6</sub> and AH<sub>3</sub> hydrate in plain calcium aluminate cement

mortar (Figure 5.2b). Minor conversion was detected for the sample with slag, and no precipitation of metastable to stable hydrates was observed in the sample with calcined clay.

In literature the reaction of calcium aluminate phases with chloride ions produces Friedel's salt [91]. It is generally considered that a high level of  $Al_2O_3$  in CAC can contribute to chloride binding and lowering of chloride attack on the reinforcement [44][93]. The most likely hydrate to react with chloride ions in calcium aluminate cement is  $CAH_{10}$  [43]. When chloride ions penetrate the hydrated calcium aluminate cement matrix,  $OH^-$  in the structure of  $CAH_{10}$  is replaced and Friedel's salt is formed [91][43][45]. Nevertheless, the formation of Friedel's salt was not observed in any of the samples in this study. The reason for this could be the instability of the Friedel's salt during the prolonged curing period or destabilisation due to carbonation [43][92]. In the reference sample cured at  $20^\circ C$ , the metastable hydrate  $CAH_{10}$  was predominantly formed, which contributed to the lowest chloride ingress compared to the other samples. In the mixture cured at  $38^\circ C$ , the conversion process and increase in capillary porosity occurred [9][10]. It is assumed that a higher capillary porosity enables greater chloride ingress [94]. Certainly, higher porosity of the capillary pore size range of the reference sample cured at  $38^\circ C$  provided a path for faster penetration of chlorides. Therefore, the amount of chlorides was lower at the surface and higher at higher depths in the case of CAC cured at  $38^\circ C$  compared to the same sample cured at  $20^\circ C$ . Furthermore at this temperature,  $C_3AH_6$  hydrate was mainly formed, which participates in the reaction with chloride ions to form Friedel salt [91].

Previous studies have shown that the addition of slag to OPC increases resistance to chloride ingress, especially at a higher replacement percentage [87]. This study shows that the replacement of 30% slag increases chloride ingress into the calcium aluminate cement

matrix. The amount of  $\text{Al}_2\text{O}_3$  plays an important role when it comes to resistance to chloride penetration. The calcium aluminate cement used in this study contained approximately 53 %  $\text{Al}_2\text{O}_3$ , while the slag had significantly lower amount (11.7 %). The replacement of 30% of CAC with slag reduced the total amount to  $\text{Al}_2\text{O}_3$  and thereby may be responsible for the reduced resistance to the chloride ingress. Moreover, binding capacity of the sample with slag cured at 20°C was lower compared to the reference sample cured at 20°C. This could be due to the lower quantity of  $\text{CAH}_{10}$  and  $\text{C}_3\text{AH}_6$  formed in the sample with slag compared to the CAC sample (Figure 5.2a). On the contrary, the sample with slag cured at 38°C, had a higher binding capacity compared to the reference sample cured at 38°C. A higher amount of  $\text{CAH}_{10}$  hydrate was formed in the sample with slag, and higher amount of  $\text{C}_3\text{AH}_6$  hydrate in the reference sample (Figure 5.2b). The initial reaction with chloride ions is mainly carried out by the metastable hydrate  $\text{CAH}_{10}$  [43].

The literature shows that the addition of calcined clay in OPC also increases the chloride resistance of concrete [88]. On the contrary, in the present study it was found that a 30% replacement of CAC with calcined clay reduced the resistance to chloride ingress. Moreover, the sample with calcined clay replacement exhibited the highest chloride penetration both for curing at 20°C and at 38°C. By curing at 20°C the lowest peak intensity for  $\text{CAH}_{10}$  was detected for the calcined clay sample, but a higher binding capacity was determined for this sample compared to the sample with slag. In the sample with calcined clay, more strätlingite and  $\text{AH}_3$  formed, which may also react with chloride ions, but with a lower intensity than  $\text{CAH}_{10}$  hydrate. By curing at 38°C, the amount of bound chlorides was comparable to the sample cured at 20°C. Similarly to the sample with slag, the formation of  $\text{CAH}_{10}$  hydrate in the sample with calcined clay provided a high binding capacity.

Chloride transport through the cement matrix is strongly influenced by its capillary porosity. However, Sakai [95] reported a good correlation between total porosity and chloride ingress in mixtures without SCMs. In this study, it was shown that the replacement of slag and calcined clay reduce total porosity, capillary porosity, critical pore entry diameter and average pore entry diameter (Figure 5.3). However, chloride ingress was higher in the sample with slag and calcined clay than in the reference mixture with higher porosity. This indicates that the phases formed during the hydration of calcium aluminate cement have a greater influence on chloride transport in CAC than the porosity of this matrix.

#### **5.4 . Conclusion**

The main objective of this study was to determine influence of slag and calcined clay on chloride transfer in CAC based mortar under the influence of ambient and elevated curing temperature. Chloride resistance was assessed through titration method and apparent diffusion coefficient.

The following conclusion were drawn:

- The reference CAC sample showed the highest resistance to chloride ingress; however, the conversion process significantly reduced the resistance, i.e. the apparent diffusion coefficient of the converted mixture was 11 times higher than that of the non-converted mixture.
- The samples containing slag and calcined clay showed a higher ingress of chlorides compared to the reference sample. Following the conversion process, the resistance to chloride penetration decreased, although this reduction was not as significant as in the CAC100 mixture.

- The formation of  $\text{CAH}_{10}$  hydrate enhanced the binding of chlorides in all samples, except in the reference sample cured at  $38^{\circ}\text{C}$ . In this sample the  $\text{CAH}_{10}$  hydrate was consumed due to the conversion process.
- It was found that the phases formed during the hydration of calcium aluminate cement have a greater influence on chloride transport in CAC than the porosity of that matrix. Even with lower porosity, samples with slag and calcined clay showed higher chloride ingress.

## **Chapter 6 Sulphate and acid resistance of CAC with slag/calced clay**

### **6.1 Introduction**

Concrete is the most important building material, and its durability can be severely impaired by the influence of aggressive substances from the environment. The resistance to aggressive substances from the environment greatly depends on the hydration products and the porosity of the cement matrix [29]. The penetration of aggressive sulphates into the concrete structure is one of the factors that causes the formation of ettringite, monosulphate and gypsum [30]. During hydration of Ordinary Portland cement (OPC) calcium hydroxide is formed. Calcium hydroxide is very reactive in the presence of sulphates and acids leads to the formation of gypsum [22][31]. This process contributes to the expansion and subsequent cracking of the concrete. Additionally, the amount of monosulphate formed depends on the proportion of tricalcium aluminate (C3A) in the Portland cement [32]. To reduce the impact of aggressive sulphates, sulphate resistant cement (sulphate resistant cement-SR) was produced. The C3A content in sulphate-resistant cement is less than 5%, which contributes to improved durability and reduced formation of secondary ettringite [31]. CAC was originally produced to increase the resistance of OPC to external sulphates, chlorides and acids [5]. Enhanced resistance of CAC cement to aggressive sulphates and acids is achieved by the absence of CH, the presence of the protective  $AH_3$  gel and the low reactivity of its hydration products (particularly  $CAH_{10}$  hydrate) [32]. CAC, during its hydration, undergoes a conversion process, forming hydrates that are more prone to reaction with sulphates and acids [22]. The occurrence of the conversion process depends on the temperature and relative humidity of the environment. At ambient temperatures, metastable hydrates ( $CAH_{10}$  and  $C_2AH_8$ ) are

initially formed providing high early strength of CAC cement [7]. When the temperature increases (above 30°C), the rapid formation of stable hydrate  $C_3AH_6$  and  $AH_3$  occurs [6]. Furthermore, the conversion process induces porosity alternations of the cement matrix and increases and enables greater penetration of substances from the environment. Compared to OPC, the metastable and stable hydrates that are formed during hydration of CAC are more stable in the presence of sulphates and acids than the hydration products of OPC [23].

Previous studies have reported that supplementary cementitious materials (SCMs) with high silica content can inhibit the conversion process of CAC [14][15][96]. During the reaction of metastable hydrate  $C_2AH_8$  and silica, strätlingite ( $C_2ASH_8$ ) is formed. The formation of this new hydrate further fills the pores, reducing porosity and increasing compressive strength under the influence of high temperatures. The formation of strätlingite, is expected to reduce the amount of stable CAC hydrates. Ground granulated blast furnace slag is a commonly used SCM for mitigating conversion in CAC [12]. However, the availability of slag is increasingly becoming a global problem [97]. Calcined clay is a natural material that is available in large quantities and due to its chemical composition (high quantity of  $Al_2O_3$  and  $SiO_2$ ), it can be a promising material for use in CAC. The possibility of using mineral additives to prevent an increase in porosity and a decrease in compressive strength is certainly an advantage, but it remains to be determined whether these materials affect the durability of CAC.

The main objective of this research is to understand the mechanism of degradation of CAC caused by sodium sulphate solution and sulphuric acid solution with partial replacement by slag or calcined clay. The replacement percentage of CAC by slag or calcined clay was 30%. The reference mixture was prepared with 100% CAC. Before exposure to sodium sulphate

solution and sulphuric acid solution, one group of samples was cured at 20°C while the other group was cured at 38°C to accelerate the conversion process. The influence of these solutions was evaluated on non-converted (cured at 20°C) and converted samples (cured at 38°C). The mass changes of each sample were recorded after a certain exposure time. To assess the influence of sulphates and acids on the mechanical properties, the compressive strength was tested before exposure and each defined exposure time. In addition, microstructure changes were investigated by thermogravimetric analysis (TGA), mercury intrusion porosimetry (MIP), and X-ray diffraction (XRD).

## 6.2 Results

### 6.2.1 Analysis of samples after exposure to sodium sulphate

#### 6.2.1.1. *Visual observations and mass change*

The samples were observed regularly to detect changes in colour, texture, the appearance of cracks or other visible signs of degradation. Figure 6.1 shows the photographs of the prism (4x4x16 cm) samples before and after 56d exposure to sodium sulphate for the reference mixture for both curing temperatures. It was observed that for both samples, after 56 days of exposure, the most degradation is at the edges of the sample, where material loss occurred. No cracks were observed for both curing temperatures. Along with the visual observations, the change in mass was measured for all samples during the 91-day of exposure to sodium sulphate. The results of the change in mass after the specified exposure time compared to the initial mass measured before exposure are shown in Figure 6.2. The reference sample, and samples with slag and calcined clay initially cured at 20°C showed continuous gain in mass during exposure to sodium sulphate. Samples that were cured at 38°C before exposure have an increase in mass during the first 7 days of exposure. Then, from the 7<sup>th</sup> to the 21<sup>st</sup> day of exposure, the mass of these samples decreases slightly, and by the 91<sup>st</sup> day of exposure, it



increases again. Samples cured at higher temperatures before exposure have a continuously lower mass increase during exposure to sodium sulphate solution. Furthermore, samples with slag and calcined clay have a similar trend of mass increase as the reference mixture for both curing temperatures.

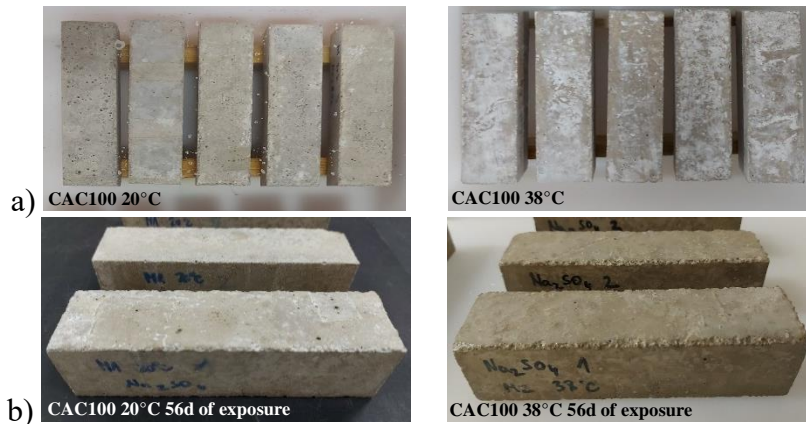


Figure 6.1 Visual observation of CAC100 sample: a) before exposure, b) after 56d of exposure to  $Na_2SO_4$

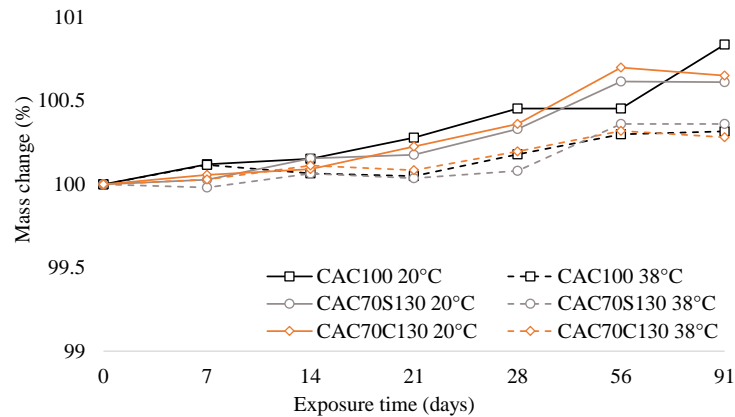


Figure 6.2 Mass change of all samples during exposure to  $Na_2SO_4$

### 6.2.1.2. Compressive strength development

The compressive strength was tested over 91 days of exposure. In addition, the compressive strength was tested after 28 days of curing and serves as the initial value of the compressive strength before exposure to the sodium sulphate solution. The results of the compressive strength are shown in Figure 6.3. The reference mixture cured at 20°C before exposure, had the highest compressive strength. However, after 21 days of exposure, the compressive

strength of this mixture decreased, and after 28 days of exposure, it increased. On the contrary, the same mixture cured at 38°C before exposure had the lowest initial compressive strength due to occurrence of the conversion process during curing at 38°C. The compressive strength of this mixture increased continuously during exposure to sodium sulphate. The mixture with slag initially cured at 20°C showed a continuous increase in compressive strength during exposure, while the compressive strength of the same mixture, initially cured at 38°C, decreased after 21 days of exposure. After 91 days of exposure the compressive strength of both mixtures with slag is comparable and higher than that of the reference mixture cured at 20°C. A mixture in which 30% of the CAC cement is replaced by calcined clay shows no significant changes in strength during exposure to sodium sulphate solution and this applies to both exposure temperatures prior to exposure. The mixture with calcined clay is the most stable in terms of compressive strength changes during exposure to sodium sulphate solution. Figure 6.4 shows the comparison of the compressive strength for samples after 56 days of curing at 20°C and 38°C and samples after 28 days of exposure to sodium sulphate solution. The compressive strength of the reference mixture was higher after exposure than after curing in water for both curing regimes. For mixtures with slag and calcined clay, the strength after curing and exposure was similar. However, for the samples initially cured at 38°C, compressive strength decreased slightly after 28 days of exposure to sodium sulphate.

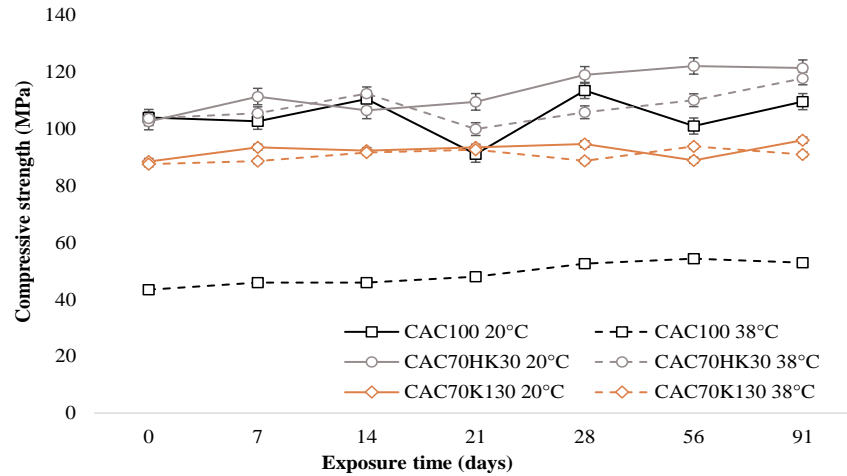


Figure 6.3 Compressive strength development during exposure to Na<sub>2</sub>SO<sub>4</sub>

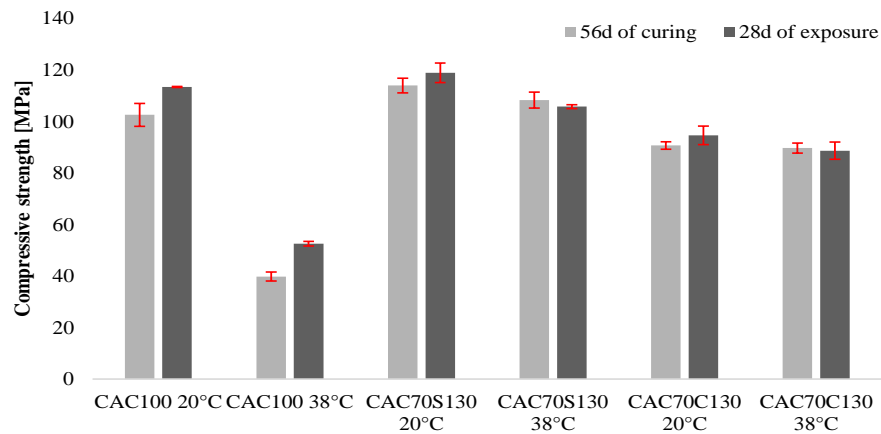


Figure 6.4 Compressive strength values after 56 days of curing and 28 days of exposure to Na<sub>2</sub>SO<sub>4</sub>

### 6.2.1.3. Microstructural changes during exposure to Na<sub>2</sub>SO<sub>4</sub>

#### Calcium aluminate cement

Figure 6.5 shows the DTG curves for the CAC100 mixture cured at 20°C (a) and 38°C (b) after 56 days of curing and after 28 days of exposure to sodium sulphate. A curing duration of 56 days in water corresponds to the same period as 28 days of exposure, as the samples were immersed in the solution only after the initial curing of 28 days. For the reference mixture cured at 20°C for 56 days, metastable hydrates CAH<sub>10</sub> and C<sub>2</sub>AH<sub>8</sub> were identified, as well as the stable hydrate C<sub>3</sub>AH<sub>6</sub> and AH<sub>3</sub> hydrate. For the same mixture exposed to sodium sulphate solution, the peak intensity for the metastable hydrate, and AH<sub>3</sub> hydrate was

higher. The reference mixture cured at 38°C for 56 days, experienced almost complete conversion of the metastable hydrates to stable hydrates compared to curing at 20°C. The DTG curve for this mixture shows slightly higher peak intensity for the metastable hydrate  $\text{CAH}_{10}$  and the stable hydrate  $\text{C}_3\text{AH}_6$  and a lower peak intensity for  $\text{AH}_3$ .

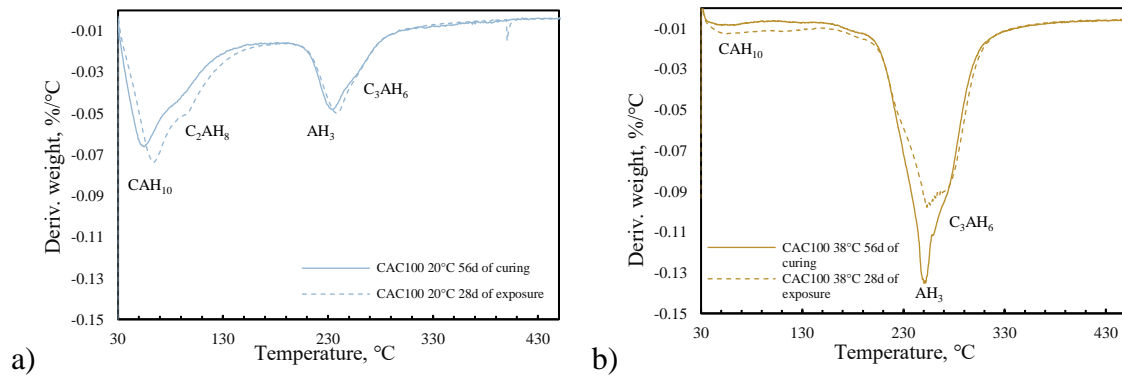


Figure 6.5 DTG curves of non-exposed and samples after 28 days of exposure to  $\text{Na}_2\text{SO}_4$  for CAC100 mix cured (a) at 20°C and at (b) 38°C

#### Calcium aluminate cement with slag

Figure 6.6 shows the DTG curves for a mixture where 30% of the CAC cement was replaced by slag, cured at 20°C (a) and 38°C (b) after 56 days of curing and 28 days of exposure to sodium sulphate solution. The addition of slag to CAC cement enhances the formation of strätlingite ( $\text{C}_2\text{ASH}_8$ ) hydrate. The decomposition of strätlingite is visible from 150°C to 190°C. Metastable and stable hydrates that normally appear in CAC cement were also detected. For the mixture cured at 20°C, a lower peak intensity is detected for metastable hydrates and a higher peak intensity for  $\text{AH}_3$  hydrate after 28 days of exposure. Also, a slightly higher peak intensity was detected for the stable  $\text{C}_3\text{AH}_6$  hydrate. Similar results were obtained for the same mixture cured at 38°C. A lower peak intensity was detected for metastable hydrates and a higher for  $\text{AH}_3$ . In this case, a lower peak intensity was detected for strätlingite and  $\text{C}_3\text{AH}_6$  hydrate after 28 days of exposure to sodium sulphate solution.

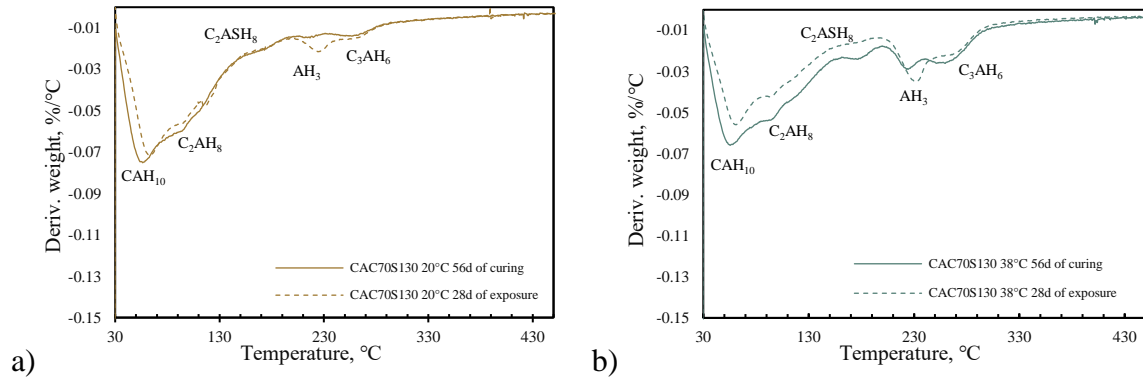


Figure 6.6 DTG curves of non-exposed and samples after 28 days of exposure to  $\text{Na}_2\text{SO}_4$  for CAC70S130 mix cured (a) at 20°C and at (b) 38°C

#### Calcium aluminate cement with calcined clay

Figure 6.7 shows the DTG curves for mix where 30% of the CAC was replaced by calcined clay cured at 20°C (a) and 38°C (b) after 56 days of curing and after 28 days of exposure to sodium sulphate. After 28 days of exposure, a higher peak intensity for both metastable hydrates and stable hydrates was detected. Also, a slightly higher peak was detected for strätlingite hydrate. In the case of the mixture cured at 38°C, only the metastable hydrate CAH<sub>10</sub> shows a lower peak intensity after 28 days of exposure. Metastable C<sub>2</sub>AH<sub>8</sub> and stable C<sub>3</sub>AH<sub>6</sub> and strätlingite have the same peak intensity as curing for 56 days in water at 38°C. Additionally, the hydrate AH<sub>3</sub> has slightly higher peak intensity after 28 days of exposure to sodium sulphate.

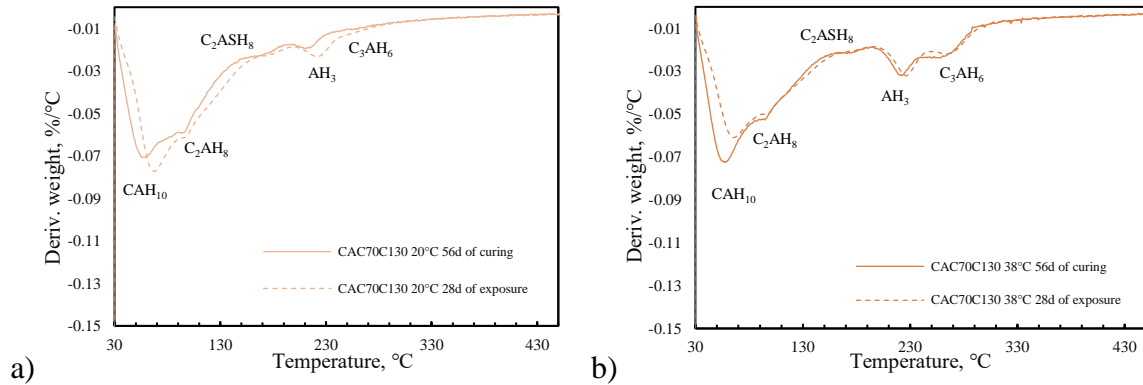


Figure 6.7 DTG curves of non-exposed and samples after 28 days of exposure to  $\text{Na}_2\text{SO}_4$  for CAC70C130 mix cured (a) at  $20^\circ\text{C}$  and at (b)  $38^\circ\text{C}$

## 6.2.2 Analysis of samples after exposure to sulphuric acid

### 6.2.2.1 Visual observations and mass change

The samples were exposed to sulphuric acid for a total of 91 days. After each exposure period, a visual inspection of the samples was conducted to note changes in colour, texture, the appearance of cracks, or other visible signs of degradation. Figure 6.8 shows the photographs of the prism (4x4x16 cm) reference samples after 7 days and 28 days of exposure to  $\text{H}_2\text{SO}_4$  solution for both curing temperatures. It can be observed that already after one week of exposure there is loss of materials on the surface of the samples. After 28 days of exposure, the loss of material and aggregate that is not surrounded by a cement matrix are even more visible. Greater degradation can be observed in the samples that were cured at  $38^\circ\text{C}$  prior to exposure. The reason for this could be a higher porosity in the sample where a conversion process occurred during curing at higher temperatures. The change in mass caused by the exposure to sulphuric acid is shown in Figure 6.9. The reference mixture cured at  $20^\circ\text{C}$ , shows an initial loss of mass after 7 days of exposure and then a gain in mass up to 21 days of exposure. Until the end of the measurement period, as loss in mass occurred, with a small increase at 56th day of measurement. The same mixture cured at  $38^\circ\text{C}$  showed continuous loss in mass during all exposure period. The mixture with slag, cured at  $20^\circ\text{C}$  and

38°C, shows a continuous increase in mass during 21-day of exposure after which the mass decreases, with an increase at the end of the experiment. Both mixtures with calcined clay behave similarly during exposure, but the mixture cured at 38°C showed a greater loss of mass.

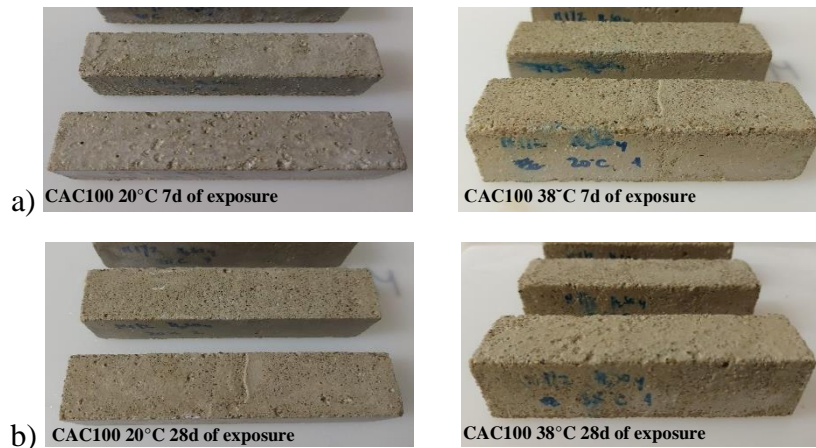


Figure 6.8 Visual observation of CAC100 sample: a) after 7d of exposure, b) after 28d of exposure to  $H_2SO_4$

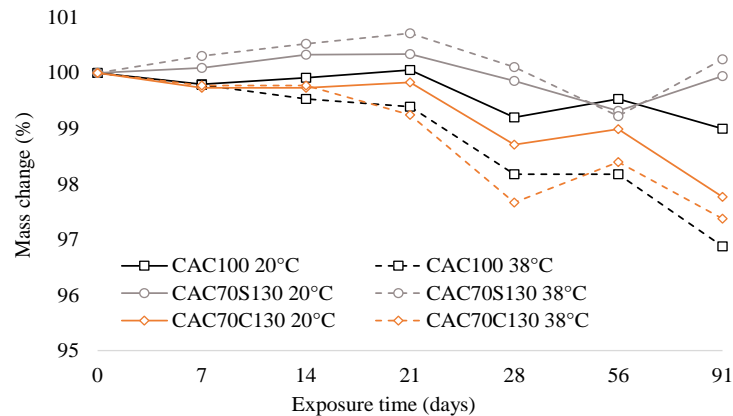


Figure 6.9 Mass change of all samples during exposure to  $H_2SO_4$

### 6.2.2.2 Compressive strength development

Similar to samples in sodium sulphate exposure, the compressive strength was tested over 91 days of exposure to  $H_2SO_4$ . Furthermore, the compressive strength was tested after 28 days of curing and serves as the initial value of the compressive strength before exposure to the sulphuric acid solution. The development of compressive strength during exposure is

shown in Figure 6.10. All mixtures showed an initial decrease in strength after 7 days of exposure. The compressive strength of the reference mixture increased slightly up to the 28<sup>th</sup> day of exposure and then decreased until end of experiment, in case of both curing regimes. The reference mixture cured at 38°C exhibited the lowest initial compressive strength due to conversion of metastable hydrates to stable hydrates. The mixture in which 30% of the CAC was replaced by slag showed a continuous decrease in compressive strength until the 91<sup>st</sup> day of exposure for curing at 20°C and until the 56<sup>th</sup> day of exposure for curing at 38°C. The compressive strength of the mixture with calcined clay, after initial decrease, showed an increase in strength until the 21<sup>st</sup> day of exposure in case of both curing temperatures. During further exposure to sulphuric acid, the compressive strength of these mixtures decreased further. Figure 6.11 shows a comparison of the compressive strength values for samples cured for 56 days at 20°C and 38°C and for samples after 28 days of exposure to sulphuric acid. The compressive strength of the reference mixture cured in water was almost equal to the compressive strength after 28 days of exposure for both curing regimes. On the contrary, the compressive strength of mixtures with slag and calcined clay decreased significantly after 28 days of exposure. The reduction in strength is lower for samples initially cured at 20°C.

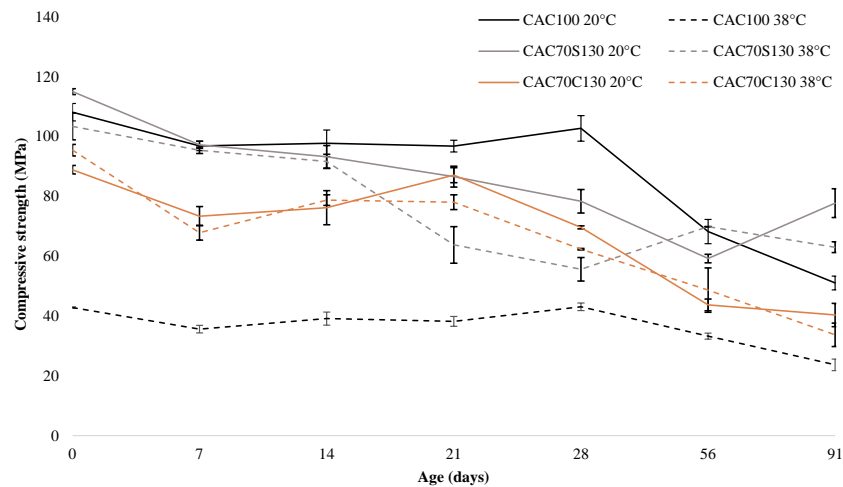


Figure 6.10 Compressive strength development during exposure to  $H_2SO_4$



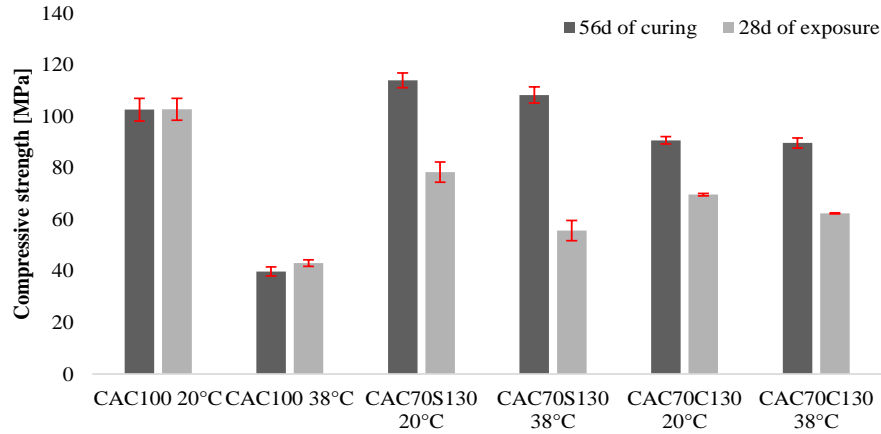


Figure 6.11 Compressive strength values after 56 days of curing and 28 days of exposure to  $H_2SO_4$

### 6.2.2.3 Microstructural changes

#### Calcium aluminate cement

Figure 6.12 shows the DTG curves for the CAC100 mixture cured at 20°C (a) and 38°C (b) after 56 days of curing, 28 days of exposure and 91 days of exposure to sulphuric acid. For the reference sample cured at 20°C, a higher peak intensity was found for metastable hydrates than for stable hydrates after 56 days of curing. For the same sample exposed to  $H_2SO_4$  solution, a higher peak intensity was detected for metastable  $CAH_{10}$  and  $C_2AH_8$  and a lower for  $C_3AH_6$  and  $AH_3$  hydrate. During exposure to  $H_2SO_4$ , stable hydrates are consumed and metastable hydrates are formed. After prolonged exposure, by the 91<sup>st</sup> day, a significantly different peak is observed at around 100°C. This peak is notably different from the peak that normally occurs at these temperatures. By the reaction of calcium aluminum hydrates with sulphuric acid gypsum is formed, and it usually occurs at these temperatures [98]. Similar behaviour can be observed in the reference sample cured at 38°C (Figure 6.12b). During curing in water for 56 days a significant amount of stable hydrates formed due to the conversion process. After 28 days in a  $H_2SO_4$  solution, a lower peak intensity is detected for  $C_3AH_6$  and  $AH_3$  hydrate and a slightly higher peak intensity for metastable  $C_2AH_8$ . With

prolonged exposure, the formation of a significant amount of  $\text{CAH}_{10}$  hydrate is detected, as well as a higher peak intensity for  $\text{AH}_3$  and  $\text{C}_3\text{AH}_6$  hydrates in comparison to 28 days of exposure. To confirm the formation of the phases formed during curing in water and exposure to sulphuric acid XRD analysis was performed. The results for the reference sample cured in water at  $20^\circ\text{C}$  for 56 days and the same sample exposed to  $\text{H}_2\text{SO}_4$  for 91 days are shown in Figure 6.13. The tests were conducted on mortar samples containing siliceous standard sand. Given that quartz has high crystallinity, the peaks of the quartz in the XRD analysis results are much larger compared to the peaks of the hydrates found in CAC. For the sample cured 56 days at  $20^\circ\text{C}$ , at a diffraction angle between 5 to 15 degrees, the metastable hydrates were detected. Higher peak intensities for metastable hydrates were detected after 91 days of exposure to sulphuric acid, indicating that metastable hydrates were formed during the exposure. In both samples, the stable hydrates hydrogarnet and  $\text{AH}_3$  were detected. However, a lower peak intensity in the sample that was exposed to  $\text{H}_2\text{SO}_4$  was detected. Furthermore, the formation of gypsum was detected in reference sample after 91 days of exposure. The formation of gypsum is associated with the consumption of  $\text{AH}_3$  and  $\text{C}_3\text{AH}_6$  hydrates, which can be seen in the results of the TGA and XRD analysis.

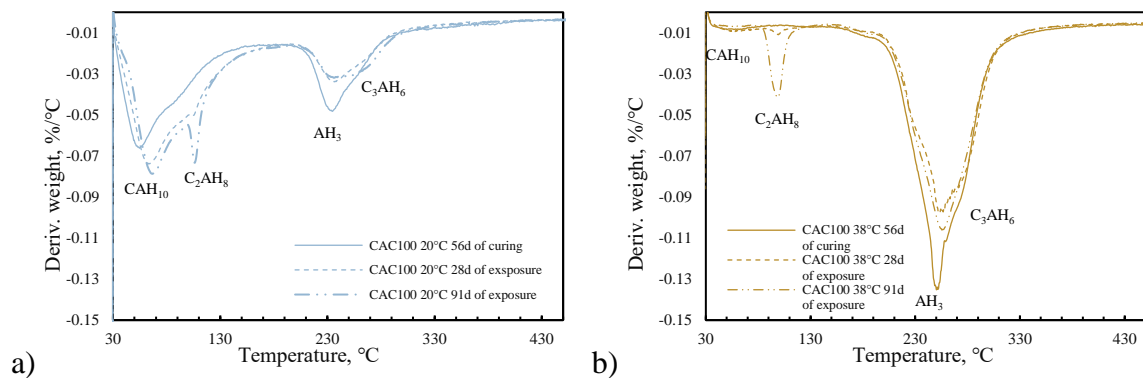


Figure 6.12 Figure 12 DTG curves of non-exposed and samples after 28 and 91 days of exposure to  $\text{H}_2\text{SO}_4$  for CAC100 mix cured (a) at  $20^\circ\text{C}$  and at (b)  $38^\circ\text{C}$

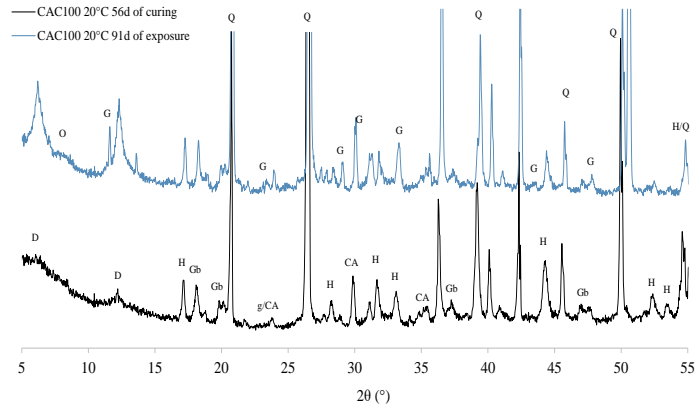


Figure 6.13 Diffractogram for non-exposed and sample after 91 days of exposure to  $H_2SO_4$  for CAC100 mix (CA=monocalcium aluminate, D= $CAH_{10}$ , Gb= $AH_3$ , g=Gehlenite, H= $C_3AH_6$ , O= $C_2AH_8$ , Q=quartz, G=Gypsum)

### Calcium aluminate cement with slag

Figure 6.14 shows the DTG curves for the CAC70S130 mixture cured at 20°C (a) and 38°C (b) after 56 days of curing and 28 days of exposure to sulphuric acid. In the sample cured 56 days at 20°C, a high proportion of metastable hydrates  $CAH_{10}$  and  $C_2AH_8$  was detected, while proportion of stable hydrogarnet and  $AH_3$  hydrate was very low. The addition of slag in CAC promotes the formation of strätlingite ( $C_2SH_8$ ) hydrate, which becomes visible at temperatures between 150°C and 200°C. After 28 days of exposure to sulphuric acid, a lower peak intensity is detected for metastable hydrates and strätlingite hydrate, while a slightly higher formation of  $AH_3$  hydrate is observed. The  $C_3AH_6$  hydrate peak intensity remained unchanged. A similar behaviour is observed for the same mixture cured at 38°C. When cured at 38°C for 56 days, a slightly higher peak intensity for strätlingite is observed compared to curing at 20°C. The formation of strätlingite at 38°C inhibits the conversion process and prevents a compressive strength decrease. Also, by curing at 38°C, higher peak intensities for stable hydrogarnet and  $AH_3$  were observed. Similar to 20°C, after 28 days of exposure, a lower peak intensity for metastable hydrates were detected. However, a lower amount of metastable hydrates was consumed during exposure to sulphuric acid. Furthermore, a lower

peak intensity was observed for strätlingite and hydrogarnet and a higher for  $\text{AH}_3$  hydrate. XRD analysis was conducted for CAC70S130 cured at  $20^\circ\text{C}$  for 56 days and after 28 days of exposure to  $\text{H}_2\text{SO}_4$ . The results are shown in Figure 6.15. After 56 days of curing at  $20^\circ\text{C}$ , higher peak intensities were detected for metastable hydrates and strätlingite hydrate, while they were lower for stable hydrates. Furthermore, after 28 days of exposure to sulphuric acid the formation of gypsum was observed which is related to the compressive strength decrease.

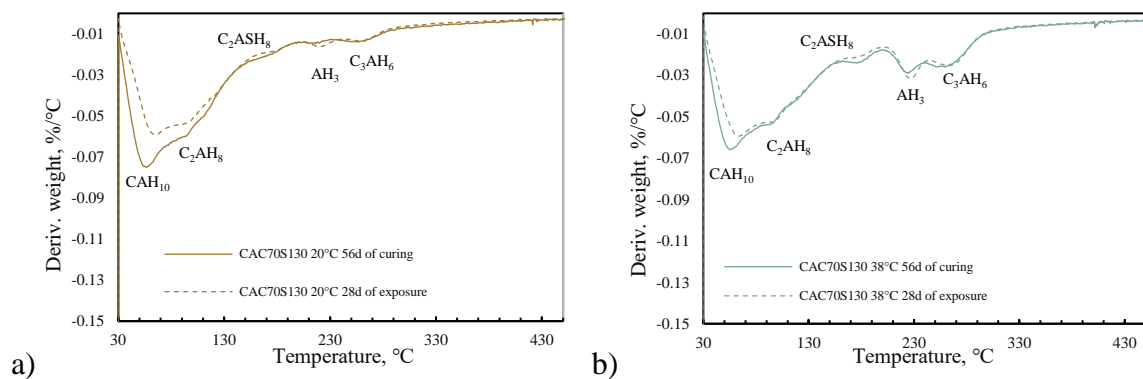


Figure 6.14 DTG curves of non-exposed and samples after 28 days of exposure to  $\text{H}_2\text{SO}_4$  for CAC70S130 mix cured (a) at  $20^\circ\text{C}$  and at (b)  $38^\circ\text{C}$

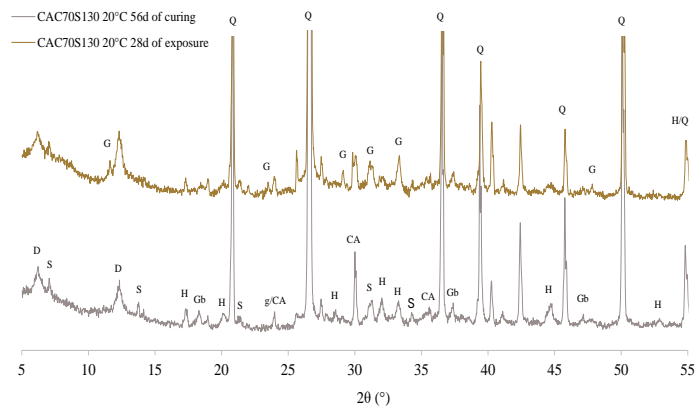


Figure 6.15 Diffractogram for non-exposed and sample after 28 days of exposure to  $\text{H}_2\text{SO}_4$  for CAC70S130 mix (CA=monocalcium aluminate, D=CAH<sub>10</sub>, Gb=AH<sub>3</sub>, g=Gehlenite, H=C<sub>3</sub>AH<sub>6</sub>, O=C<sub>2</sub>AH<sub>8</sub>, Q=quartz, G=Gypsum)

### Calcium aluminate cement with calcined clay

Figure 6.16 shows the DTG curves for the CAC70C130 mixture cured at  $20^\circ\text{C}$  (a) and  $38^\circ\text{C}$  (b) after 56 days of curing and 28 days of exposure to sulphuric acid. When calcined clay is

added to the CAC cement, strätlingite hydrate is formed at both curing temperatures. By curing at 20°C for 56 days, both metastable hydrates and AH<sub>3</sub> hydrate were detected, however stable C<sub>3</sub>AH<sub>6</sub> was not detected. After 28 days of exposure, a lower peak intensity was observed for metastable hydrates, while it was higher for strätlingite and AH<sub>3</sub> hydrate. Hydrogarnet was not detected after exposure to sulphuric acid. After 56 days of curing the same mixture at 38°C (Figure 6.16b) both metastable hydrates, strätlingite and AH<sub>3</sub> hydrate were observed. The peak intensity attributed to the formation of stable hydrogarnet was also detected. After 28 days of exposure, a lower peak intensity was detected for the metastable CAH<sub>10</sub> hydrate, while it was higher for the C<sub>2</sub>AH<sub>8</sub> hydrate. Furthermore, lower peak intensities were detected for both stable hydrates. XRD analysis was performed on a sample cured at 20°C for 56 days and on the same sample exposed to sulphuric acid for 28 days (Figure 6.17). For the sample cured at 20°C, at the diffraction angle between 5 to 15 degrees, both metastable hydrates and strätlingite hydrate were detected. However, after exposure to sulphuric acid peak intensity detected for metastable hydrates was lower, and for strätlingite hydrate slightly higher. The formation of gypsum is also visible at lower and higher diffraction angles.

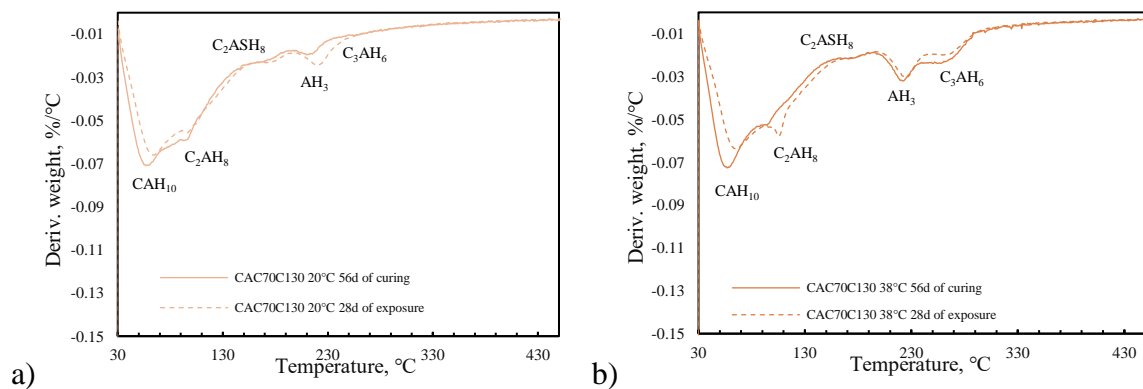


Figure 6.16 DTG curves of non-exposed and samples after 28 days of exposure to H<sub>2</sub>SO<sub>4</sub> for CAC70C130 mix cured (a) at 20°C and at (b) 38°C

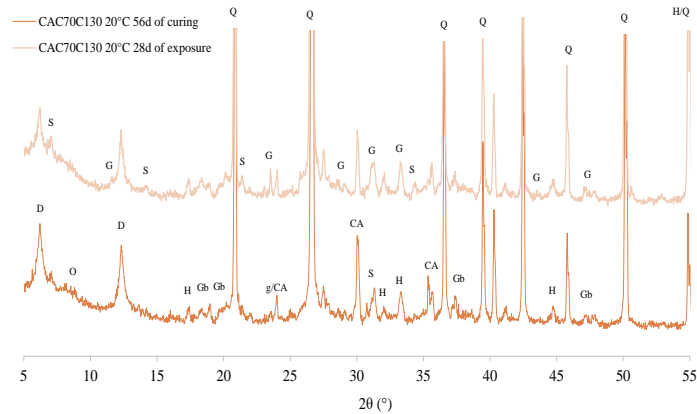


Figure 6.17 Diffractogram for non-exposed and sample after 28 days of exposure to  $H_2SO_4$  for CAC70C130 mix (CA=monocalcium aluminate, D= $CAH_{10}$ , Gb= $AH_3$ , g=Gehlenite, H= $C_3AH_6$ , O= $C_2AH_8$ , Q=quartz, G=Gypsum)

#### 6.2.2.4. Pore structure changes

The pore structure analysis was conducted on reference samples as well as on samples with slag and calcined clay after 56 days of curing at 20°C. Also, measurements were conducted after 91 days of exposure to sulphuric acid for the reference mixture, and after 28 days of exposure for the mixtures with addition of slag and calcined clay. The results of the total accessible porosity (a) and the pore volume distribution (b) for all mixtures are shown in Figure 6.18. The reference mixture cured for 56 days had a significantly higher porosity compared to the same mix exposed to sulphuric acid for 28 days, although the compressive strength of these two samples was the same. The total accessible porosity and average pore diameter for all mixtures cured at 20 °C and exposed to  $H_2SO_4$  are shown in Table 6.1. It was observed that the total porosity of the reference mixture after exposure was 5.6 % lower than after curing at 20°C for 56 days. However, the average pore diameter of this sample was higher than that of the sample cured in water, which can also be seen in Figure 6.18b, where the curve of the reference mixture is shifted to the right after exposure to sulphuric acid. When CAC is replaced by 30% slag or calcined clay, the total porosity is decreased for approximately 5.5% for the sample with slag, and 4% for the sample with calcined clay after 56 days of curing in water. In the case of these two mixtures, the total porosity was

significantly increased by 28 days of exposure to sulphuric acid. The total porosity increased by almost 4% for both the slag and calcined clay mix. The average pore diameter of both mixtures also increased. As with the reference mixture, this can also be seen in Figure 6.18b, curves are shifted right after exposure to sulfuric acid.

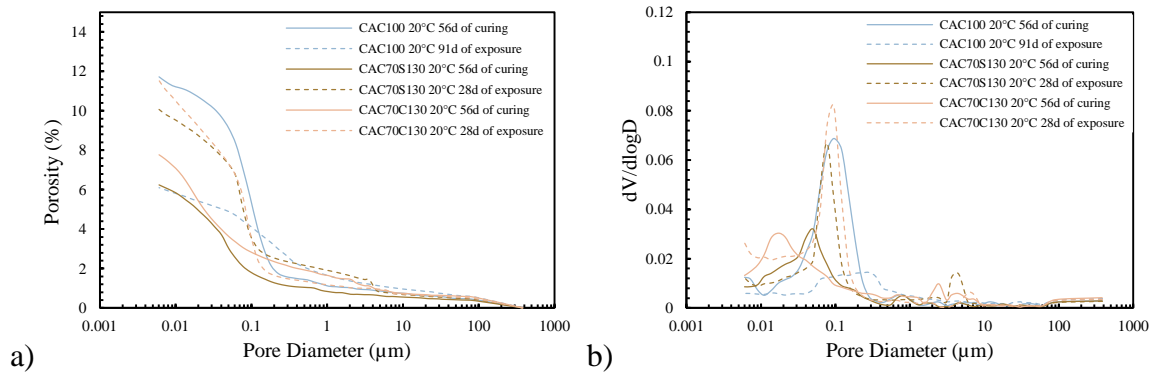


Figure 6.18 a) Total porosity for non-exposed and samples after 28 and 91 days of exposure to  $H_2SO_4$ , b)  $dV/d\log D$

Table 6.1 Total porosity and average pore diameter after 56 days of curing and 28 days of exposure to  $H_2SO_4$

Mix	Exposure time	Porosity (%)	Average pore diameter (nm)
CAC100 20°C	56d of curing	11.7	51.02
	91d of exposure	6.1	58.07
CAC70S130 20°C	56d of curing	6.24	31.75
	28d of exposure	10.07	42.96
CAC70C130 20°C	56d of curing	7.78	27.55
	28d of exposure	11.54	32.39

### 6.3 Discussion

The behaviour of CAC under the influence of sulphates and acids has not yet been investigated to this extent. Also, there is not many studies on the influence of aggressive solutions on CAC with the addition of slag and calcined clay cured at ambient and high temperature. Before exposure to the sulphate and acid solutions the samples were cured at two different temperatures. One part of the samples was cured at 20°C and the other part at 38°C to accelerate the conversion process.

### 6.3.1 Exposure to sodium sulphate solution

It has been reported that no significant damage to CAC samples is expected after exposure to sodium sulphate [29]. After exposure to 5% Na<sub>2</sub>SO<sub>4</sub> solution, visual inspection did not reveal any significant changes in the samples cured at both temperatures. Only a slight material loss was observed at the edges of the samples (Figure 6.1). As the conversion process increases the total porosity of the sample, it is assumed that more sulphate ions penetrate the cement matrix. The analysis, of the reference mixture after 28 days of exposure to sodium sulphate solution shows that there are no significant differences in the mass change and compressive strength, regardless of the curing temperature, prior and after exposure to sodium sulphate solution. The mass of the reference sample increases after exposure to the sodium sulphate solution, regardless of the curing temperature. The reaction of sulphate ions with the aluminates in the CAC forms ettringite, and the formation of the new phase increases the weight of the sample [23]. Kurtis et al. [29] reported that hydration of cements can continue during exposure to sulphate solutions, which consequently increases compressive strength. Therefore, an increase in compressive strength does not necessarily represent a higher resistance to sulphates, but the resistance can only be expressed by a decrease in compressive strength. The reference mixture cured at 38°C, had the lowest compressive strength due to the conversion process. However, after exposure to sodium sulphate, the compressive strength slightly increased. The compressive strength of the same mixture cured at 20°C was mostly stable during exposure, with a minor decrease in strength after 3 weeks of exposure. Furthermore, the compressive strength of samples cured in water for 56 days was lower than the strength of samples exposed to sulphates (Figure 6.4). The reason for this could be the formation of a new phase (ettringite) that fills the pores and reduces the porosity of the samples. By conducting TGA analysis, it was determined that the exposure of



reference sample to sodium sulphate solution consumes  $AH_3$  hydrate, and at the same time a larger amount of metastable hydrates is formed and lower amount of stable  $C_3AH_6$  hydrate was observed [23]. The same mechanism is observed for the sample initially cured at  $38^\circ\text{C}$ . However, in this case, a higher amount of  $AH_3$  is formed during hydration and a higher amount is consumed during exposure to  $Na_2SO_4$ .

In previous studies it was confirmed that the addition of slag to OPC improves resistance to sulphates depending on the  $Al_2O_3$  content in slag. The resistance to sulphate attack decreases with increasing content of aluminium oxide [99][100][101]. The addition of slag to CAC does not compromise its sulphate resistance in terms of compressive strength. At the end of the experiment, the compressive strength remained at least as high as before exposure to sodium sulphate. The slag used in this study had 11.7% of aluminium oxide which is considered a low alumina content [101]. The compressive strength of the sample with the slag cured at  $20^\circ\text{C}$  follows the trend of the reference sample cured at the same temperature. In comparison with reference sample cured at  $38^\circ\text{C}$ , the sample with slag had a higher initial compressive strength due to inhibition of conversion process by the formation of strätlingite hydrate. During exposure to sulphates, there was no significant decrease in compressive strength. Furthermore, the mass change during exposure follows the trend of the reference mixture for both curing temperatures. The microstructural analysis showed that under influence of sulphate ions, metastable hydrates and strätlingite hydrate are decomposed, while  $AH_3$  hydrate and hydrogarnet are forming when sample is cured at  $20^\circ\text{C}$ . In the sample initially cured at  $38^\circ\text{C}$ , the hydrogarnet also decomposes after 28 days of exposure to sulphates. Compared to the reference sample, when slag is added to CAC, metastable hydrates react first. The reason for this could be the lack of stable hydrates that could react

with sulphate ions, so that metastable hydrates take over this function. A higher amount of consumed metastable hydrates results in reduced compressive strength in comparison with the same mixture cured for 56 days at 38°C (Figure 6.4).

Similar to the addition of slag to OPC, it was reported that the addition of calcined clay increases the sulphate resistance of OPC cement [101, 102, 103, 104]. By replacing part of the OPC with calcined clay, portlandite consumption and a lower amount of calcium ions occur, which prevents the secondary formation of ettringite and gypsum [104]. Calcined clay is preferably combined with CAC to prevent the conversion process through the formation of strätlingite hydrate, which reduces porosity. Reduced porosity also reduces the penetration of sulphate ions into the cement matrix. As with the reference sample and the sample with slag, during exposure to the sulphate solution, the mass of sample with clay increases due to the formation of new phase ettringite. The compressive strength of the sample with calcined clay is lower before and after exposure, compared to the reference sample and the sample with slag. However, during exposure to sodium sulphate solution, there was no decrease in strength, as with the other mixtures. In the sample with calcined clay cured at 20°C, the formation of metastable hydrates and  $AH_3$  hydrate was detected, while strätlingite hydrate and hydrogarnet remained unaffected by the sulphate ions. In the same sample cured at 38°C, the decomposition of metastable  $CAH_{10}$  was detected, as well as small amount of newly formed  $AH_3$  hydrate. Similar to the sample with slag, the formation of a higher amount of stable hydrates in the sample initially cured at 38°C (then exposed to sulphates) results in a slightly lower compressive strength compared to the strength after 56 days of curing at 38°C.

### 6.3.2 Exposure to sulfuric acid solution

Compared to the sodium sulphate solution, significant damage was observed after sulphuric acid exposure. When sulphate ions from the sulphuric acid diffuse into the cement matrix, the calcium bearing phases CA and hydrogarnet ( $C_3AH_6$ ) react first. As a result of this reaction, secondary  $AH_3$ , and gypsum are formed [22].  $AH_3$  hydrate is stable when the pH is above 3-4, has a high neutralization capacity during acid exposure, and prevents further degradation of the sample [105, 106]. The surface of the sample exposed to the sulphuric acid solution has a pH lower than 3, leading to the dissociation of the  $AH_3$  hydrate [107]. When the  $AH_3$  hydrate dissolves, noticeable changes appear on the samples. After 7 days of exposure, aggregate pop-outs and loss of material were observed in the reference mixture cured both at 20°C and 38°C. After 28 days of exposure to sulphuric acid solution, the deterioration is even more visible (Figure 6.8). The initial gain in mass from the 7<sup>th</sup> to the 21<sup>st</sup> day of exposure is connected to the formation of gypsum and  $AH_3$  hydrate, which are densifying the structure of the cement matrix [22]. During prolonged exposure, weight loss of the samples, of the reference mixture cured both on 20°C and 38°C, was observed due to loss of material. The compressive strength is increasing until 28<sup>th</sup> day of exposure to sulphuric acid solution for the reference mixture cured both at 20°C and 38°C. Strength of sample cured at 38°C is initially lower due to the conversion process. The compressive strength increase is related to the continuation of hydration of the cement in sulphuric acid and the formation of secondary  $AH_3$ , which fills the pores. The decrease in compressive strength was observed after 28 days of exposure for both curing temperatures as a result of the dissociation of  $AH_3$  when the pH of the cement matrix reaches a value below 3. A higher decrease in compressive strength was observed for the mixture cured at 20°C. The reason for this could be the lower amount of  $AH_3$  hydrate that could prevent diffusion of sulphate ions

into the cement matrix. However, the primary factor in the degradation of CAC due to sulphuric acid exposure is the formation of gypsum [105]. By conducting XRD analysis formation of gypsum was confirmed for the reference mixture cured at 20°C (Figure 6.13). The formation of gypsum induces microcracks in the area affected by the sulphuric acid, resulting in a decrease in the mechanical properties. Exposure to the sulphuric acid solution strongly influenced the pore structure of the reference mixture. The total porosity significantly decreased; however the average pore diameter increased after 91 days of exposure influencing the compressive strength decrease (Figure 6.18).

The addition of more than 20% slag to CAC inhibits the conversion process and reduces the porosity of the cement matrix [12]. Slag with  $C_2AH_8$  hydrate forms strätlingite hydrate ( $C_2ASH_8$ ), and thus the formation of the stable phases  $C_3AH_6$  and  $AH_3$  is reduced. Given that  $AH_3$  hydrate is crucial for neutralizing the solution and preventing sulphate ion precipitation, the sample containing slag may be more susceptible to degradation by sulphuric acid. The weight of the sample increases during the 21-day of exposure due to the formation of gypsum, however after prolonged exposure the mass decreases because of loss of the material (Figure 6.8). The compressive strength is continuously decreasing during exposure for both samples cured at 20°C and 38°C. A smaller decrease in compressive strength was observed for the sample initially cured at 20°C compared to the same mixture cured at 38°C. The sample cured at 20°C forms less stable hydrates, which results in lower porosity and thus higher compressive strength. The significantly lower strength observed after 28 days of exposure to sulphuric acid, compared to the compressive strength of the sample cured at 20°C for 56 days, indicates changes in the structure of the cement matrix and the formation of microcracks (Figure 6.11). TGA analysis showed the formation of  $AH_3$  hydrate and the

consumption of metastable hydrates under the influence of sulphuric acid. This process differs from that observed in the reference mixture without slag. Additionally, an insufficient amount of  $C_3AH_6$  hydrate was formed during hydration, and the reaction with sulphate ions is mainly carried out by metastable hydrates. The degradation of the sample with slag is observed immediately after exposure in the terms of a decrease in compressive strength. The XRD analysis also confirmed the formation of gypsum, which contributes to the degradation. Less gypsum formation was observed compared to the reference mixture, but the measurements were performed after a shorter exposure time. These results indicate that the sample containing slag requires a shorter period of exposure to the sulphuric acid solution for degradation to occur. In contrast to the reference sample, the total accessible porosity of the sample with slag increased after 28 days of exposure, along with an increase in the average pore diameter.

The addition of calcined clay has a comparable effect to the addition of slag to CAC in the presence of sulphuric acid. Also, calcined clay, as well as slag, contributes to the mitigation of the conversion process to CAC by forming stralingite, which densifies the cement matrix and prevents a decrease in compressive strength. The degradation process due to the influence of sulphuric acid solution is not prevented compared to the reference mixture due to the lack of  $AH_3$  hydrate formed during cement hydration. Moreover, in the sample initially cured at  $38^\circ\text{C}$ , the formation of  $AH_3$  hydrate after exposure to sulphuric acid solution was not observed (Figure 6.16). The compressive strength is constantly lower during exposure compared to the reference mixture, however, the trend of compressive strength decrease followed by an increase is similar to the reference sample cured at  $20^\circ\text{C}$ . Similar to the sample containing slag, a significant decrease in compressive strength was observed after 28 days of

exposure, in contrast to the compressive strength achieved after 56 days of curing in water. By analysing TGA results it was determined that the metastable hydrate  $CAH_{10}$  for sample cured at  $20^{\circ}\text{C}$  first reacts with sulphate ions to form acid solution. In the sample cured at  $38^{\circ}\text{C}$ , along with the metastable hydrate,  $C_3AH_6$  hydrate reacts with the sulphate ions. The formation of gypsum was also observed in the sample containing calcined clay after 28 days of exposure (Figure 6.17). However, compared to the slag-containing sample, the formation of gypsum is less prominent. The total porosity and the average pore diameter of the sample with calcined clay increased after 28 days of exposure. However, the difference between the non-exposed and exposed samples is less pronounced than in the sample with slag.

#### **6.4 Conclusion**

This study aimed to evaluate the sulphate and acid resistance of CAC-based mortar without and with the addition of slag or calcined clay. In addition, the influence of the conversion process on changes in the microstructure that affect sulphate and acid penetration was investigated. It has been shown that CAC based mortar is more susceptible to degradation in acid solutions than in sulphate solutions.

Following conclusions are drawn from the study:

- Exposure to a sulphate solution has no significant influence on the compressive strength of plain CAC mortar, regardless of the curing temperature.
- A 30% replacement of CAC with slag or calcined clay slightly improves the stability of the compressive strength under the influence of sulphates at both curing temperatures.
- Gypsum formation and  $AH_3$  dissociation significantly influenced the compressive strength of plain CAC mortar after 28 days of exposure to sulphuric acid solution.

- Exposure to sulphuric acid increased the total porosity of the sample with slag, leading to a decrease in compressive strength. Additionally, the early formation of gypsum during exposure contributed to the lower resistance to sulphuric acid of the sample with slag compared to the reference sample.
- In the sample with calcined clay, the formation of gypsum and an increase in total porosity were observed, resulting in decreased compressive strength and, consequently, lower resistance compared to the reference sample.

## Chapter 7 Conclusions

### 7.1 Conclusions

This research provided information on the behaviour of calcium aluminate cement-based mortar and concrete under the influence of various environmental conditions. In order to determine the effects of the conversion process on the mechanical and durability properties, the process was accelerated by curing the samples at 38°C. To inhibit the conversion process, slag and calcined clay were utilised in this research, and their effects on the mechanical and durability properties were evaluated.

The main conclusions of this thesis are:

1. Incorporating slag and calcined clay can inhibit the conversion process and promote densification of CAC-based mortar. However, the addition of slag to CAC-based concrete leads to a slight decline in basic durability properties.
2. Carbonation has the greatest effect on the plain CAC sample cured at ambient temperatures in terms of a decrease in compressive strength. Higher carbonation was observed in samples containing slag and calcined clay, despite the lower porosity of the matrix at both curing temperatures. However, the compressive strength of these samples increased after carbonation.
3. The reference sample cured at 20°C, showed the highest resistance to chloride ingress, however the conversion process significantly decreased its resistance. The addition of slag or calcined clay reduces the effect of the conversion process on the resistance to chloride ingress.
4. Exposure to a 5% sulphate solution does not affect the mechanical properties of CAC mortar. Furthermore, the addition of slag or calcined clay does not affect these



properties either; in fact, the strength of the samples exposed to the sulphates is even more stable.

5. Exposure to 1.5% sulphuric acid leads to considerable degradation in all three systems observed, which is mainly due to the dissociation of  $AH_3$  and the formation of gypsum.

The research within this dissertation determined the effects of slag and calcined clay on microstructural changes, their contribution to mitigating the effects of the conversion process and their effects on durability properties. Therefore, this research serves as a basis for a broader application of CAC-based systems.

## 7.2 Scientific contribution

The achieved original scientific contributions of the dissertation are:

- **The influence of SCMs on changes in the microstructure of calcium-aluminate cement was determined.**

This research has shown that the addition of SCMs with high silica content promotes the formation of a new phase, strätlingite ( $C_2ASH_8$ ). The formation of strätlingite reduces the rate of the conversion process, which is unavoidable in CAC. It was demonstrated that 30% slag or calcined clay is an adequate replacement percentage to ensure mitigation of the conversion process. Already after 5 days of curing at 38°C, the compressive strength of the pure CAC sample was 60% lower compared to a sample cured at 20°C. For samples with slag or calcined clay, the compressive strength was stable over the entire testing period regardless of curing temperature.

- **The influence of changes in the microstructure on the durability properties of calcium-aluminate cement was determined.**

It was determined that the carbonation resistance of CAC depends on the amount of phases formed during curing at 20°C or 38°C. The formation of stable hydrates ( $C_3AH_6$  and  $AH_3$ ) provided higher carbonation resistance compared to the systems where mostly metastable hydrates ( $CAH_{10}$  and  $C_2AH_8$ ) were formed. For the pure CAC sample, the resistance to chloride ingress was reduced after curing at 38°C due to the increase in porosity. The samples with slag and calcined clay also showed a higher chloride penetration after curing at 38°C, however, this reduction was not as significant as in the case of the CAC mixture, as a similar amount of metastable and stable hydrates were formed during curing at 20°C and 38°C. In terms of sulphate resistance, it was determined that exposure to sodium sulphate does not have a significant effect on the mechanical properties and microstructural changes in any of the systems tested. However, when CAC was exposed to sulphuric acid, significant changes were determined for non-converted and converted samples. Gypsum formation and  $AH_3$  dissociation influenced the compressive strength reduction and porosity changes in all three systems tested.

- **Changes which occur at the microstructural and macrostructural levels of calcium-aluminate cement with and without SCMs, when exposed to different environmental conditions were quantified.**

In this research, the influence of two different curing temperatures (20°C and 38°C) on the properties on microstructural and macrostructural levels was observed. The curing temperature of 38°C was used to accelerate the conversion process. It was shown that the

influence of the conversion process on the durability properties is reduced when slag and calcined clay were incorporated into CAC. In samples with slag and calcined clay exposed to carbonation, a similar amount of calcium carbonate was found before and after the conversion process. In contrast, the reference sample cured at 38°C showed a significantly larger amount of calcium carbonate compared to that cured at 20°C. The compressive strength of non-converted reference mixture cured at 20°C decreased by almost 30% after 56 days of carbonation, while the same converted mixture showed an increase in compressive strength of almost 40% after carbonation due to the formation of carbonates. For mixtures with slag and calcined clay, a slight increase in strength was observed for all mixtures after 56 days of carbonation, regardless of the curing conditions prior to carbonation. In terms of chloride diffusion, the apparent chloride diffusion of the reference sample was 11 times higher after conversion, while the samples with slag and calcined clay showed 2.8 and 1.3 times higher apparent diffusion coefficients after curing at 38°C, respectively. In terms of sulphate resistance, no decrease in resistance was observed both for reference and samples with slag and calcined clay after curing at 38°C. However, the sulphuric acid solution had significant effect before and after conversion for all samples, resulting in a decrease in compressive strength of 52% and 44% for the pure CAC sample cured at 20°C and 38°C, respectively, after exposure to H<sub>2</sub>SO<sub>4</sub> for 91 days. The compressive strength of the samples with slag and calcined clay also decreased after exposure to sulphuric acid. For the sample with slag, the compressive strength decreased by 32% for curing at 20°C and by 39% for curing at 38°C after 91 days of exposure to H<sub>2</sub>SO<sub>4</sub>. For the sample with calcined clay, the compressive strength decreased by 54% for curing at 20°C and 64% for curing at 38°C after 91 days of exposure to H<sub>2</sub>SO<sub>4</sub>.

This research provided the basis for a more efficient production and application of calcium-aluminate cement. Therefore, in addition to the original scientific contribution, the industrial contribution of the proposed work is also achieved.

### **7.3 Future recommendations**

Several recommendations for future research based on this dissertation are listed below:

1. This study showed promising results in terms of mechanical properties when SCMs are added to CAC. It was also shown that durability of CAC with the addition of SCMs is not compromised after occurrence of the conversion process. However, the present study comprised monitoring the properties up to a maximum of 90 days. Longer studies would be needed to evaluate the performance of CAC-based mortars under prolonged exposure to aggressive environmental conditions.
2. It has been demonstrated that calcined clay could be a promising material for use in combination with CAC. The performance of calcined clay depends mainly on the kaolinite content. In the present study, two clays with different kaolinite content were analysed. Future research could include calcined clay with different kaolinite content to determine its influence on the development of compressive strength and long-term durability.
3. In the absence of standards for the behaviour of CAC mortar/concrete, standards and recommendations for OPC were used. Since OPC and CAC have significantly different chemistry, the use of standards for OPC could influence the obtained results for CAC. Further research is needed to establish protocols for testing CAC-based mortar/concrete under different exposure conditions.

## References

- [1] Snellings, R., Assessing, Understanding and Unlocking Supplementary Cementitious Materials, RILEM Tech. Lett., vol. 1, p. 50, 2016, doi: 10.21809/rilemtechlett.2016.12.
- [2] International Energy Agency, <https://www.iea.org/reports/cement>, 2024 (accessed 15 April 2024).
- [3] Burris, L. E., Alapati, P., Moser, R. D., Ley, M. T., Berke, N., and Kurtis, K. E., Alternative cementitious materials: Challenges and opportunities, Am. Concr. Institute, ACI Spec. Publ., vol. 2015-Janua, no. SP 305, pp. 27.1-27.10, 2015.
- [4] Scrivener, K.: “Calcium aluminate cements (Chapter)”, Advanced Concrete Technology (ur. Newman, J., Choo, B.S.) England: Elsevier Science Publishers Ltd., 2003.
- [5] Ideker, J.H., Scrivener, K.L., Fryda, H. and Touzo, B.: “Calcium aluminate cements (Chapter)”, Lea’s Chemistry of Cement and Concrete (ur. Hewlett, P., Liska, M.), England: Elsevier Science Publishers Ltd., 2019
- [6] Fu, T., Adams, M. P., and Ideker, J. H., A Preliminary Study on A Calcium Aluminate Cement Concrete Maturity Theory in Predicting Conversion, 14th Int. Congr. Chem. Cem., no. November, 2016, doi: 10.13140/RG.2.1.2606.5369.
- [7] Bizzozero, J., Hydration and dimensional stability of calcium aluminate cement-based systems, École Polytechnique Fédérale de Lausanne, vol. 6336, 2014.
- [8] Adams, M.P., Lute, R.D., Moffatt, E.G. and Ideker, J.H.: Evaluation of a Procedure for Determining the Converted Strength of Calcium Aluminate Cement Concrete, Journal of Testing and Evaluation 46, no. 4, pp. 1659–1672, 2018
- [9] Pacewska, B. and Nowacka, M., Studies of conversion progress of calcium aluminate cement hydrates by thermal analysis method, Journal of Thermal Analysis and Calorimetry, vol. 117, no. 2. pp. 653–660, 2014, doi: 10.1007/s10973-014-3804-5.

- 
- [10] Yang, H. J., Ann, K. Y., and Jung, M. S., Development of strength for calcium aluminate cement mortars blended with GGBS, *Adv. Mater. Sci. Eng.*, vol. 2019, 2019, doi: 10.1155/2019/9896012.
- [11] EN 14647, Calcium aluminate cement – Composition, specifications and conformity criteria, pp. 1-41, 2005
- [12] Kirca, Ö., Özgür Yaman, I., and Tokyay, M., Compressive strength development of calcium aluminate cement-GGBFS blends, *Cem. Concr. Compos.*, vol. 35, no. 1, pp. 163–170, 2013, doi: 10.1016/j.cemconcomp.2012.08.016.
- [13] Kotwica, L.: “The influence of mineral additives on properties of calcium aluminate cement mortars”, *Cement Wapno Beton*, 3, p. 191–198, 2016
- [14] Collepari, M., Monosi, S., and Piccioli, P., The influence of pozzolanic materials on the mechanical stability of aluminous cement, *Cement and Concrete Research*, vol. 25, no. 5. pp. 961–968, 1995, doi: 10.1016/0008-8846(95)00091-P.
- [15] López, A. H., Calvo, J. L. G., Olmo, J. G., Petit, S., and Alonso, M. C., Microstructural evolution of calcium aluminate cements hydration with silica fume and fly ash additions by scanning electron microscopy, and mid and near-infrared spectroscopy, *Journal of the American Ceramic Society*, vol. 91, no. 4. pp. 1258–1265, 2008, doi: 10.1111/j.1551-2916.2008.02283.x.
- [16] Win, T. T., Panwisawas, C., Jongvivatsakul, P., Pansuk, W., and Prasittisopin, L., Effects of Fly Ash Composition to Mitigate Conversion of Calcium Aluminate Cement Composites, pp. 1–19, 2023.
- [17] De Belie, N., Soutsos, M., and Gruyaert, E., Properties of Fresh and Hardened Concrete Containing Supplementary Cementitious Materials: State-of-the-Art Report of the RILEM Technical Committee 238-SCM, Working Group 4. 2018.
- [18] Quillin, K., Osborne, G., Majumdar, A., and Singh, B., Effects of w/c ratio and curing conditions on strength development in BRECEM concretes, *Cement and Concrete Research*, vol. 31, no. 4. pp. 627–632, 2001, doi: 10.1016/S0008-8846(00)00494-4.

- [19] Bougara, A., Lynsdale, C., Milestone, N.B., The influence of slag properties, mix parameters and curing temperature on hydration and strength development of slag/cement blends, *Construction and Building Materials*, 187, pp. 339-347, 2018, doi.org/10.1016/j.conbuildmat.2018.07.16
- [20] Majumdar, A. J., Singh, B., and Edmonds, R. N., Hydration of mixtures of “Ciment Fondu” aluminous cement and granulated blast furnace slag, *Cement and Concrete Research*, vol. 20, no. 2. pp. 197–208, 1990, doi: 10.1016/0008-8846(90)90072-6.
- [21] Ö. Kirca, Temperature Effect on Calcium Aluminate Cement Based Composite Binders, The Graduate School of Natural and Applied Sciences, Middle East Technical University, 230, (2006)
- [22] Khan, H.A., Castel, A., Khan, M.S.H, Mahmood, A.H., Durability of calcium aluminate and sulphate resistant Portland cement based mortars in aggressive sewer environment and sulfuric acid, *Cement and Concrete Research*, 124, 2019, doi.org/10.1016/j.cemconres.2019.105852
- [23] R.D. Lute, Durability of Calcium-Aluminate Based Binders for Rapid Repair Applications, Faculty of the Graduate School, University of Texas Austin, (2016)
- [24] Zhang, H., 4—Cement (Chapter), *Building Materials in Civil Engineering*, 423, pp. 46-80, 2011, doi: 10.1533/9781845699567.46.
- [25] Pöllmann, H., Calcium aluminate cements - Raw materials, differences, hydration and properties, *Reviews in Mineralogy and Geochemistry*, vol. 74. pp. 1–82, 2012, doi: 10.2138/rmg.2012.74.1.
- [26] Shirani, S. et al., Calcium aluminate cement conversion analysed by ptychographic nanotomography, *Cement and Concrete Research*, vol. 137. 2020, doi: 10.1016/j.cemconres.2020.106201.
- [27] Lee, J., Jun, H., Jang, I., Kyum, S., and Jung, D., Case Studies in Construction Materials Comparison of calcium aluminate cements on hydration and strength development at different initial curing regimes, *Case Stud. Constr. Mater.*, vol. 17, no. October, p. e01596, 2022, doi: 10.1016/j.cscm.2022.e01596.

- [28] Lamberet, S., Durability of ternary binders based on portland cement, calcium aluminate cement and calcium sulfate, PhD thesis N°3151, Ecole Polytechnique Fédérale de Lausanne, vol. 3151, 2005.
- [29] Kurtis, K. E., Shomglin, K., Monteiro, P. J. M., Harvey, J., Roesler, J.: Accelerated test for measuring sulfate resistance of calcium sulfoaluminate, calcium aluminate, and Portland cements, *Journal of Materials in Civil Engineering*, vol. 13, pp. 216-221, 2001
- [30] El Sökkary, T. M., Assal, H. H., and Kandeel, A. M., Effect of silica fume or granulated slag on sulphate attack of ordinary Portland and alumina cement blend, *Ceramics International*, vol. 30, no. 2. pp. 133–138, 2004, doi: 10.1016/S0272-8842(03)00025-7.
- [31] Bescher, E., Rice, E. K., Ramseyer, C., and Roswurm, S., Sulfate resistance of calcium sulphoaluminate cement, *J. Struct. Integr. Maint.*, vol. 1, no. 3, pp. 131–139, 2016, doi: 10.1080/24705314.2016.1211235.
- [32] Aye, T., Oguchi, C. T., and Takaya, Y., Evaluation of sulfate resistance of Portland and high alumina cement mortars using hardness test, *Construction and Building Materials*, vol. 24, no. 6. pp. 1020–1026, 2010, doi: 10.1016/j.conbuildmat.2009.11.016.
- [33] Liu, Z. and Meng, W., Fundamental understanding of carbonation curing and durability of carbonation-cured cement-based composites: A review, *J. CO2 Util.*, vol. 44, no. December 2020, p. 101428, 2021, doi: 10.1016/j.jcou.2020.101428.
- [34] Lippiatt, N., Ling, T. C., and Pan, S. Y., Towards carbon-neutral construction materials: Carbonation of cement-based materials and the future perspective, *J. Build. Eng.*, vol. 28, p. 101062, 2020, doi: 10.1016/j.job.2019.101062.
- [35] Goñi, S., Gaztanaga, M. T., Guerrero, A.: Role of cement type on carbonation attack, *J. Mater. Res.*, Vol. 17, No. 7, 2002, doi: 10.1557/JMR.2002.0271
- [36] Goñi, S. and Guerrero, A., Accelerated carbonation of Friedel's salt in calcium aluminate cement paste, *Cement and Concrete Research*, vol. 33, no. 1. pp. 21–26, 2003, doi: 10.1016/S0008-8846(02)00910-9.



- [37] Alapati, P., Kurtis, K.E., Carbonation in Alternative Cementitious Materials: Implications on Durability and Mechanical Properties, Sixth Int. Con. Dur. Concr. Struct ICC02, (2018).
- [38] Fernández-Carrasco, L., Rius, J., and Miravittles, C., Supercritical carbonation of calcium aluminate cement, *Cement and Concrete Research*, vol. 38, no. 8–9. pp. 1033–1037, 2008, doi: 10.1016/j.cemconres.2008.02.013.
- [39] Park, S. M., Jang, J. G., Son, H. M., and Lee, H. K., Stable conversion of metastable hydrates in calcium aluminate cement by early carbonation curing, *Journal of CO2 Utilization*, vol. 21. pp. 224–226, 2017, doi: 10.1016/j.jcou.2017.07.002.
- [40] Zhang, Y. et al., Chloride binding of monosulfate hydrate (AFm) and its effect on steel corrosion in simulated concrete pore solution, *J. Build. Eng.*, vol. 67, p. 105945, 2023, doi: <https://doi.org/10.1016/j.jobbe.2023.105945>.
- [41] Wolofsky, R., Corrosion Initiation of Concrete Bridge Elements Exposed to De-icing Salts., Department of Civil Engineering and Applied Mechanics McGill University, Canasa, November, 2011.
- [42] Khan, M. U., Ahmad, S., and Al-Gahtani, H. J., Chloride-Induced Corrosion of Steel in Concrete: An Overview on Chloride Diffusion and Prediction of Corrosion Initiation Time, *Int. J. Corros.*, vol. 2017, 2017, doi: 10.1155/2017/5819202.
- [43] Wang, Z. et al., Influence of sodium chloride on the hydration of calcium aluminate cement constantly cured at 5, 20 and 40°C, *Advances in Cement Research*, vol. 33, no. 2. pp. 84–95, 2021, doi: 10.1680/jadcr.19.00041.
- [44] Ann, K. Y. and Cho, C. G., Corrosion resistance of calcium aluminate cement concrete exposed to a chloride environment, *Materials*, vol. 7, no. 2. pp. 887–898, 2014, doi: 10.3390/ma7020887.
- [45] Osma, J. F. and Sá, M., Electrical characterization of Calcium Aluminate ( CA ) in presence of chloride ions, 14th International Congress on the Chemistry of Cement. 2015

- [46] Li, G., Zhang, A., Song, Z., Shi, C., Wang, Y., Zhang, J, Study on the resistance to seawater corrosion of the cementitious systems containing ordinary Portland cement or/and calcium aluminate cement, *Construction and Building Materials*, vol. 157, pp. 852-859, 2017
- [47] HRN EN 933-1, Tests for geometrical properties of aggregates – Part 1: Determination of particle size distribution- Sieving method, pp. 1-20, 2012
- [48] ASTM C1897-20, Standard Test Methods for Measuring the Reactivity of Supplementary Cementitious Materials by Isothermal Calorimetry and Bound Water Measurements, *ASTM Int. West Conshohocken, PA*, vol. 04, no. August, pp. 7–11, 2020, doi: 10.1520/C1897-20.2.
- [49] HRN EN 480-2 2007, Admixtures for concrete, mortar and grout – Test methods - Part 2: Determination of setting time, pp. 1-16, 2006
- [50] HRN EN 1015-3 2000 A2 008, Methods of test for mortar for masonry – Part 3: Determination of consistence of fresh mortar (by flow table), pp. 1-8, 2006
- [51] HRN EN 206-1, Beton-1.dio Specifikacije, svojstva, proizvodnja i sukladnost (uključuje amandmane A1:2004 I A2:2005), pp.1-70, 2005
- [52] EN 12390-12, Testing hardened concrete – Part 12: Determination of the carbonation resistance of concrete – Accelerated carbonation method, pp. 1-20, 2020
- [53] EN 933-4, Methods of test for dense shaped refractory products, Part 4: Determination of permeability of gases, 1995
- [54] NT Build 492, Concrete, mortar and cement-based repair materials: Chloride migration coefficient from non-steady-state migration experiments, *Measurement*, pp. 1–8, 1999.
- [55] Lebedev, A. V., The synthesis of multi-channel adaptive control system for the autonomous underwater robot, *RPC 2010 - 1st Russ. Pacific Conf. Comput. Technol. Appl.*, pp. 324–328, 2010.
- [56] EN 12390.8, Testing hardened concrete – Part 8: Depth of penetration of water under pressure, pp. 1-11, 2009.

- [57] HRN 1128, Concrete – Guidelines for the implementation of HRN EN 206-1, PP.1-46, 2007
- [58] HRN CEN TS 12390-9, Testing hardened concrete – Part 9: Freeze-thaw resistance with de-icing salts- Scaling, pp.1-36, 2016
- [59] ASTM C1012-04, Standard Test Method for Length Change of Hydraulic-Cement Mortars Exposed to a Sulfate Solution, ASTM Int., pp. 1–6, 2004.
- [60] International Energy Agency, <https://www.iea.org/reports/cement>, 2024 (accessed 20 May 2024).
- [61] Scrivener, K. L., John, V. M., and Gartner, E. M., Eco-efficient cements: Potential economically viable solutions for a low-CO<sub>2</sub> cement-based materials industry, *Cem. Concr. Res.*, vol. 114, pp. 2–26, 2018, doi: 10.1016/j.cemconres.2018.03.015.
- [62] Panesar, D. K. and Zhang, R., Performance comparison of cement replacing materials in concrete: Limestone fillers and supplementary cementing materials – A review, *Constr. Build. Mater.*, vol. 251, 2020, doi: 10.1016/j.conbuildmat.2020.118866.
- [63] Juenger, M. C. G., Winnefeld, F., Provis, J. L., and Ideker, J. H., Advances in alternative cementitious binders, *Cem. Concr. Res.*, vol. 41, no. 12, pp. 1232–1243, 2011, doi: 10.1016/j.cemconres.2010.11.012.
- [64] Ram, K., Flegar, M., Serdar, M., and Scrivener, K., Influence of Low-to Medium-Kaolinite Clay on the Durability of Limestone Calcined Clay Cement (LC3) Concrete. *Materials* 16, no. 1 (2023): 374.
- [65] Scrivener, K., Martirena, F., Bishnoi, S., and Maity, S., Calcined clay limestone cements (LC3), *Cem. Concr. Res.*, vol. 114, no. August 2017, pp. 49–56, 2018, doi: 10.1016/j.cemconres.2017.08.017.
- [66] Zunino, F. and Scrivener, K., Microstructural developments of limestone calcined clay cement (LC3) pastes after long-term (3 years) hydration, *Cem. Concr. Res.*, vol. 153, p. 106693, 2022, doi: 10.1016/j.cemconres.2021.106693.

- 
- [67] Ram, K., Serdar, M., Londono-Zuluaga, D., and Scrivener, K., The effect of pore microstructure on strength and chloride ingress in blended cement based on low kaolin clay, *Case Studies in Construction Materials* 17 (2022): e01242
- [68] Zunino, F. et al., Hydration and mixture design of calcined clay blended cements : review by the RILEM TC 282-CCL, vol. 1, 2022, doi: 10.1617/s11527-022-02060-1.
- [69] Cheng, X., Dong, Q., Ma, Y., Zhang, C., Gao, X., Yu, Y., Wen, Z., Zhang, C., Guo, X., Mechanical and thermal properties of aluminate cement paste with blast furnace slag at high temperatures, *Construction and Building Materials*, 228, 2019, doi.org/10.1016/j.conbuildmat.2019.116747
- [70] Arvaniti, E. C. et al., Determination of particle size, surface area, and shape of supplementary cementitious materials by different techniques, *Mater. Struct. Constr.*, vol. 48, no. 11, pp. 3687–3701, 2015, doi: 10.1617/s11527-014-0431-3.
- [71] Gluth, G. J. G. and Hillemeier, B., Pore structure and permeability of hardened calcium aluminate cement pastes of low w/c ratio, *Materials and Structures/Materiaux et Constructions*, vol. 46, no. 9. pp. 1497–1506, 2013, doi: 10.1617/s11527-012-9991-2.
- [72] Engineering, H., Relationship between pore structure and compressive strength of concrete : Experiments and statistical modelling, vol. 41, no. 3, pp. 337–344, 2016.
- [73] Kumar, R. and Bhattacharjee, B., Porosity, pore size distribution and in situ strength of concrete, *Cem. Concr. Res.*, vol. 33, pp. 155–164, 2003, doi: 10.1016/S0008-8846(02)00942-0.
- [74] Mehta, P. K., *Concrete. Structure, properties and materials*, 1986.
- [75] Gosselin, C., *Microstructural Development of Calcium Aluminate Cement Based Systems with and without Supplementary Cementitious Materials*, vol. 4443, p. 234, 2009.
- [76] Scheinherrová, L. and Trník, A., Hydration of calcium aluminate cement determined by thermal analysis, 2017, doi: 10.1063/1.4994514.

- 
- [77] Fan, W. et al., Effects of carbonation on mechanical properties of CAC-GGBFS blended strain hardening cementitious composites, *Low-carbon Mater. Green Constr.*, vol. 1, no. 1, pp. 1–18, 2023, doi: 10.1007/s44242-022-00001-3.
- [78] Fernández-Carrasco, L., Puertas, F., Blanco-Varela, M. T., and Vázquez, T., Carbonation of calcium aluminate cement pastes, *Mater. Constr.*, vol. 2001, no. 263–264, pp. 127–136, 2001, doi: 10.3989/mc.2001.v51.i263-264.358.
- [79] Sanjuán, M. Á., Estévez, E., Argiz, C., and Barrio, D. del, Effect of curing time on granulated blast-furnace slag cement mortars carbonation, *Cem. Concr. Compos.*, vol. 90, pp. 257–265, 2018, doi: 10.1016/j.cemconcomp.2018.04.006.
- [80] Khan, M. S. H., Nguyen, Q. D., and Castel, A., Carbonation of Limestone Calcined Clay Cement Concrete, in *Calcined Clays for Sustainable Concrete*, 2018, pp. 238–243.
- [81] De Weerd, K., Wilson, W., Machner, A., and Georget, F., Chloride profiles – What do they tell us and how should they be used?, *Cem. Concr. Res.*, vol. 173, no. March, 2023, doi: 10.1016/j.cemconres.2023.107287.
- [82] Liu, J. et al., Chloride distribution and steel corrosion in a concrete bridge after long-term exposure to natural marine environment, *Materials (Basel)*, vol. 13, no. 17, 2020, doi: 10.3390/ma13173900.
- [83] Bašić, Alma-Dina; Serdar, Marijana; Hartmann, Florian; Mikanovic, Ingrid; Walenta, G., Possibilities and Challenges of adding Ground Granulated Blast Furnace Slag to Calcium Aluminate Cement, *ECS2023*, pp. 1–6. 2023
- [84] Idrees, M., Ekincioglu, O., and Sonyal, M. S., Hydration behavior of calcium aluminate cement mortars with mineral admixtures at different curing temperatures, *Constr. Build. Mater.*, vol. 285, p. 122839, 2021, doi: 10.1016/j.conbuildmat.2021.122839.
- [85] Lee, J. M., Yang, H. J., Jang, I. Y., Kim, S. K., and Jung, D. H., Comparison of calcium aluminate cements on hydration and strength development at different initial curing regimes, *Case Stud. Constr. Mater.*, vol. 17, no. August, p. e01596, 2022, doi: 10.1016/j.cscm.2022.e01596.

- [86] Son, H. M., Park, S. M., Jang, J. G., and Lee, H. K., Effect of nano-silica on hydration and conversion of calcium aluminate cement, *Constr. Build. Mater.*, vol. 169, pp. 819–825, 2018, doi: 10.1016/j.conbuildmat.2018.03.011.
- [87] Otieno, M., Beushausen, H., and Alexander, M., Effect of chemical composition of slag on chloride penetration resistance of concrete, *Cem. Concr. Compos.*, vol. 46, pp. 56–64, 2014, doi: 10.1016/j.cemconcomp.2013.11.003.
- [88] Ram, K., Development of high-performance concrete with lower ecological footprint concrete with lower ecological, Faculty of Civil Engineering, University of Zagreb, 2024.
- [89] Balázs, G., Csizmadia, J., and Kovács, K., Chloride ion binding ability of calcium-aluminate, -ferrite and -silicate phases, *Period. Polytech. Civ. Eng.*, vol. 41, no. 2, pp. 147–168, 1997.
- [90] Macias, A., Kindness, A., Glasser, F.P., Corrosion behaviour of steel in high alumina cement mortar cured at 5, 25 and 55°C: chemical and physical factors, *Journal of Materials Science*, vol.31, pp. 2279-2289, 1996
- [91] Sanjuán, M. A., Effect of curing temperature on corrosion of steel bars embedded in calcium aluminate mortars exposed to chloride solutions, *Corrosion Science*, vol. 41, no. 2, pp. 335–350, 1998, doi: 10.1016/S0010-938X(98)00075-4.
- [92] Galan, I. and Glasser, F. P., Chloride in cement, *Adv. Cem. Res.*, vol. 27, no. 2, pp. 63–97, 2015, doi: 10.1680/adcr.13.00067.
- [93] Ann, K. Y., Kim, T. S., Kim, J. H., and Kim, S. H., The resistance of high alumina cement against corrosion of steel in concrete, *Constr. Build. Mater.*, vol. 24, no. 8, pp. 1502–1510, 2010, doi: 10.1016/j.conbuildmat.2010.01.022.
- [94] Sanjuán, M. A., Formation of chloroaluminates in calcium aluminate cements cured at high temperatures and exposed to chloride solutions, *J. Mater. Sci.*, vol. 32, no. 23, pp. 6207–6213, 1997, doi: 10.1023/A:1018624824702.

- [95] Sakai, Y., Relationship between pore structure and chloride diffusion in cementitious materials, *Constr. Build. Mater.*, vol. 229, p. 116868, 2019, doi: 10.1016/j.conbuildmat.2019.116868.
- [96] Astoveza, J., Trauchessec, R., Soth, R., and Pontikes, Y., Properties of calcium aluminate blended cement incorporating iron-rich slag: Evolution over a curing period of 1 year, *Construction and Building Materials*, vol. 282. 2021, doi: 10.1016/j.conbuildmat.2021.122569.
- [97] UN Environment, Scrivener, K. L., John, V.M., Gartner, E.M., *Eco-efficient cements: Potential, economically viable solutions for a low-CO<sub>2</sub> cement based industry*, p. 64, 2016.
- [98] Dorol Sio, J., *Influence of Pozzolanic Material in the Conversion and Corrosion Behaviour of Calcium Aluminate Cement*, University of Sydney, 2014.
- [99] Nosouhian, F., Fincan, M., Shanahan, N., Stetsko, Y. P., Riding, K. A., and Zayed, A., Effects of slag characteristics on sulfate durability of Portland cement-slag blended systems, *Constr. Build. Mater.*, vol. 229, p. 116882, 2019, doi: 10.1016/j.conbuildmat.2019.116882.
- [100] Whittaker, M., Zajac, M., Ben Haha, M., and Black, L., The impact of alumina availability on sulfate resistance of slag composite cements, *Constr. Build. Mater.*, vol. 119, pp. 356–369, 2016, doi: 10.1016/j.conbuildmat.2016.05.015.
- [101] Elahi, M. M. A. et al., Improving the sulfate attack resistance of concrete by using supplementary cementitious materials (SCMs): A review, *Constr. Build. Mater.*, vol. 281, p. 122628, 2021, doi: 10.1016/j.conbuildmat.2021.122628.
- [102] Rossetti, A., Ikumi, T., Segura, I., and Irassar, E. F., Sulfate performance of blended cements (limestone and illite calcined clay) exposed to aggressive environment after casting, *Cem. Concr. Res.*, vol. 147, no. June, p. 106495, 2021, doi: 10.1016/j.cemconres.2021.106495.

- [103] Aramburo, C. H., Pedrajas, C., and Talero, R., Portland cements with high content of calcined clay: Mechanical strength behaviour and sulfate durability, *Materials (Basel)*., vol. 13, no. 18, 2020, doi: 10.3390/MA13184206.
- [104] Shi, Z. et al., Sulfate resistance of calcined clay – Limestone – Portland cements, *Cem. Concr. Res.*, vol. 116, no. March 2018, pp. 238–251, 2019, doi: 10.1016/j.cemconres.2018.11.003.
- [105] Wei, F. et al., Durability of Fibre-Reinforced Calcium Aluminate Cement ( CAC )–Ground Granulated Blast Furnace Acid Attack, *Materials (Basel)*., vol. 13, 2020.
- [106] Herisson, J., Gueguen-Minerbe, M., Hullebusch, E.D., Chaussadent, T., Behaviour of different cementitious material formulations in sewer networks, *Water Science and Tchnology*, 2014, doi: 10.2166/wst.2014.009
- [107] Scrivener, K. L., Cabiron, J. L., and Letourneux, R., High-performance concretes from calcium aluminate cements, *Cem. Concr. Res.*, vol. 29, no. 8, pp. 1215–1223, 1999, doi: 10.1016/S0008-8846(99)00103-9.



## List of figures

Figure 1.1 Formation of the main phases under the influence of temperature .....	16
Figure 1.2 Development of compressive strength in relation to curing temperature [5] .....	17
Figure 1.3 Compressive strength development of mortar in relation to curing time [10]....	19
Figure 1.4 Change in compressive strength in relation to exposure time [22] .....	21
Figure 1.5 a) XRD of non-carbonated and carbonated CAC, b) dTG of non-carbonated and carbonated CAC [39].....	22
Figure 1.6 a) Free chloride content, b) Total chloride content .....	23
Figure 2.1 Particle size distribution of slags (as received) .....	28
Figure 2.2 dTG of raw clay.....	29
Figure 2.3 Heat of hydration obtained by R3 test using calorimetry for 7 days.....	30
Figure 3.1 Particle size distribution-air jet sieving for different time of milling.....	40
Figure 3.2 Particle size distribution - air jet sieving .....	41
Figure 3.3 Particle size distribution - laser diffraction .....	41
Figure 3.4 Flow value and temperature of fresh mortar .....	43
Figure 3.5 Initial and final setting time of fresh mortar .....	43
Figure 3.6 Compressive strength of mortars of the following ages: 6 hours, 24 hours, 7 days and 28 days .....	45
Figure 3.7 Relative compressive strength of mortars of the following ages: 6 hours, 24 hours, 7 days and 28 days .....	45
Figure 3.8 Particle size distribution of CAC cement and slag S1.....	46
Figure 3.9 Development of compressive strength over 56 days for samples cured at: a) 20°C, b) 38°C.....	48
Figure 3.10 DTG for mixes cured at 20°C and 38°C after 28 days: a) CAC100, b) CAC70S130 .....	50
Figure 3.11 Diffractogram for samples cured 56 days at 20°C and 38°C: a) CAC100, b) CAC70S130 (CA=monocalcium aluminate, D=CAH10, Gb=AH3, G=Gehlenite, H=C3AH6, O=C2AH8, S=strätlingite Q=quartz) .....	51
Figure 3.12 Total porosity after 28 days of curing at 20°C and 38°C for CAC100 and CAC70S130 mix .....	53

---

Figure 3.13 Differential intrusion curve after 28 days of curing at 20°C and 38°C for CAC100 and CAC70S130 mix.....	53
Figure 3.14 Critical pore entry diameter after 28 days of curing at 20°C and 38°C for CAC100 and CAC70S130 mix.....	54
Figure 3.15 Compressive strength of CAC100 and CAC70S130 concrete mix.....	55
Figure 3.16 Compressive strength relative to CAC100 mix.....	55
Figure 3.17 Water penetration depth for CAC100 and CAC70S130 mix.....	56
Figure 3.18 Gas permeability coefficient for CAC100 and CAC70S130 mix .....	57
Figure 3.19 Chloride migration coefficient for CAC100 and CAC70S130 mix .....	57
Figure 3.20 Mean value of scaled material per cycle of freezing and thawing .....	58
Figure 3.21 Carbonation depth for CAC100 and CAC70S130 mix .....	59
Figure 3.22 Samples sprayed with phenolphthalein after 7 days of carbonation: a) CAC100, b) CAC70S130, and 28 days of carbonation: c) CAC100, d) CAC70S130.....	59
Figure 3.23 dTG curves of non-carbonated and carbonated samples a) CAC100, b) CAC70S130.....	60
Figure 3.24 Pore size distribution of non-carbonated and carbonated samples a) CAC100, b) CAC70S130.....	61
Figure 3.25 Compressive strength of non-carbonated and carbonated samples.....	62
Figure 3.26 Heat of hydration obtained by R3 test using calorimetry for 7 days.....	63
Figure 3.27 Particle size distribution of CAC cement and clay C1, C2.....	64
Figure 3.28 Development of compressive strength over 28 days.....	65
Figure 3.29 Development of compressive strength over 56 days for samples cured at: a) 20°C, b) 38°C.....	67
Figure 3.30 DTG for mixes cured at 20°C and 38°C after 28 days: a) CAC100, b) CAC70C130.....	69
Figure 3.31 Diffractogram for samples cured 56 days at 20°C and 38°C: a) CAC100, b) CAC70C130 (CA=monocalcium aluminate, D=CAH10, Gb=AH3, G=Gehlenite, H=C3AH6, O=C2AH8, S=strätlingite Q=quartz) .....	70
Figure 3.32 Total porosity after 28 days of curing at 20°C and 38°C for CAC100 and CAC70C130 mix.....	71
Figure 3.33 Differential intrusion curve after 28 days of curing at 20°C and 38°C for CAC100 and CAC70C130 mix .....	72

---

Figure 3.34 Critical pore entry diameter after 28 days of curing at 20°C and 38°C for CAC100 and CAC70S130 mix .....	72
Figure 3.35 Pore classification based on their entry diameter .....	76
Figure 3.36 Capillary pores classification .....	76
Figure 4.1 Carbonation depth values for all mixes .....	81
Figure 4.2 Samples sprayed with phenolphthalein after 56 days of exposure for CAC70S130 mix: a) 20°C, b) 38°C.....	81
Figure 4.3 Compressive strength values after 28 days and 56 days of curing at 20°C and 38°C .....	82
Figure 4.4 Compressive strength values before and after 56 days of carbonation compared to compressive strength prior to carbonation.....	83
Figure 4.5 DTG curves of carbonated CAC100 mix cured at (a) 20°C and at (b) 38°C after 28 days and 56 days of exposure .....	84
Figure 4.6 Diffractogram for non-carbonated and carbonated CAC100 20°C mix (CA=monocalcium aluminate, D=CAH10, Gb=AH3, G=Gehlenite, H=C3AH6, O=C2AH8, Q=quartz, A=aragonite, C=calcite, V=vaterite).....	85
Figure 4.7 Diffractogram for non-carbonated and carbonated CAC100 38°C mix (CA=monocalcium aluminate, D=CAH10, Gb=AH3, G=Gehlenite, H=C3AH6, O=C2AH8, Q=quartz, A=aragonite, C=calcite, V=vaterite).....	86
Figure 4.8 DTG curves of carbonated CAC70S130 (a) 20°C and (b) 38°C mix after 28 days and 56 days of exposure .....	87
Figure 4.9 Diffractogram for non-carbonated and carbonated CAC70S130 20°C mix (CA=monocalcium aluminate, D=CAH10, Gb=AH3, G=Gehlenite, S=Strätlingite, H=C3AH6, O=C2AH8, Q=quartz, A=aragonite, C=calcite, V=vaterite).....	88
Figure 4.10 Diffractogram for non-carbonated and carbonated CAC70S130 38°C mix (CA=monocalcium aluminate, D=CAH10, Gb=AH3, G=Gehlenite, S=Strätlingite, H=C3AH6, O=C2AH8, Q=quartz, A=aragonite, C=calcite, V=vaterite).....	88
Figure 4.11 DTG curves of carbonated CAC70C130 (a) 20°C and (b) 38°C mix after 28 days and 56 days of exposure .....	89
Figure 4.12 Diffractogram for non-carbonated and carbonated CAC70C130 20°C mix (CA=monocalcium aluminate, D=CAH10, Gb=AH3, G=Gehlenite, S=Strätlingite, H=C3AH6, O=C2AH8, Q=quartz, A=aragonite, C=calcite, V=vaterite).....	90
Figure 4.13 Diffractogram for non-carbonated and carbonated CAC70C130 38°C mix (CA=monocalcium aluminate, D=CAH10, Gb=AH3, G=Gehlenite, S=Strätlingite, H=C3AH6, O=C2AH8, Q=quartz, A=aragonite, C=calcite, V=vaterite).....	90

Figure 4.14 CAC100 mix: a) Total porosity for non-carbonated and carbonated samples, b) $dV/d\log D$ .....	91
Figure 4.15 CAC70S130 mix: a) Total porosity for non-carbonated and carbonated samples, b) $dV/d\log D$ .....	92
Figure 4.16 CAC70C130 mix: a) Total porosity for non-carbonated and carbonated samples, b) $dV/d\log D$ .....	92
Figure 5.1 Compressive strength of each mixture after 7 and 28 days of curing .....	102
Figure 5.2 DTG curves of all mixes after 28 days of curing at (a) 20°C and at (b) 38°C..	103
Figure 5.3 Results of a) Total porosity, b) $dV/d\log D$ .....	104
Figure 5.4 Apparent diffusion coefficient: relation between curing at 38°C and 20°C .....	106
Figure 5.5 Total chloride content of each mixture cured at 20°C categorized into bound and free chloride content.....	107
Figure 5.6 Total chloride content of each mixture cured at 20°C categorized into bound and free chloride content.....	107
Figure 5.7 Bound chlorides in relation to total chlorides for: a) CAC100, b) CAC70S130, and c) CAC70C130 mixes .....	108
Figure 5.8 Diffractogram of samples cured 56 days in water and after exposure to NaCl: a) CAC100 20°C, b) CAC100 38°C (CA=monocalcium aluminate, D=CAH10, Gb=AH3, G=Gehlenite, H=C3AH6, O=C2AH8, Q=quartz, S=Strätlingite) .....	110
Figure 5.9 Diffractogram of samples cured 56 days in water and after exposure to NaCl: a) CAC70S130 20°C, b) CAC70S130 38°C (CA=monocalcium aluminate, D=CAH10, Gb=AH3, G=Gehlenite, H=C3AH6, O=C2AH8, Q=quartz, S=Strätlingite).....	111
Figure 5.10 Diffractogram of samples cured 56 days in water and after exposure to NaCl: a) CAC70C130 20°C, b) CAC70C130 38°C (CA=monocalcium aluminate, D=CAH10, Gb=AH3, G=Gehlenite, H=C3AH6, O=C2AH8, Q=quartz, S=Strätlingite).....	111
Figure 6.1 Visual observation of CAC100 sample: a) before exposure, b) after 56d of exposure to Na <sub>2</sub> SO <sub>4</sub> .....	119
Figure 6.2 Weight change of all samples during exposure to Na <sub>2</sub> SO <sub>4</sub> .....	119
Figure 6.3 Compressive strength development during exposure to Na <sub>2</sub> SO <sub>4</sub> .....	121
Figure 6.4 Compressive strength values after 56 days of curing and 28 days of exposure to Na <sub>2</sub> SO <sub>4</sub> .....	121
Figure 6.5 DTG curves of non-exposed and samples after 28 days of exposure to Na <sub>2</sub> SO <sub>4</sub> for CAC100 mix cured (a) at 20°C and at (b) 38°C .....	122
Figure 6.6 DTG curves of non-exposed and samples after 28 days of exposure to Na <sub>2</sub> SO <sub>4</sub> for CAC70S130 mix cured (a) at 20°C and at (b) 38°C .....	123

---

Figure 6.7 DTG curves of non-exposed and samples after 28 days of exposure to Na <sub>2</sub> SO <sub>4</sub> for CAC70C130 mix cured (a) at 20°C and at (b) 38°C.....	124
Figure 6.8 Visual observation of CAC100 sample: a) before exposure, b) after d of exposure to H <sub>2</sub> SO <sub>4</sub> .....	125
Figure 6.9 Weight change of all samples during exposure to H <sub>2</sub> SO <sub>4</sub> .....	125
Figure 6.10 Compressive strength development during exposure to H <sub>2</sub> SO <sub>4</sub> .....	126
Figure 6.11 Compressive strength values after 56 days of curing and 28 days of exposure to H <sub>2</sub> SO <sub>4</sub> .....	127
Figure 6.12 Figure 12 DTG curves of non-exposed and samples after 28 and 91 days of exposure to H <sub>2</sub> SO <sub>4</sub> for CAC100 mix cured (a) at 20°C and at (b) 38°C.....	128
Figure 6.13 Diffractogram for non-exposed and sample after 91 days of exposure to H <sub>2</sub> SO <sub>4</sub> for CAC100 mix (CA=monocalcium aluminate, D=CAH10, Gb=AH3, g=Gehlenite, H=C3AH6, O=C2AH8, Q=quartz, G=Gypsum) .....	129
Figure 6.14 DTG curves of non-exposed and samples after 28 days of exposure to H <sub>2</sub> SO <sub>4</sub> for CAC70S130 mix cured (a) at 20°C and at (b) 38°C .....	130
Figure 6.15 Diffractogram for non-exposed and sample after 28 days of exposure to H <sub>2</sub> SO <sub>4</sub> for CAC70S130 mix (CA=monocalcium aluminate, D=CAH10, Gb=AH3, g=Gehlenite, H=C3AH6, O=C2AH8, Q=quartz, G=Gypsum) .....	130
Figure 6.16 DTG curves of non-exposed and samples after 28 days of exposure to H <sub>2</sub> SO <sub>4</sub> for CAC70C130 mix cured (a) at 20°C and at (b) 38°C.....	131
Figure 6.17 Diffractogram for non-exposed and sample after 28 days of exposure to H <sub>2</sub> SO <sub>4</sub> for CAC70C130 mix (CA=monocalcium aluminate, D=CAH10, Gb=AH3, g=Gehlenite, H=C3AH6, O=C2AH8, Q=quartz, G=Gypsum) .....	132
Figure 6.18 a) Total porosity for non-exposed and samples after 28 and 91 days of exposure to H <sub>2</sub> SO <sub>4</sub> , b) dV/dlogD .....	133

**List of tables**

Table 1.1 Densities of the calcium aluminate cement hydrates.....	16
Table 2.1 Chemical composition of used materials .....	29
Table 2.2 The resistance of concrete according to chloride migration coefficient values ...	34
Table 2.3 Limiting water permeability values for different quality classes of concrete .....	35
Table 3.1 Comparison of Blaine, $d_{10}$ , $d_{50}$ and $d_{90}$ .....	42
Table 3.2 Total porosity of non-carbonated and carbonated samples.....	61
Table 4.1 Total porosity and average pore diameter values of non-carbonated and carbonated samples .....	92
Table 4.2 Parameters quantified from thermogravimetric analysis before and after 56 days of accelerated carbonation .....	97
Table 5.1 Total porosity and average pore diameter values of non-carbonated and carbonated samples .....	105
Table 6.1 Total porosity and average pore diameter after 56 days of curing and 28 days of exposure to $H_2SO_4$ .....	133

---

## **Biography**

Alma-Dina Bašić was born on September 13, 1995, in Zagreb, Croatia. She obtained her bachelor's degree in civil engineering in 2018 at Faculty of Civil Engineering, University of Zagreb, Croatia. In September 2020 she obtained a master's degree in the field of Construction Materials at the Faculty of Civil Engineering, University of Zagreb. Focus of her Master thesis was Binders based on calcined clay in concrete for general application. In the year 2019/2020 her work with colleague Katarina Didulica "Development of sustainable binders based on locally available materials" was awarded with Rector's Award. Since December 16, 2020, she has been a PhD student at the Department of Materials, Faculty of Civil Engineering at University of Zagreb, Croatia. Her research topic is influence of supplementary cementitious materials on durability of calcium aluminate cement under different curing regimes.

## **List of published papers**

### **Papers in journal**

1. Skočibušić Pejić, Josipa, Bašić, Alma-Dina, Grubor, Martina, Serdar, Marijana, "Link between the reactivity of slag and the strength development of calcium aluminate cement", *Materials*, 2024, 17 (14), 3551, <https://doi.org/10.3390/ma17143551>

### **Papers, posters, and presentations in conferences**

1. Bašić, Alma-Dina, Grubor, Martina, Serdar, Marijana, Mikanovic, Ingrid and Walenta, Günther, "Strength development of calcium aluminate cement with slag", 7th Symposium on Doctoral Studies in Civil Engineering, Faculty of Civil

- 
- Engineering, University of Zagreb, Zagreb, Croatia: University of Zagreb Faculty of Civil Engineering, 2021
2. Bašić, Alma-Dina, Grubor, Martina, Serdar, Marijana, Mikanovic, Ingrid and Walenta, Günther “Influence of supplementary cementitious materials on compressive strength of calcium aluminate cement” 15<sup>th</sup> International Scientific Conference iNDiS 2021, Novi Sad, Serbia, 24-26 November 2021
  3. Skočibušić Pejić, Josipa; Bašić, Alma-Dina; Serdar, Marijana; Hartman, Florian, International Conference on Calcium Aluminates, “Development of a new innovative product - ECO2Flex project”, presentation, International Conference on Calcium Aluminates 2022, Cambridge, UK, 18-20 July 2022
  4. Bašić, Alma-Dina; Serdar, Marijana; Mikanović, Ingrid; Walenta, Günther, “Influence of slag on durability of calcium aluminate cement concrete”, 76th RILEM Annual Week International Conference on Regeneration and Conservation of Structures, Kyoto, Japan, 3-9 September 2022
  5. Bašić, Alma-Dina; Serdar, Marijana; Mikanovic, Ingrid; Walenta, Günther, “Impact of slag on carbonation rate of concrete based on calcium aluminate cement”, MATEC Web of Conferences Volume 364 / Alexander, M.G. ; Beushausen, H.; Dehn,F.; Ndawula,J.;Moyo,P.(ur.),October,CapeTown,2022,<https://doi.org/10.1051/mateconf/202236402020>
  6. Bašić, Alma-Dina; Serdar, Marijana; Hartmann, Florian; Mikanovic, Ingrid; Walenta, Günther, “Possibilities and Challenges of adding Ground Granulated Blast Furnace Slag to Calcium Aluminate Cement”, European Coatings Show Conference (ECS2023), 27-28 March. 2023, Nuremberg, Germany



- 
7. Flegar, .M, Bašić, AD., Bukvić, O., Serdar, M., “Carbonation of Concretes with Different Binder Chemistry – A Comparative Analysis” In: Jędrzejewska, A., Kanavaris, F., Azenha, M., Benboudjema, F., Schlicke, D. (eds) International RILEM Conference on Synergising Expertise towards Sustainability and Robustness of Cement-based Materials and Concrete Structures. SynerCrete 2023. RILEM Bookseries, vol 44. Springer
  8. Bašić, Alma-Dina; Serdar, Marijana, “Changes in the durability of calcium aluminate cement based concrete induced by slag addition”, 9<sup>th</sup> International conference “Civil Engineering – Science and Practice”, GNP2024, 5-9 March, 2024, Kolašin, Montenegro